P~ .gamon

0360-1285(94)00015-8

LASER TECHNIQUES FOR THE QUANTITATIVE DETECTION OF REACTIVE INTERMEDIATES IN COMBUSTION SYSTEMS

KATHARINA KOHSE-HÖINGHAUS

Physikalische Chemie I, Universität Bielefeld, Universitätsstraße 25, D-33615 Bielefeld, Germany

Abstract—An overview is given of recent developments in laser diagnostic methods for the quantitative measurement of trace species concentrations and, in conjunction, of temperature in combustion systems. After a short introduction illustrating some experiments from the pre-laser era, the article presents typical applications and discusses advantages and limitations of laser techniques including laser absorption, linear, saturated, predissociative and multi-photon-excited laser-induced fluorescence (LIF), resonance-enhanced multiphoton ionization (REMPI), electronically resonant coherent anti-Stokes Raman scattering (resonance CARS), degenerate four-wave mixing (DFWM) and amplified spontaneous emission (ASE). Recent trends including two-dimensional imaging, multi-species detection and high-pressure applications will also be discussed. Throughout the article, an attempt is made to present typical results from a large portion of the relevant technical literature. A concluding section gives a short summary of the current status and comments on the perspectives for further research.

CONTENTS

NOTATION
Symbols

A_{ji}	Einstein coefficient for spontaneous emission	t	Time	
B_{ij}, B_{ji}	Einstein coefficients for absorption and stimulated emission	V	Volume	
		v	Vibrational quantum number	
c	Velocity of light	v	Frequency	
c_i	Concentration	Φ	Equivalence ratio	
E	Energy	χ	Mole fraction	
e	Electron charge	Ω	Detection solid angle	
f	Oscillator strength			
f_B	Boltzmann fraction			
g	Degeneracy			
h	Planck's constant			
I	Intensity			
J	Quantum number for total angular momentum			
k	Boltzmann's constant			
k_v	Absorption coefficient			
l	Path length			
m	Electron mass			
N	Rotational quantum number			
N_i	Number density			
n	Fundamental quantum number			
p	Pressure			
T	Temperature			

Units
Pressure is given in bar: $1 \text{ bar} = 10^5 \text{ Pa (Nm}^{-2})$

Abbreviations

ASE	Amplified spontaneous emission
CARS	Coherent anti-Stokes Raman scattering
DFWM	Degenerate four-wave mixing
DPCFWM	Double phase-conjugate four-wave mixing
LIF	Laser-induced fluorescence
LIPF	Laser-induced predissociative fluorescence
MPLIF	Multi-photon laser-induced fluroescence
PLIF	Planar laser-induced fluorescence
REMPI	Resonance-enhanced multi-photon ionization
CVD	Chemical vapor deposition

1. INTRODUCTION

Regarding the global dependence on fossil fuels and increasing constraints with respect to the emission of combustion-generated pollutants, the importance of a more detailed understanding of combustion processes can hardly be overestimated. A multitude of interdependent parameters determines the general performance of technical combustion systems in terms of efficiency, fuel consumption, pollutant formation, cost and reliability. Computer simulation of combustion processes thus plays an increasingly important role in design and optimization procedures. To date, many significant features of technical combustion systems cannot, however, be modelled in adequate detail. While progress is currently being made in simulating the interaction of a turbulent flow field with the complex network of chemical reactions for prediction of local flame extinction and associated hydrocarbon emission and for modelling soot formation and engine knock, a comprehensive description of practical combustion (e.g. the Diesel

combustion process) is far beyond the capability of current computer models.

In this situation, laser spectroscopic techniques serve two main purposes: they provide in situ, real-time information on technical combustion processes and they furnish data for a thorough inspection of current model assumptions. Laser diagnostic techniques have superseded more traditional probe and sampling methods for many applications due to their high temporal and spatial resolution, their excellent selectivity and sensitivity, and in particular their non-invasive nature. Various parameters of interest, such as particle and droplet sizes, velocity, temperature and concentration distributions, can be determined using laser spectroscopic methods. For a thorough analysis of the chemical processes governing combustion situations such as ignition, heat release, quenching or pollutant formation, accurate information, particularly on the behavior of reactive intermediates in combustion systems, can be measured using laser absorption, laser-induced fluorescence, multi-photon spectroscopy or other less estab-

lished techniques capable of detecting ppm levels of atomic and molecular radicals in combustion environments.

Several books and review articles can be recommended for an excellent introduction into the field of combustion diagnostics. Although written in pre-laser times, the wealth of information in Gaydon's book on flame spectroscopy[1] should not be overlooked. Established laser techniques for combustion diagnostics are discussed in detail by Eckbreth[2] and Taylor[3] who give, besides Chigier,[4] the most recent comprehensive overviews. Further reviews, particularly of the diagnostics of intermediate species, can be found in the literature.[5-10] Laser diagnostics in turbulent diffusion flames was most recently reviewed by Stepowski.[11] Laurendeau[12] has surveyed optical techniques for the measurement of temperature in reactive systems. Fluorescence techniques have been reviewed by Schofield and Steinberg[13] and by Crosley.[14,15] Two-dimensional applications of laser-induced fluorescence have been discussed by Hanson[16] and Hanson et al.[17] Some specific applications of laser spectroscopic techniques to combustion diagnostics have been compiled by Wolfrum[18] and by Kompa et al.[19] in recent journal editions.

The intention of this article is to report on the present status of development of techniques for the detection of combustion intermediates, in particular with respect to their potential for quantitative concentration measurements. Since temperature, one of the most important quantities in combustion systems, is related to the determination of concentrations, comments on the capability of methods for accurate temperature measurements shall be given when applicable. Although care was taken to survey a substantial part of the recent literature, the list of references is by no means complete. It should also be noted that the views expressed in this review necessarily reflect the author's personal opinions and experience. The article is organized in the following way. Section 2 gives some background information on quantitative measurement of intermediate concentrations without the aid of laser radiation. Section 3 reports briefly on laser absorption and related techniques. Major parts of the article are devoted to laser-induced fluorescence (Section 4) and multiphoton excitation (Section 5). Techniques and experimental procedures which are still being developed and applications of which are, to a large extent, of a qualitative nature, are covered in Section 6. A brief summary and suggestions for further research are given in Section 7.

2. DETERMINATION OF RADICAL CONCENTRATIONS AND TEMPERATURES WITHOUT LASERS

Combustion proceeds through a multitude of elementary reaction steps. Molecular radicals and atoms play a dominant role in controlling the network of chemical processes. Three quite abundant intermediate species, H, O and OH, take part in most pyrolysis or oxidation reactions and are thus of eminent influence on ignition, heat release, flame propagation and flame quenching. Furthermore, the presence of certain hydrocarbon radicals may indicate specific reaction paths followed in the fuel degradation process or may provide clues for the generation of aromatic compounds and soot. Nitrogen- and sulfur-containing radicals are involved in NO_x and SO_x formation. For a thorough analysis of the detailed reaction mechanism it is therefore important to detect at least some key intermediate species in specific combustion situations and to measure their concentrations in combination with the local temperature.

Such investigations are usually performed in laminar, premixed low-pressure flames with extended reaction zones. Three probe techniques are established for these experiments: electron spin resonance (ESR) and mass spectrometry for the measurement of concentrations, and thermocouples for temperature measurements. Mass spectrometry in combination with probe sampling is well suited for an overview of the flame composition since all radicals can in principle be detected. Especially for determination of the concentrations of large hydrocarbon radicals, which exhibit complicated spectra and a high density of states (resulting in poor optical detection sensitivities), mass spectrometry has proved to be far more successful than absorption or fluorescence techniques. However, careful control of the sampling procedure is crucial for reliable results. Microprobes or molecular beam sampling systems have been used in a large number of investigations; typical applications can be found in the article of Foner and Hudson,[20] in the studies on soot formation of Bonne et al.[21] and Homann and Wagner,[22] the work on methane flames of Fristrom,[23] Peeters and Mahnen,[24] Milne and Greene,[25] Lazzara et al.,[26] Biordi et al.,[27] on ethane flames by Blauwens et al.[28] and on acetylene flames by several groups.[29-31] Examples of recent studies include those of Vandooren[32] in ammonia-seeded, rich $H_2/O_2/Ar$ flames at low pressure and of Garo et al.[33] in low-pressure CH_4/O_2 flames doped with NO or NH_3.

In order to avoid recombination losses of radicals in the sampling system, scavengers may be used instead of molecular beam sampling. Scavengers like NO_2 or D atoms react rapidly with the radical under investigation to form stable compounds which are then detected. However, scavenger reactions may not be specific enough to distinguish between different original species. For example, H, O and OH react rapidly with NO_2 so that only the sum of their concentrations may be detectable. Corresponding experiments have been described by Fristrom[23,34] and Volponi et al.[35]

ESR spectroscopy has been used mainly for measuring H, O and N atom concentrations in flow systems and flames. Again, probe sampling is required. The distance to the spectrometer is preferably kept
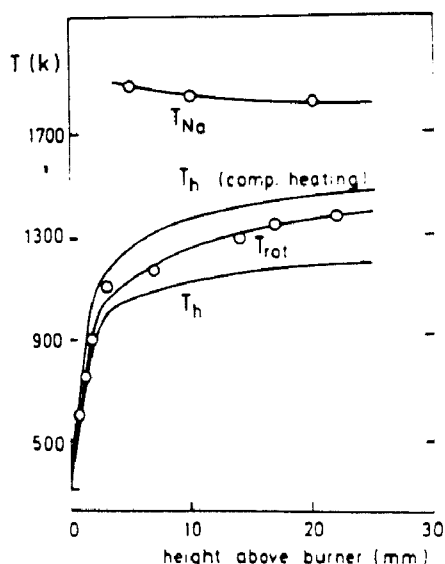
FIG. 1. Temperature profile in a lean acetylene/oxygen flame at low pressure,[53] measured with different techniques. T_{Na}: sodium line reversal; T_h: thermocouple, with and without compensatory heating; T_{rot}: rotational spectra of OH, monitored in absorption.

short to minimize recombination losses. Calibration of the radical detection efficiency can be performed using O_2 or NO. The quantitative determination of radical concentrations by ESR is reported in the fundamental work of Westenberg and de Haas,[36] Westenberg and Fristrom[37] and Westenberg.[38] More recent applications can be found in the literature.[39-41]

Temperature in flames has often been measured with thermocouples, although the accuracy and reliability of such measurements may be questionable. Not only can the flame be disturbed by the thermocouple, but in addition, the presence of high radical concentrations may lead to catalytic processes on the thermocouple surface and thus to substantial experimental errors. Further uncertainties originate from radiation losses. Also, the application of thermocouples is necessarily limited at high temperatures due to material considerations.

Photometric techniques using alkali metal compounds have found a limited range of application for the measurement of atom concentrations and temperature in flames. H atom concentrations can be determined in an indirect way from the reactions H + LiOH = Li + H_2O or H + NaCl = Na + HCl by monitoring the spectral intensity of Li or Na radiation at 671 and 589 nm, respectively. This method was used by James and Sugden,[42] Bulewicz et al.,[43] McEwan and Phillips[44] and Halstead and Jenkins.[45] It is not very accurate; Bulewicz et al.[43] observed variations of up to a factor of 4 in the measured H atom concentration when using the NaCl versus the LiOH reaction. A potential uncertainty results from the addition of alkali metal salts to the flame. Also, it was observed that the method tends to be unreliable below about 1600 K.[44]

A commonly applied technique is the doping of

flames with alkali atoms as temperature indicators. In particular, the Na line reversal technique[46] has received considerable attention for the measurement of temperature in flames. This method has been applied by James and Sugden,[42] Zeegers and Alkemade[47] and Milne and Green.[25] Furthermore, atomic tracers such as Tl, In, Ga or Pb have been used for the determination of temperature.[48] If carefully applied, these methods may be quite accurate.

A large number of investigations have been performed using emission and absorption spectroscopy. While emission of radicals such as OH, CH and C_2 is indicative of the presence of excited states of these species in flames, absorption of these and other radicals may be used for concentration and temperature measurements. Before lasers were available, accidental spectral coincidences of atomic lines with absorption lines of the radical under investigation were exploited. The OH radical, for example, can be excited with a Bi lamp (Carrington[49]). Furthermore, broadband sources like Hg and Xe lamps can be employed. In large diameter flat flames, where cool zones at the edges are of little influence, radical concentrations can be very accurately determined by absorption. Many authors have measured concentrations and determined rotational temperatures from UV absorption of the OH radical.[47,50-53] Porter et al.[54] as well as Bulewicz et al.[55] have in addition measured CH and C_2 concentrations using multiple reflection geometries to increase the path length. CH and C_2 concentrations have also been determined by Bleekrode and Nieuwpoort[56] and Jessen and Gaydon;[57] they had to use very long absorption path lengths as well. Le and Vanpee[58] have measured CH, C_2, CN, NH, OH and NO concentrations in a low-pressure flame by absorption. Emission of OH, CH or C_2 in flames has been monitored.[51,59] Recently, emission and absorption studies in solid propellant flames for the measurement of absolute OH, NH and CN concentrations were reported.[60]

In several studies, optical techniques have been used to examine the perturbation of the flame by probes. Eberius et al.[52,53] have combined mass spectrometry, gas chromatography, ESR and UV absorption in their investigations of low-pressure flames. Figure 1 compares the temperature profile Eberius et al.[53] obtained with different methods; deviations on the order of several hundred degrees were observed between the results of the Na line reversal technique, OH rotational spectra from UV absorption spectroscopy, and measurements with a thermocouple. Revet et al.[61] and Stepowski et al.[62] have compared optical and probe sampling techniques for the measurement of concentrations: in zones with steep gradients, OH concentrations obtained with both methods differed by about a factor of 2. Schoenung and Hanson[63] have measured CO in methane flames with both probe and optical techniques and defined conditions under which the two methods gave identical results.

Cattolica et al.[64] have detected OH by laser absorption and mass spectrometry and discussed the observed deviations. A detailed comparison of UV absorption and mass spectrometry for NO measurements in flames was carried out by Zabielski et al.[65] In addition, Seery and Zabielski[66] have detected the OH radical with both absorption and probe techniques. Smith and Chandler[67] have measured CN concentration profiles by laser-induced fluorescence with and without the presence of a probe in the flame. Recently, Desgroux et al.[68] have determined flame perturbation by a probe in a premixed methanol/air flame at low pressure. They measured OH concentrations and rotational temperatures by laser-induced fluorescence with and without a quartz sampling probe present. Discrepancies in the OH concentration in the order of 30% and cooling effects by the probe of about 100–120 K were observed.

All these investigations demonstrate that both probe and optical methods, when carefully applied, can measure accurate radical concentrations. Probe measurements tend, however, to be questionable in zones exhibiting large temperature and concentration gradients. Since temperature and concentration measurements are often related, considerable errors may result. Whereas probe measurements are possible in clean laboratory environments, such as one-dimensional low-pressure flames, where they may be the only way to gain information on a wide range of species, including large hydrocarbon radicals, their application to practical combustion systems is rather limited. Temporal and spatial resolution obtained with probe sampling methods are insufficient for following temperature and concentration fluctuations in turbulent or unsteady flames. Soot, particles or droplets may have adverse effects on the probes. Also, the combustion process may be affected by the presence of the probe, e.g. by catalytic effects on the probe surface. The disadvantages of probe measurements may be seen as advantages of optical techniques, which may be used in a non-invasive manner directly at the location of interest, where they offer high sensitivity, temporal and spatial resolution, and which, in addition, may provide special features such as laser-like signal beams or two-dimensional images.

3. LASER ABSORPTION

Absorption is one of the most simple optical techniques in both instrumentation and data evaluation. The previous section has given a few examples for absorption measurements in flames using incoherent light sources. Here, typical applications of laser absorption in combustion diagnostics shall be presented.

The absorption in a sample of path length l and absorber concentration c_A is obtained by measuring the incident intensity I_0 of the light source and the intensity I transmitted by the sample. The decrease of the intensity by the absorption in the sample is given by Beer's law

$$I = I_0 \exp - (l\, c_A\, k_v);\qquad(1)$$

k_v is the frequency-dependent absorption coefficient. For gaseous absorbers, c_A is often expressed as the partial pressure p_A of the absorbing molecule $p_A = p\chi_A$, where p is the total pressure and χ_A is the mole fraction of the absorbing molecule. The absorption coefficient is then given in the units $atm^{-1}cm^{-1}$. Oscillator strength f and absorption coefficient are related by

$$\int k_v \mathrm{d}v = (\pi e^2/mc^2)\,(N_A/p\chi_A)f\qquad(2)$$

if induced emission can be neglected; m and e are the mass and charge of the electron and c is the velocity of light. Integration is performed over the entire absorption line. Besides the shape of the absorption line, the spectral distribution of the light source may be of influence. Detailed information on absorption spectroscopy in general and on lineshape functions can be found in the books of Penner[69] and Mitchell and Zemansky.[70]

One of the most significant features of the absorption technique results in a severe disadvantage for use in combustion experiments: it is a line-of-sight technique which does in general not allow for spatial resolution along the beam path. Its application is limited to flames or zones of combustion systems with homogeneous density and absorber concentration. Also, the presence of soot, particles and droplets in the beam path may cause difficulties.

3.1. Laser Absorption in Flames and Shock Tube Experiments

In clean laboratory flames, radical concentrations can be measured directly, without further calibration, by absorption techniques, since the populations of quantum levels within the electronic ground state are monitored. Thus, the number density in a specific quantum state is easily obtained if the absorption coefficient is known, and it can be related to the total radical concentration (via the Boltzmann fraction) if the ground state population may be assumed to be thermally distributed. In contrast, laser-induced fluorescence (LIF) provides information on the population in both the ground and excited electronic states; the evaluation therefore requires information about the influence of collisions on the populations in the excited state, as will be detailed in Section 4.

Absorption using narrowband laser radiation has found an interesting application in shock tube experiments, where pyrolysis and oxidation mechanisms may be studied in the absence of flow, diffusion or heat conduction. In these investigations, the temporal evolution of specific molecular radical concentrations is examined by laser absorption in order to provide
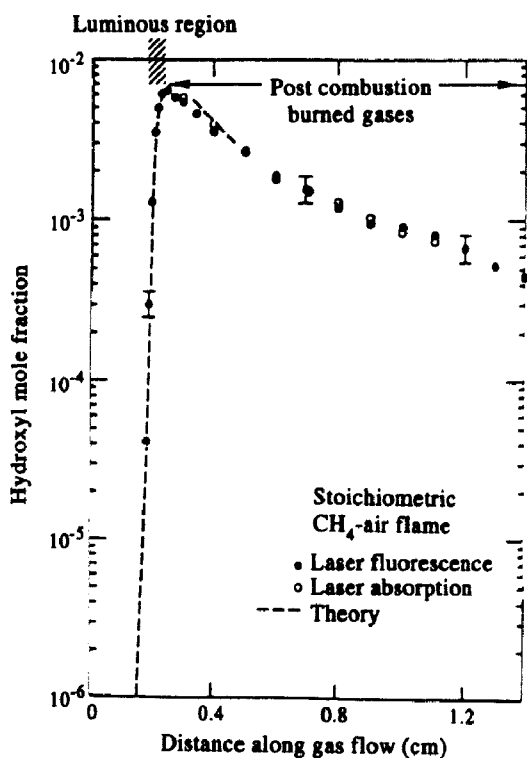
FIG. 2. OH concentration in a stoichiometric methane/air flame.[92] Quantitative concentration measurements with absorption were used to calibrate the LIF results.

rate coefficients for elementary combustion reactions, particularly for radical–molecule or radical–radical reactions, or information on reaction mechanisms. Hanson et al.[71] have been the first to observe narrowband laser absorption of the OH radical in a shock tube. The technique was refined by Rea et al.[72] In a similar approach, Fujii and Shin[73] have detected OH in shock tube experiments by laser absorption. Using narrowband laser absorption schemes, several other radicals have been detected with good sensitivity and accuracy, including NCO,[74,75] NH,[76] CH,[77] NH$_2$,[78] CN,[79,80] and CH$_3$.[81] Chang et al.[82] have rapidly tuned a narrowband laser across two neighboring OH lines and thus obtained accurate temperature measurements in a shock tube experiment. The narrowband laser absorption technique is not limited to chemical-kinetic investigations or measurements of absorption lineshapes, as has been demonstrated by Chang et al.[83] and DiRosa et al.[84] who simultaneously determined velocity, temperature, pressure, density and mass flux from NO absorption in a shock tube. Velocity was obtained from the Doppler shift, temperature and pressure from peak intensity ratios and lineshapes, density from the measured temperature and pressure, and mass flux from density and the measured velocity. Similar measurements of OH were reported by Davidson et al.[85] This method is capable of complete characterization of high-speed combustion systems, when the flow is sufficiently uniform along the line-of-sight.

While laser absorption allows for species-specific detection, selective production of radicals may also

be desirable. Instead of thermal radical sources, flash photolysis[86,87] or excimer laser photolysis[88,90] in combination with absorption were used in order to prepare significant amounts of a specific radical and to investigate its kinetic behavior in a largely undisturbed fashion. In general, however, the combined application of laser photolysis and laser absorption to complex reaction systems requires detailed information on the spectroscopy, photodissociation dynamics and collisional deactivation of the molecules or radicals under study. An example of a kinetic investigation, in this case of ammonia pyrolysis, with the combined laser photolysis/laser absorption technique is given by Davidson et al.[91]

One of the most frequent applications of laser absorption measurements in combustion diagnostics is the calibration of LIF experiments. Examples in the literature are numerous. Bechtel and Teets[92] have measured the concentration of the OH radical in the burnt gases of a methane/air flame by absorption and used this information for the calibration of their LIF signals; the results are shown in Fig. 2. Lucht et al.[93] have used OH absorption measurements in non-sooting flames to obtain calibration factors for their saturated LIF experiments in sooting flames where OH concentrations were too small for detection by absorption. Further examples for calibration of LIF measurements by absorption are found in the articles of Anderson et al.,[94] who measured OH and NH concentrations in CH$_4$/N$_2$O flames, of Chou et al.[95] for the detection of NO in ammonia flames, of Kaiser et al.[96] for the detection of OH in propane flames and in our own work for measuring OH concentrations at pressures above 1 bar.[97]

For many absorption experiments in flames the bandwidth of the light source, even of a laser, is larger than the width of the absorption line. Thus the radical concentration is inferred from the measured integral absorption, as described by Cattolica,[98] Cattolica et al.[64] and Chou et al.[99] In this case the shape of the absorption line and the influences of temperature, pressure and gas composition on its broadening behavior must be known from independent sources. If narrowband lasers are used instead, the absorption line profile can be measured directly. With narrowband laser absorption, Lück and Thielen[100] and Tsatsaronis and Lück[101] have obtained OH concentrations in a methane flame, Green and Miller[102] have determined relative NH$_2$ profiles in low-pressure ammonia flames, and Joklik et al.[103] have measured CH concentrations in low-pressure acetylene flames. In some of these investigations,[100,101,104] temperature was measured in conjunction with the OH concentration.

3.2. Special Absorption Techniques

Some absorption techniques offer special features and therefore deserve a separate description. In typi-
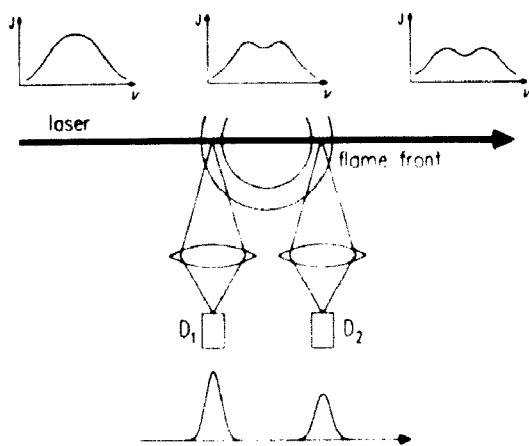
Fig. 3. Spatially resolved absorption measurement using a combination of absorption and fluorescence.[114] The fluorescence intensities (curves at the bottom) measured by the detectors D_1 and D_2 serve as a measure of absorption (curves at the top). After the first transition through the flame front, the incident radiation (top left curve) is attenuated by absorption (top center). The first fluorescence signal (bottom left) corresponds to the original incident radiation, the second (bottom right) to a lower laser intensity. A second transition of the flame front causes additional absorption (top right).

cal experimental arrangements, about 0.1% absorption can reliably be measured. A limiting factor is often the stability of the light source. Higher sensitivity is achievable with intracavity techniques, where the absorbing medium is placed inside the resonator. Harris and Weiner[105,106] have detected O atoms and C_2 radicals, respectively, by intracavity absorption. Compared to a conventional absorption experiment, the estimated increase in sensitivity was about a factor of 5000 for C_2 detection. Anderson et al.[107] have detected small amounts of NCO in a CH_4/N_2O flame with this method. However, the quantitative interpretation of these experiments may be difficult. A detailed examination of the potential of intracavity absorption measurements for combustion diagnostics is given by Harris.[108] Different means for increasing the sensitivity of absorption measurements are provided by modulation techniques. A detailed analysis of frequency modulation for high sensitivity absorption experiments is found in the recent article of Silver.[109]

Some modifications of the conventional absorption set-up aim at providing spatial resolution in the direction of the laser beam. Inversion routines as described by Grabner and Hastie[110] may correct for the influence of varying concentration or temperature on the absorption signal. Good spatial resolution may be obtained with absorption experiments in crossed-beam geometry, where the measured signal originates only from the region of spatial overlap of both beams. Goldsmith[111] and Kychakoff et al.[112] report saturated absorption experiments with a powerful, pulsed pump beam and a weak cw probe beam which are both tuned to the same absorption transition. The pump pulse temporarily depletes the population in a given (ground state) level; this deple-

tion is registered as a decrease of absorption by the probe signal. Goldsmith[111] has detected Na atoms and Kychakoff et al.[112] have measured OH radicals in a flame using this technique. In turbulent media, however, where beam steering may affect the overlap of both beams, application of saturated absorption is questionable. For a quantitative interpretation of the measured absorption signals, the saturation behavior must be known. This is easier than in the case of saturated fluorescence (Section 4.3), since only the population in the electronic ground state must be considered, avoiding the need to accurately describe collisional processes in the excited state. However, the sensitivity of saturated absorption is smaller than that of saturated fluorescence, since a small absorption signal has to be distinguished from a large background.

Spatial resolution in absorption measurements can also be achieved with a combination of absorption and fluorescence. This technique was demonstrated by Stepowski and Garo[113] for the detection of OH in a centro-symmetric diffusion flame. Two fluorescence detectors at right angles to the direction of the laser radiation serve as monitors for the absorption between the two observation volumes on the laser beam axis, as illustrated in Fig. 3. For non-negligible absorption in the flame front, the second fluorescence signal exhibits lower intensity than the first. The absorption can be determined from the two fluorescence intensities. In principle, the technique can also be applied for flames without radial symmetry; then, two counterpropagating laser beams are used, generating four fluorescence signals.[114] In this arrangement, the method allows for correction of varying absorption, fluorescence quantum yields or detector sensitivities. It may also be used as an in situ calibration for fluorescence measurements.[115]

3.3. Photothermal and Photoacoustic Techniques

Photothermal and photoacoustic detection of radicals can be regarded as complementary to absorption measurements. Laser radiation is tuned to an absorption transition; the energy thus deposited in the system is at atmospheric pressure, rapidly dissipated by collisions. This leads to a local increase in temperature and a corresponding change in density and index of refraction. Thermal waves or pressure waves originating from the absorption volume can be detected. Depending on the measured quantity, the technique is termed photothermal or photoacoustic. Both variants are advantageous at high pressures, since the signal increases with collision rate. This is in contrast to laser-induced fluorescence measurements, where a higher collision frequency leads to a decrease in fluorescence quantum yield.

Sound waves generated by local absorption can be detected with a microphone. A few applications have been demonstrated in a flame environment. Allen et

al.[116] have detected Na and Li atoms in an acetylene flame, and Tennal et al.[117] have measured NO_2 in a methane flame at atmospheric pressure. Also, Smith et al.[118] have detected OH and NH_2 in a flame environment. The detection of sound waves is, however, not very well suited to the measurement of radical concentrations in flames since the spatial resolution is rather limited. Furthermore, a quantitative interpretation of the measured signals is difficult, if the sound waves are reflected or pass through thermally or chemically inhomogeneous zones in the flame.

Optical detection of heat or pressure waves with the aid of a second laser is thus preferable. Pump and probe laser beams are crossed so that the signal arises only from the overlapping zone. The deflection of the probe beam by the induced pressure or heat wave generated by absorption of the pump laser radiation is monitored with a position-sensitive detector. The observed deflection is a function of the locally deposited energy and thus of the concentration of the absorbing molecule. Rose et al.[119] have determined the OH concentration in a methane flame with the photoacoustic technique and Kizirnis et al.[120] have monitored the OH concentration in a propane/air flame with the photothermal method. The latter group has in addition measured the flame temperature photoacoustically by determining the sound velocity between two probe volumes. For this experiment, the pressure wave was generated by directing the laser onto a wire, since the production of a measurable pressure effect in the flame itself would require very high laser intensities which could cause breakdown. Lawton[121] and Rose and Gupta[122] modified this technique for measurements in sooting flames where the soot particles induced a pressure wave when hit by the laser radiation. As mentioned before, for the quantitative interpretation of such measurements, it is required that the pressure wave travels in a homogeneous medium. Also, the use of a wire in a flame environment, an inherent source of perturbations, is questionable. For these reasons, photothermal and photoacoustic techniques are of limited value for the determination of radical concentrations and temperature in flames; they are not suited for investigations in turbulent systems.

In general, this restriction holds for all absorption techniques: they are not suited for measurements in environments which exhibit steep density, temperature or concentration gradients. Furthermore, their sensitivity may not be sufficient for detection of sub-ppm radical mole fractions even in laboratory flames, and thus multi-pass arrangements may be required. The great advantage of laser absorption techniques is their relative ease of application and straightforward interpretation. Spatial resolution in the direction of the laser beam may be obtained in special applications, but this is usually at the cost of additional complexity in apparatus and data evaluation.

Applications of laser absorption measurements in combustion are, for the above reasons, typically limited to the investigation of flat, premixed flames and the calibration of fluorescence experiments. The potential of narrowband laser absorption techniques for the characterization of high-velocity flow or combustion environments as well as for detailed studies of chemical-kinetic mechanisms should, however, not be overlooked.

4. LASER-INDUCED FLUORESCENCE (LIF)

Laser-induced fluorescence is one of the most widely used techniques in combustion diagnostics. This is undoubtedly due to its high sensitivity combined with its potential for two-dimensional imaging. Furthermore, a wealth of molecules, predominantly intermediate species, can be detected by LIF in combustion environments. One important advantage in comparison with absorption techniques is the good spatial resolution obtainable with LIF: typically the fluorescence intensity originating from a small observation volume (< 1 mm^3) is monitored at right angles with respect to the laser beam direction. Compared to special non-linear techniques for the detection of radicals—such as electronically resonant CARS (see Section 4.5) or degenerate four-wave mixing, DFWM (see Section 6.3)—LIF experiments and data evaluation procedures are quite simple; they require neither multiple laser beams nor complex theoretical treatment.

Several aspects of LIF relevant to combustion measurements will be discussed in the following sections. As a short introduction to LIF, the qualitative and quantitative detection of various radical species in flames will be reviewed. This will be followed by several individual sections on the importance of collision processes for LIF measurements, on saturated LIF techniques, on temperature determination with LIF and on the potential of different variants of LIF for measurements in high-pressure environments, in comparison with alternative techniques. LIF imaging experiments will be covered in Section 6.2.

4.1. General Aspects

Fluorescence is often understood as an absorption process followed by light emission. The energy level diagram in Fig. 4 summarizes the important processes here for the OH radical. By absorption of a photon of suitable energy, an excited energy level is populated, and light is emitted at the same and different wavelengths according to selection rules for allowed transitions. This radiative decay, termed spontaneous emission, competes with stimulated emission, collision processes and in some cases, predissociation. In typical LIF experiments, light emitted
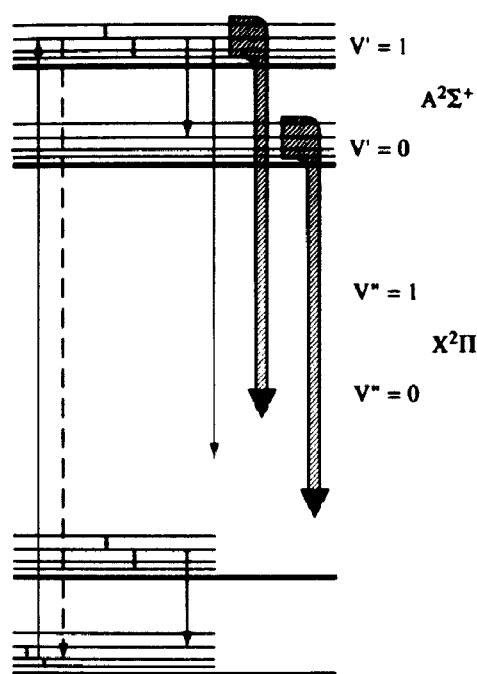
FIG. 4. Schematic energy level diagram for the OH radical. Excitation in the (1,0) transition of the A-X system is shown (upward arrow) along with the relevant depopulation processes (downward arrows), including stimulated emission (dashed), rotational energy transfer (short bidirectional arrows), vibrational energy transfer (short arrows), electronic quenching (long arrows) and spontaneous emission (hatched arrows). Broadband detection in the (0,0) and (1,1) bands is assumed.

either from a single quantum state or broadband radiation originating from a variety of states (as shown in Fig. 4 by the broad arrows) is detected. The fluorescence intensity provides information on the concentration of the emitting species. For quantitative interpretation, all competing depopulation processes need to be considered.

4.1.1. Qualitative detection of radicals with LIF

A prerequisite for the detection of a radical with LIF is a known absorption and emission spectrum in accessible wavelength ranges. Most electronic transitions for small molecules are found in the visible or ultraviolet spectral range. In special cases, e.g. for the detection of light atoms, excitation with vacuum UV radiation is required. Since this is often not possible in combustion environments, simultaneous excitation by more than one photon may offer a solution (see Section 5). Almost all important 2-, 3- and 4-atom molecules in combustion chemistry that consist of H, O, C, N and S have, besides these atoms themselves, already been detected by LIF, and many of these measurements have been made in flames.[123] Quantitative information is not always necessary. For example, LIF may be used to follow the progress of an elementary reaction or to monitor the dynamic behavior of specific quantum states, thus gaining insight into chemical mechanisms or into the formation and destruction of chemical

bonds. The review articles of Hack[124] and Wolfrum[125] describe related studies.

Spatially-resolved detection of a particular radical in specific combustion zones may yield valuable information, as detailed by Crosley.[123] Jeffries and Crosley[126] have observed the NS radical by LIF in various flames and have concluded from the shape of the measured NS profiles and from a concentration estimate that NS may form a link between the reactions of fuel-bound sulfur and nitrogen. Anderson et al.[94] have applied LIF of NH to investigate several flames burning with H_2 or CH_4 as fuels, and air, N_2O or NO as oxidizers. They found enormous differences in the NH concentrations. For example, NH was observed in flames with N_2O oxidizer in concentrations of about 5 orders of magnitude above equilibrium, whereas NH could not be detected at all in the other flames. Due to this large effect, some conclusions on potential reaction mechanisms were obtained without accurate, absolute NH concentration measurements. Similar concepts were pursued by Zabarnick[127,128] as well as Branch et al.,[129] who measured a variety of relative radical concentration profiles in different low-pressure flames in order to examine flame chemistry mechanisms. For most radicals with three or more atoms, quantitative detection is difficult because of the large number of quantum states and the lack of complete spectroscopic information. However, merely detecting their presence in particular regions of a flame may allow comparisons with model predictions.

4.1.2. Quantitative determination of radical concentrations in flames

For the examination of chemical-kinetic models, accurate radical concentration measurements are preferable. The concentration can be deduced from the measured fluorescence signal. Regarding the simplest case of a two-level system with the quantum states m and n, the fluorescence intensity I_{fl} and the number density in the excited state N_n are related by

$$I_{fl} = A_{nm} h \nu_{nm} (\Omega/4\pi) V N_n \qquad (3)$$

where A_{nm} is the Einstein coefficient for spontaneous emission, h is Planck's constant, ν_{nm} is the frequency of the emitted radiation, Ω is the detection solid angle and V is the observation volume. Under typical combustion conditions, however, a large number of quantum states populated by collision processes will be involved in the generation of the observed fluorescence signal. A general equation for the evaluation of the concentration from multi-level systems can thus not be given, since this relation would depend on the spectroscopic and dynamic features of the molecular system as well as on the experimental procedure.

In particular, experimental parameters which are of importance for the evaluation of LIF experiments include observation volume, solid angle and detec-

tion efficiencies of filters, monochromators, photo-multipliers or cameras, and the power density, spectral profile and pulse duration of the laser radiation. In addition, spectroscopic parameters such as transition probability, absorption lineshape and fluorescence quantum yield are of influence. The latter quantity represents the ratio of the number of spontaneously emitting molecules to the total number of excited molecules. Furthermore, polarization of the fluorescence may have to be considered,[130,131] especially under low-pressure conditions. Using suitable calibration techniques, most of the required information is obtained without difficulty and with good accuracy for the particular experimental situation. However, the determination of the fluorescence quantum yield may pose a problem. Besides collision processes, stimulated emission or predissociation may compete with spontaneous emission; it may be advantageous to make them the dominant loss processes from the excited state, as will be discussed later in this chapter.

Collision processes influence the fluorescence intensity and spectral distribution, and for excitation with a pulsed laser, they also affect the temporal decay of the fluorescence. Pressure, temperature and chemical composition at the observation volume determine the local collision efficiency and are thus of influence on the fluorescence quantum yield. In flames where cold zones of unburnt fuel and oxidizer may exist in close vicinity to hot, burnt gases, the fluorescence quantum yield may vary drastically with position, thus rendering quantitative LIF measurements in such environments problematic.

Several strategies have been proposed to facilitate the quantitative interpretation of LIF signal if the quantum yield is not precisely known. It has been mentioned before that it may be advantageous to calibrate fluorescence measurements with absorption measured under the same conditions. Alternatively, the influence of collisions can be estimated if the gas composition and the (temperature-dependent) collision efficiencies for the dominant collision partners are known. This approach was followed by Bechtel and Teets[92] and Morley.[132,133] However, accurate measurements then require a large amount of information on the flame chemistry as well as on the collision processes of the detected radical; the availability of such data is limited, but is rapidly improving as detailed in Section 4.2.

To unambiguously determine the influence of collisions, it is recommended, whenever possible, to measure directly the temporal evolution of the fluorescence signal, as was demonstrated by Stepowski and Cottereau.[134] For low-pressure conditions, commonly available laser systems with nanosecond pulse lengths allow for sufficient temporal resolution; at atmospheric pressure and above, picosecond laser pulse lengths are required. Several authors[135-141] have measured effective fluorescence lifetimes, particularly for the OH radical, in atmospheric pres-

sure flames. Effective fluorescence lifetimes of CO in atmospheric pressure flames have been reported by Agrup and Alden.[142] In the recent experiment of Dreizler et al.,[141] picosecond temporal resolution was combined with spatial resolution along a line. The time-resolved measurements largely confirmed predicted effective lifetimes, which were obtained from (calculated) gas compositions and measured quenching coefficients. Direct measurements of fluorescence lifetimes in flames at higher pressures are not known to the author.

Alternative strategies for quantitative concentration measurements with LIF aim at reducing the influence of collisions. This is achieved by choosing the experimental conditions in such a way that quenching is not the dominant loss process from the excited level. For the so-called saturated fluorescence technique, this is done by enhancing the influence of stimulated emission. The method has been applied by various groups; a more detailed discussion is given in Section 4.3. Another possibility to reduce the sensitivity of the fluorescence signal to collisions is to excite predissociative states. Laser-induced predissociative fluorescence (often abbreviated LIPF), based on the work of Massey and Lemon,[143] was demonstrated by Lee et al.[144] and Andresen et al.[145,146] and has been widely used since. Some typical applications will be discussed in Section 4.5. Whereas saturated fluorescence intensities are very high, predissociation leads to a decrease in fluorescence intensity; the signal loss may, however, be compensated in part with higher excitation power densities. With both approaches, quantitative concentration measurements in atmospheric pressure flames have been demonstrated with some potential for application at higher pressures.

4.1.3. Detection of the OH radical in flames

A large number of combustion studies with LIF have reported detection of the OH radical. OH is an important intermediate in hydrocarbon oxidation and is present in most flames in relatively large concentrations. Its spectroscopy is well known, and a large database on its collisional behavior is available. Therefore, quantitative interpretation of OH LIF measurements is more easily achieved than for most other radicals. The current status of OH detection in typical combustion environments is illustrated in Fig. 5. OH has been detected by laser-induced fluorescence in flames with pressures ranging from about 0.01 to 30 bar. Experimental procedures are listed in the rectangular boxes and motivations of various studies are given in the oval boxes. The lines connecting the boxes show which techniques have predominantly been applied under specific conditions. For example, single-pulse point-wise OH detection with linear LIF has been used to obtain statistical information on turbulent flames at atmospheric pressure; single-pulse 2D imaging of OH by LIF or
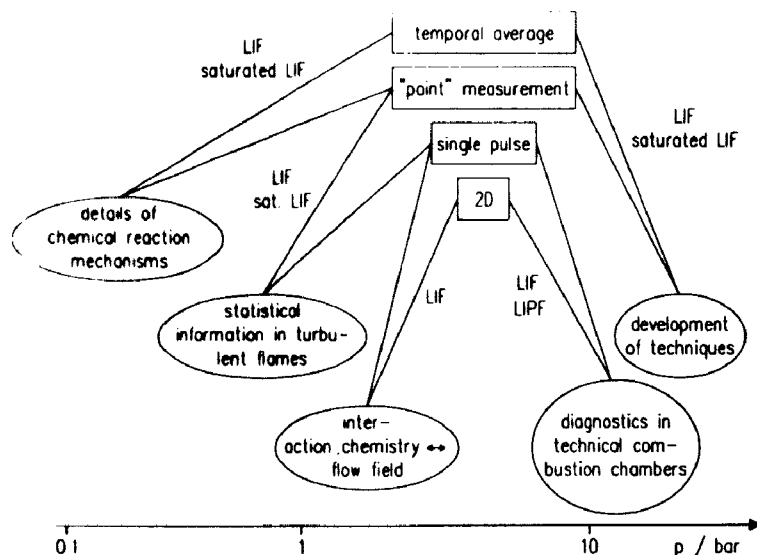
FIG. 5. Current status of OH detection in typical combustion environments. The pressure range in which OH LIF is regularly used is illustrated by the x-axis. Measurement procedures are given in the rectangular boxes, motivations for corresponding experiments in the oval boxes. Connecting lines represent typical OH LIF investigations. As an example for the interpretation of this schematic representation, single-pulse two-dimensional LIF has been used in turbulent flame experiments at atmospheric pressure to study flow field-chemistry interaction.

LIPF has been employed in investigations of practical combustion processes at pressures of 1–10 bar and above.

Most OH concentrations measurements have been performed in laminar, premixed, flat flames at sub-atmospheric pressure. Examples are found in some studies which have already been mentioned as well as in the articles of Anderson et al.[94] and Kaiser et al.[96] Laurendeau and Goldsmith[147] have compared five different approaches for the detection of the OH radical with LIF. In our own work,[148] we have discussed various aspects of quantitative OH LIF detection in low-pressure flames. Furthermore, a variety of studies have used saturated LIF of OH for quantitative concentration measurements.

LIF can also be applied to study various aspects of technical combustion systems. Such experiments yield information on the chemistry and structure of turbulent diffusion flames, mixing processes, ignition, flame propagation and local flame extinction. Azzazy and Daily[149] have measured probability density functions of the OH concentration in a turbulent methane flame. Lucht et al.[150] and Drake et al.[151] have measured absolute OH concentrations in turbulent hydrogen diffusion flames by saturated LIF. Barlow et al.[152,153] have investigated turbulent jet flames with several laser diagnostic techniques including quantitative OH detection by LIF. The calibration of the OH fluorescence signals relied on simultaneous measurements of the chemical composition with spontaneous Raman spectroscopy, tabulated quenching coefficients and LIF measurements under comparable conditions in a flame of known OH concentration. Several similar applications of LIF in

combination with Raman and Rayleigh measurements have been published by the same group, one of the more recent studies being that of Masri et al.[154] A similar concept has been pursued by Cheng et al.[155] as well as in the recent investigations of Barlow and Carter[156] and Carter and Barlow,[157] where OH and NO are quantitatively detected in conjunction with the measurement of stable species concentrations and temperature. Combinations of two-dimensional LIF and single-pulse multiple-species Raman measurements have been reported by Stårner et al.[158] and in the joint studies of Meier et al.[159] and Prucker et al.[160] Smyth et al.[161] and Smyth and Tjossem[162] describe quantitative OH concentration measurements in laminar diffusion flames. In their studies, too, LIF was combined with several other diagnostic techniques. This work is reviewed and compared with flame model computations in the recent article of Norton et al.[163] Lucht et al.[93] and Puri et al.[164] have measured OH concentrations in sooting flames at atmospheric pressure. Cattolica and Schefer[165] have determined the OH concentration in the vicinity of a hot plate. Similarly, Pfefferle et al.[166,167] and Griffin et al.[168] have detected OH near catalytic surfaces. Berglind and Sunner[169] have used OH LIF in order to characterize the ignition of methane/air mixtures. Various groups have studied internal combustion engines with the aid of two-dimensional LIF techniques; examples will be given in Section 6.2.

4.1.4. Detection of molecules other than OH

A variety of radicals, in particular diatomic species, have been detected in flames using LIF; how-
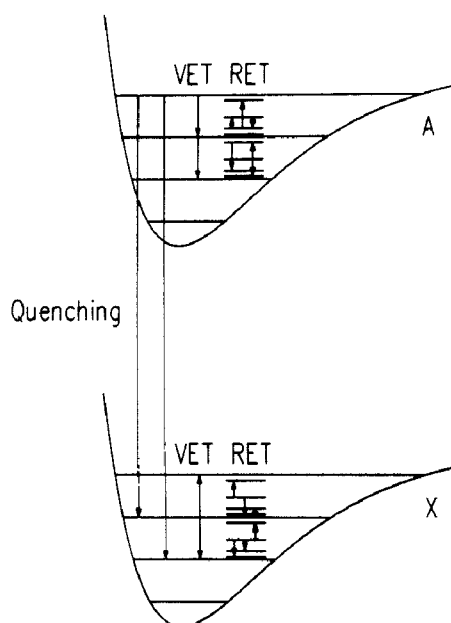
FIG. 6. Schematic energy level diagram illustrating different inelastic collision processes of relevance for LIF detection of OH: electronic quenching, vibrational energy transfer (VET) and rotational energy transfer (RET).

ever, absolute concentrations have been determined in only a few of these investigations. Some examples besides those already cited before shall be given. Fujiwara et al.[170] have detected OH, CH, C_2 and CN in flames. In a recent study investigating prompt NO formation, Heard et al.[171] have measured concentrations of OH, CH and NO in low-pressure methane/air flames. Filseth et al.[172] and Cattolica et al.[173] reported detection of CH, and Puechberty and Cottereau[174] and Vanderhoff et al.[175] detected the CN radical. C_2 was detected by Vanderhoff et al.,[176] NH_2 by Wong et al.[177] and Copeland et al.,[178] NCO by Anderson et al.[107] and Copeland et al.[178] Several sulfur-containing radicals were monitored by Muller et al.[179] Recently, HCO^{180} and $^1CH_2{}^{181}$ have been detected in flames. Furthermore, LIF detection of the C_2H radical has been achieved by Hsu et al.[182] in a photolysis reactor. Various stable molecules of importance in combustion have also been observed by LIF. Detection of NO and/or NO_2 has been reported for example by Barnes and Kircher,[183] Grieser and Barnes,[184] Chou et al.,[95] Cole and Swords[185] and Cattolica.[186] In the latter investigation, NO_2 was used as an indicator of cold, unburnt zones in jet flames since this species is consumed rapidly by H atoms produced in the reaction zone. Recently, Harrington and Smyth[187] have achieved detection of nascent formaldehyde in flames by LIF and Williams and Fleming[188] have detected CH_3O in $CH_4/O_2/N_2O/N_2$ flames by LIF. Broadband fluorescence of larger hydrocarbons has been monitored by Fujiwara et al.,[189] Miller et al.,[190] Beretta et al.[191] and Cignoli et al.[192]

4.1.5. Influence of temperature and pressure on LIF investigations

The quantitative detection of radicals by LIF should not be viewed as independent from an accurate temperature measurement. Temperature is an important quantity, since density, Boltzmann fractions and collision efficiencies are temperature-dependent, and also because accurate temperature data is often needed for computer simulations of the combustion process. Although CARS is one of the most established laser-diagnostic techniques for measuring temperature,[2] it may be advantageous to determine the local temperature in conjunction with radical concentrations using the same LIF apparatus. Also, LIF offers the potential for instantaneous two-dimensional temperature measurements.

The application of LIF to high-pressure combustion environments is a rapidly developing area of research. Limitations are imposed by the loss of fluorescence intensity caused by quenching and collisional broadening, and increasing number densities may lead to optical thickness of the medium under study. More detailed discussions of the use of LIF for temperature measurements and of the perspectives of accurate concentration measurements with LIF in high-pressure systems are found in Sections 4.4 and 4.5, respectively. Some related aspects have also been treated in detail in the literature.[5,14,148,193-195]

4.2. Collision Processes

The fluorescence quantum yield is one of the most important quantities necessary for the determination of concentrations and temperatures from measured fluorescence signals. For a given LIF experiment, it is dependent on pressure, temperature and chemical composition at the measurement location. Also, the quantum yield may vary with the quantum state of the radical. Different types of collision processes influence the fluorescence signal and quantum yield; this is illustrated schematically in Fig. 6. The excited level in the electronic state can be depopulated by electronic quenching, vibrational energy transfer (VET) and rotational energy transfer (RET). Quenching is commonly understood as collisional deactivation to a lower electronic state, whereas VET and RET denote collisional transfer to different vibrational or rotational levels* in the same electronic state. In a typical LIF experiment—for example the measurement of OH concentrations by excitation of a single line in the (1,0) band of the $A^2\Sigma^+$-$X^2\Pi$ transition and detection of the broadband fluorescence in the combined (1,1) and (0,0) bands—several vibrational states and a multitude of rotational levels (each with two fine structure levels corresponding to

---

*In this work, collisional energy transfer between different fine structure levels is also termed RET.
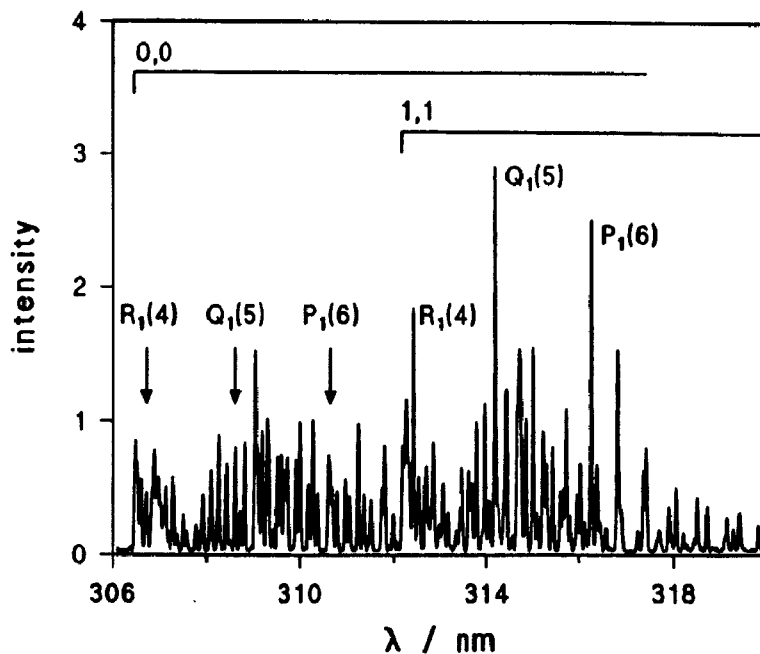
FIG. 7. OH fluorescence spectrum following excitation of the $Q_1 5$ line in the A-X (1,0) band in a CH_4/air flame at atmospheric pressure.

opposite spin components) are populated and contribute to the fluorescence signal (see Fig. 7). The transfer of energy between these levels is described by a large number of rate coefficients which are dependent on collision partner and temperature. The quantitative detection of only a single radical species by LIF therefore requires an enormous amount of information on collision processes. It is evident that for most experiments, this data on the complete matrix of relevant collisional energy transfer coefficients will not be available.

Instead of measuring all necessary coefficients as a function of quantum state, collision partner and temperature, it may therefore be preferable to simulate the collisional energy transfer with an appropriate formalism in order to describe the entire matrix of energy transfer coefficients on the basis of a few measured ones. In two limiting situations, the representation of the energy transfer processes can be simplified. If electronic quenching is much faster than RET and VET, the population in the laser-excited level is 'frozen'; the fluorescence spectrum then is dominated by lines originating from this excited level. In the opposite situation (with rapid RET and/or VET), a fast redistribution of the population between neighboring states takes place; the 'memory' of the excited state is lost in the fluorescence spectrum.

In general, the time scales of electronic quenching, RET and VET are of the same order, and one of these limiting cases is not reached. Figure 7 demonstrates this for the detection of OH; the fluorescence spectrum show here was obtained following excitation of the $Q_1 5$ line in the A-X (1,0) band. Only a small fraction of the initial population remains in the laser-excited $v' = 1$, $F_1 5$ level; the corresponding fluorescence lines $R_1 4$, $Q_1 5$ and $P_1 6$ in the (1,1) band are marked in Fig. 7. Although the population in the

laser-excited state is still greatest, rotational energy transfer in the $v' = 1$ state has already populated many other levels. Also, VET to the $v' = 0$ state has taken place. In the (0,0) band emission, however, a preference for radiation from $F_1 5$ is not discernible. The rotational distributions in both vibrational states are not in equilibrium with the gas temperature.

A comprehensive model of the collisional energy transfer should be able to describe the different collision processes independently. It is therefore desirable to understand the physical principles underlying each process. Carefully selected experiments, supported by ab initio calculations whenever feasible, will prove extremely helpful in finding suitable relations for a detailed description of collisional energy transfer.

4.2.1. Electronic quenching

With respect to the detection of minority species in combustion, the most extensive data bases on electronic quenching exist for OH and NO. The results of a large number of studies on OH, covering also the quenching of some other diatomic hydrides such as NH and CH, have been reviewed by Garland and Crosley[196] and Crosley,[197] whereas quenching data for NO are compiled in the recent studies of Gray et al.[198] and Drake and Ratcliffe.[199] Different types of information are available. In several studies, rotationally averaged quenching cross sections for individual quenchers as a function of temperature in the range of about 200–1200 K have been measured. In addition, some investigations have provided rotational-state-specific cross sections for different collision partners at room temperature. Also, experiments in the burnt gas regions of flames have yielded information on the effective quenching cross sections under these conditions.
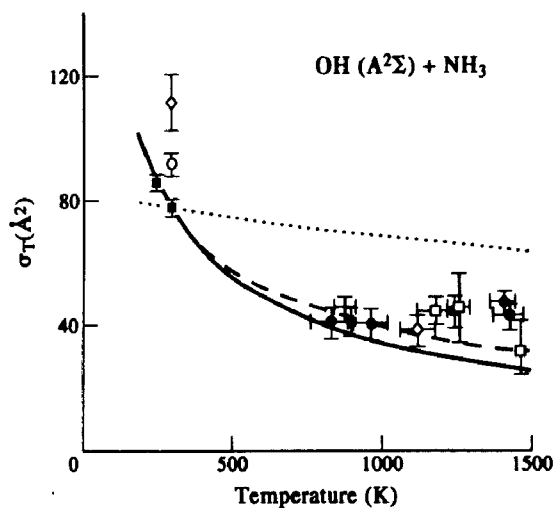
FIG. 8. Quenching cross section for OH ($A^2\Sigma^+$, $v' = 0$) with NH_3 as a function of temperature.[215] Symbols represent different experimental series, lines illustrate different models for the interpretation.

4.2.1.1. *Quenching of OH* ($A^2\Sigma^+$). Wysong et al.[200] have recently measured quenching cross sections of OH with various collision partners at room temperature; their article also reviews previous literature. McDermid and Laudenslager,[201] Copeland and Crosley,[202] Copeland et al.,[203] Papagiannakopoulos and Fotakis[204] and Cleveland and Wiesenfeld[205] have studied the dependence of the cross section on rotational level. Most results—apart from those of Papagiannakopoulos and Fotakis[204] for very high rotational levels—indicate a decrease of the cross section with increasing rotational quantum number.

Detailed information is available on the temperature dependence of the quenching cross sections of OH (A) with several flame-relevant collision partners. For example, Hooymayers and Alkemade[206] and Stepowski and Cottereau[207] have investigated OH quenching at flame temperatures with the colliders H_2O, N_2 and O_2. Also, several groups have studied quenching at flame temperatures in the burnt gases of low-pressure hydrogen flames (where H_2O is the dominant collision partner), including Jeffries et al.,[208] Cattolica and Mataga[209] and Lee et al.[210] Temperature-dependent cross sections for a variety of colliders have been obtained in a laser pyrolysis experiment by Fairchild et al.[211,212] and Smith and Crosley.[213] In most cases, a decrease of the cross section with increasing temperature was observed. This behavior was also found by Copeland and Crosley[214] in the temperature range 230–310 K. Jeffries et al.[215] have measured the cross section for quenching of OH by NH_3 in the range of 250–1400 K; as shown in Fig. 8, they observed a decrease of the cross section by a factor of 2 between 300 and 900 K and a nearly constant cross section above 900 K. Most of the results can qualitatively be represented by a mechanism based upon a long-range attractive interaction potential. In particular, a decrease of the cross section with increasing temperature is expected

for this type of interaction. For larger collider molecules, such as some hydrocarbons, steric factors may play a role;[213] simplified models of the collision dynamics are less appropriate in these cases.

Quenching of OH ($A^2\Sigma^+$, $v' = 1$) has, for example, been studied by German,[216] Copeland et al.[217] and Burris et al.[218] The cross sections tend to be of similar magnitude as those for $v' = 0$; again, a decrease of the cross section with rotational quantum number was observed. It thus seems not unlikely that similar mechanisms govern the electronic quenching of OH in both vibrational states.

4.2.1.2. *Quenching of combustion-relevant molecules other than OH.* The quenching of other diatomic hydrides has been studied in detail, partly with the intention to detect potential analogies to the quenching of OH. The recent review of Kenner et al.[219] summarizes the information on temperature-dependent quenching (in the range 240–420 K) of CH ($A^2\Delta$), NH ($A^3\Pi$), NH ($c^1\Pi$) and PH ($A^3\Pi$) and examines several models for the representation of the experimental results. Quenching of NH($A^3\Pi$) at room temperature was investigated by Hofzuma-haus and Stuhl;[220] they report slightly smaller cross sections than for OH, and a less pronounced decrease with rotational level. The results of Garland and Crosley[221] are in good agreement with this study. High-temperature quenching cross sections for NH ($A^3\Pi$) were measured by Garland et al.[222] Most recently, Chappell et al.[223] have investigated the rotational level dependence of the quenching of NH ($A^3\Pi$), and Kaes and Stuhl[224] have studied the quenching of isolated levels in NH ($A^3\Pi$) as a function of Λ doubling, spin and rotational energy. Quenching of NH ($c^1\Pi$) was investigated by Kenner et al.[225] For many colliders, essential features of the quenching behavior of NH ($c^1\Pi$) largely resemble those of OH ($A^2\Sigma^+$). This is true in particular for the decrease of the cross section with both temperature and rotational level.

Nokes and Donovan[226] have studied the quenching of CH ($A^2\Delta$) at room temperature, and Garland and Crosley[227] have performed high-temperature quenching measurements for this radical. Also, Garland and Crosley[228] have measured the ratios of electronic quenching, VET and RET for CH ($A^2\Delta$) and CH ($B^2\Sigma^-$) in atmospheric pressure methane flames. In contrast to the behavior observed for OH ($A^2\Sigma^+$) and NH ($A^3\Pi$), the cross sections for electronic quenching of CH ($A^2\Delta$) increase with rotational level for most colliders. Some recent information is available on the quenching of NH_2, HCO and NO. Wysong et al.[200] have measured rotational-level-dependent quenching of NH_2 ($\tilde{A}^2A_1$) by He and N_2. Meier et al.[229] have reported quenching coefficients for HCO ($\tilde{B}^2A'$) with a variety of collision partners.

Raiche and Crosley[230] have investigated quenching of the ($A^2\Sigma^+$) and ($B^2\Pi$) states of NO. Furthermore, quenching of the NO ($A^2\Sigma^+$, $v' = 0$) state has
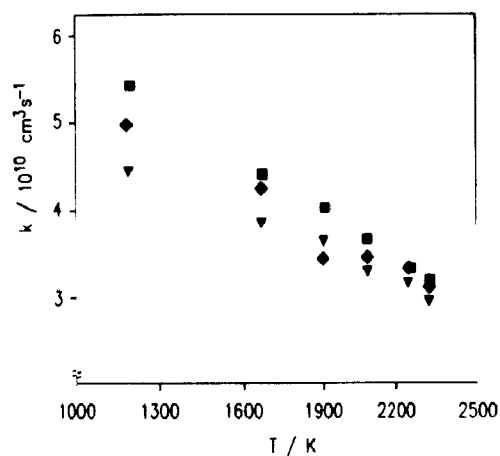
FIG. 9. Effective fluorescence decay rates for different rotational states of OH ($A^2\Sigma^+$, $v' = 0$) at elevated temperatures.[208] Squares: $N' = 3$, diamonds: $N' = 8$, triangles: $N' = 16$.

been studied by Cattolica et al.[231] and Heard et al.[232] Quenching coefficients for the $v' = 1$ state were measured by Burris et al.[233] for N_2 and O_2 as collision partners. Drake and Ratcliffe[199] have provided a detailed data base for quenching of NO ($A^2\Sigma^+$). Recently, high-temperature quenching cross sections for NO ($A^2\Sigma^+$) have been measured for N_2 as collision partner by Meier et al.[234] and for He, Ar, NO and CO_2 as colliders by Gray et al.[198] Thoman et al.[235] have studied the temperature dependence of the quenching of NO ($A^2\Sigma^+$) by N_2. With the model described by Paul et al.,[236] which is based upon the assumption of a curve-crossing or 'harpoon' mechanism, magnitude and temperature dependence of the measured quenching cross sections for NO ($A^2\Sigma^+$) and several colliders could be represented quite successfully; it should not be forgotten, however, that the calculations must be normalized to an experimental value, usually that at room temperature is chosen. Most recently, a similar modelling approach has been used to describe OH quenching.[237]

4.2.1.3. *Quenching and effective decay rates in flames.* Information on the variation of collisional deactivation of the excited level with stoichiometry or with chemical composition and temperature throughout the reaction zone is of considerable significance for the interpretation of two-dimensional LIF measurements in turbulent flames. With the tabulated quenching cross sections of Garland and Crosley,[196] collisional decay rates—or effective lifetimes—may be calculated for many flame conditions for which temperature and chemical composition are known. In most situations, this leads to an accuracy of about 30% in OH concentration. The calculated decay rates for OH can be compared with the experimental results of Jeffries et al.,[208] Kohse-Höinghaus et al.[148] and Lee et al.[210] in low-pressure flames. A decrease of the decay rates with increasing height above the burner has been observed in these flames; as an example, Fig. 9 displays the results of

Jeffries et al.[208] in a low-pressure H_2/N_2O flame. Measurements of OH lifetimes in flames at atmospheric pressure were performed by Schwarzwald et al.,[137,138] Köllner et al.[140] and Dreizler et al.[141] Garland and Crosley[196] have noted that data is more limited for NH and CH. More recently, Rensberger et al.[238,239] and Copeland et al.[240] have measured decay rates for NH ($A^3\Pi$), CH ($A^2\Delta$) and CH ($B^2\Sigma^-$) in flat low-pressure flames. With increasing distance from the burner surface, a decrease in decay rate was observed for NH, whereas an increase was noted for CH. The dependence on stoichiometry was small in all cases.

For other radicals and small molecules of interest in combustion, data on quenching in flames is even more scarce than for the diatomic hydrides. Some information, mostly in the burnt gas of atmospheric pressure flames, is available from the lifetime measurements of Schwarzwald et al.[138,139] for CN and NO, respectively. Recently, Agrup and Aldén[142] have measured the lifetime of CO ($B^1\Sigma^+$) in the reaction zone of an atmospheric pressure CO/air flame. It should, however, be noted, that in all investigations listed above, electronic quenching is not observed as an isolated process. Rotational relaxation influences the measured decay rates or lifetimes to an amount which cannot be determined easily, because several energy levels are involved besides the laser-excited state.

Some features of electronic quenching processes remain largely unexplored, even for the often-studied OH radical. For example, more information is needed on the rotational level dependence of quenching as a function of temperature. A pioneering study of this relation for the OH radical is that of Jeffries et al.[208] Also, quenching by radicals has seldom been investigated. H atoms, for example, may be very abundant in low-pressure hydrogen flames and may contribute significantly to the effective decay rate. The high temperature cross section for OH quenching by H atoms estimated in the work of Jeffries et al.[208] is in good agreement with the room temperature value of Becker et al.[241] Almost no information exists on the vibrational (and rotational) distribution in the electronic ground state generated by electronic quenching. Although knowledge on product state distributions is essential for the quantitative interpretation of saturated LIF measurements in flames at atmospheric or higher pressures (see Section 4.3), the only studies addressing this question known to the author are those of Crosley and Copeland[242] on the OH ($X^2\Pi$) state following quenching from the OH ($A^2\Sigma^+$) state and of Meier et al.[243] on NO ($X^2\Pi$) following quenching from NO ($A^2\Sigma^+$). Quantitative information has not been published on this subject; from these preliminary results it appears, however, that quenching is not necessarily governed by Franck-Condon rules. Although not in quantitative agreement with the measurements of Meier et al.,[243] a more recent,

unpublished study has confirmed the result that high vibrational levels are populated.[244] Similar observations have recently been made for OH quenching by the same group.[244]

While the existing data base on electronic quenching of some important combustion-relevant radicals and molecules is already large enough to permit quantitative interpretation of measured LIF signals under many combustion conditions, details of the molecular dynamics of the quenching process remain largely unclear. For some radical-collider pairs, the observations seem to be consistent with a simplified attractive forces interaction model, in particular for collisions of the OH radical. Expectations that a similar approach would at least be generally applicable for diatomic hydrides have, however, been unrealistic. Reliable predictions of the magnitude, level and temperature dependence of electronic quenching for a specific radical-collider pair cannot be made without a solid foundation in either experimental data or quantum mechanical calculation.

4.2.2. Vibrational energy transfer (VET)

Vibrational energy transfer is a very complex process which cannot be generally treated by a simple physical model. A detailed discussion of VET is beyond the scope of this paper. The purpose of this section is, however, to compile the existing experimental data on VET of several diatomic radicals important for combustion. Several physical processes are summarized under the term 'vibrational energy transfer', and this renders its description even more complex than that of RET. These processes are distinguished by their final states as $V \rightarrow V$, $V \rightarrow R$ and $V \rightarrow T$ transfer, depending on whether the energy is transferred to vibration, rotation or translation of the collider, respectively. All these processes may appear in combination so that both target molecule and collider may experience changes in vibrational, rotational and translational energies as a result of the collision.

Several simplified models allow representation of VET in special cases. Some account only for attractive parts of the interaction potential, some only for the repulsive ones. However, they are in general not capable of describing the transfer of more than one vibrational quantum nor the dependence of the VET cross section on rotational state. Apart from some data for NO (including those of Cattolica et al.[231]), information on VET of combustion-relevant radical species exists mainly for OH. The experiments described in the literature do not distinguish between $V \rightarrow V$, $V \rightarrow R$ and $V \rightarrow T$ processes.

Lengel and Crosley[245,246] have studied VET of OH ($A^2\Sigma^+$). They have—similar to electronic quenching—observed a decrease in VET cross section with increasing rotational quantum number N'. Their results agree well with those of German.[216]

Smith and Crosley[247] have also noted a decrease of the cross section with N' in flame experiments. Copeland et al.[217] have investigated VET and quenching of OH ($A^2\Sigma^+$, $v' = 1$) with several colliders. They distinguish three types of collision partners: strongly polar ones such as H_2O and NH_3, which cause rapid quenching but inefficient VET; inert colliders such as N_2, CF_4 and SF_6, which exhibit the opposite behavior; and other molecules such as CO_2, N_2O and CH_4, where VET and quenching cross sections are of similar magnitude.

In addition, VET in the OH ($X^2\Pi$) state has recently been studied. Rensberger et al.,[248] Raiche et al.[249] and Dodd et al.[250] have investigated the vibrational energy transfer in OH ($X^2\Pi$, $v'' \leq 3$) with different collision partners and have measured cross sections that were in general about two orders of magnitude smaller than those for the OH ($A^2\Sigma^+$) state. For high vibrational levels in OH ($X^2\Pi$), Sappey and Copeland[251] have reported VET cross sections which are between those for the OH ($A^2\Sigma^+$) state and those for the lower vibrational levels in the OH ($X^2\Pi$) state. For OH ($X^2\Pi$, $v'' = 12$) the cross sections are more than a factor of 50 larger than those for $v'' = 1$ or 2, but still smaller than those for OH ($A^2\Sigma^+$). This difference in collision efficiency between the two electronic states cannot be a function of internal energy alone, since the energy difference between $X^2\Pi$, $v'' = 12$ and $A^2\Sigma^+$, $v' = 0$ is only about 750 cm^{-1}, less than a vibrational quantum.

Some further observations will be briefly reported. Cross sections for VET in OH ($A^2\Sigma^+$) are quite large. Smith and Crosley[247] have noted that part of the transferred energy following VET in OH ($A^2\Sigma^+$) appears as rotational energy. Cross sections for transfer of several vibrational quanta ($v' = 2 \rightarrow v' = 0$) in OH ($A^2\Sigma^+$) are of similar magnitude to those for single-quantum transfer ($v' = 2 \rightarrow v' = 1$), according to Lengel and Crosley.[246] Colliders with similar degrees of freedom may have very different VET behavior.[217] The dependence of the VET cross section on rotational quantum number is quite similar for different vibrational levels in the OH ($A^2\Sigma^+$) state.[246]

It is very difficult to arrive at general conclusions concerning VET in OH from the rather small number of studies. Considering the large differences in the measured cross sections, the mechanism for VET in the electronic ground state of OH seems to be significantly different from that for VET in the OH ($A^2\Sigma^+$) state. Details in the VET behavior of the two electronic states may only be understood on the basis of the interaction potentials for corresponding radical-collider pairs. Although results on OH in particular should not be generalized, the conclusion seems permitted that many features of detailed, state-specific vibrational energy transfer for combustion-relevant molecules are still not fully understood.

4.2.3. Rotational energy transfer (RET)

State-specific rotational energy transfer has been investigated with several different methods for a variety of diatomic molecules such as alkali dimers, alkali hydrides and halogen compounds; however, a comparatively poor database exists for radicals of interest in combustion. An excellent overview by Dagdigian[252] reviews most of the related experiments. For example, RET in the electronic ground state of NO has been studied by Sudbo and Loy.[253,254] Smith and Johnson[255] and Imajo et al.[256] have measured rate coefficients for RET of NO ($A^2\Sigma^+$) with He and Ar as collision partners. RET in NO ($A^2\Sigma^+$) has also been studied by Broida and Carrington[257] and Ebata et al.[258] From fluorescence spectra of CH ($A^2\Delta$) measured in low-pressure flames, Cattolica et al.[173] and Joklik and Daily[259] have deduced ratios of total RET* and quenching for different initial levels. Both groups observed that RET is faster than quenching by about a factor of 3–4 under these conditions. Dixon et al.[260] have studied RET of CH ($A^2\Delta$) at room temperature with He as collision partner; the RET coefficients are especially large for transfer with $\Delta N = \pm 1$, they decrease as a function of the transferred energy and thus may be represented with a simple model. In a recent article, Dagdigian[261] reports the investigation of RET in NH ($X^3\Sigma^-$).

Carrington[49] was the first to study the population distribution in OH ($A^2\Sigma^+$, $v' = 0$) after excitation of a selected rotational line; for this measurement, the accidental coincidence of the $R_2 10$ transition with a bismuth resonance line was exploited. Cross sections for total RET of OH ($A^2\Sigma^+$, $v' = 0$) with colliders Ar and N_2 have been measured by Stepowski et al.[262] and, for H_2O as collision partner, by Lucht et al.[263] Burris et al.[218] have studied total RET in OH ($A^2\Sigma^+$, $v' = 1$) with colliders O_2 and N_2 at room temperature, and a similar investigation for OH ($A^2\Sigma^+$, $v' = 0$) has been performed by Burris et al.[264] Andresen et al.[145] have measured the rotational distribution in OH ($A^2\Sigma^+$, $v' = 3$) after excitation of a single rotational level. Because of the very short lifetime of this predissociative state, the authors find, even in an atmospheric pressure H_2/O_2 flame, that most of the fluorescence originates from the initial level. Under their conditions, a strong tendency for symmetry conservation ($F_2 \rightarrow F_2$ and $F_1 \rightarrow F_1$) was noted. Similar observations were made by Crosley and Smith[265] in the burnt gases of a CH_4/air flame, whereas Anderson et al.[266] have found no indication for this behavior in a CH_4/N_2O flame. Lengel and Crosley[267] have performed a de-

tailed study of rotational energy transfer in OH ($A^2\Sigma^+$, $v' = 0$). In their experiment, state-specific RET coefficients for Ar, N_2 and H_2 were obtained from fluorescence spectra. However, since the fluorescence was not time-resolved, corrections for multiple collisions were necessary.

At DLR, we have developed a method for the determination of state-specific RET coefficients[268,269] which combines high temporal and spectral resolution. Each individual RET coefficient is determined from a pair of time-resolved single-line fluorescence signals, one of them arising from the laser-excited level, the other from a level populated by collisions. The influence of multiple collisions can be accounted for by using an extrapolation technique. In a series of investigations, RET coefficients at 300 K for a variety of initial levels and collision partners have been obtained with this method. At first, the applicability of the method was examined for OH ($A^2\Sigma^+$, $v' = 0$) and He and Ar as collision partners.[269] Most interestingly, the RET caused by the two rare gases was observed to be strikingly different. The RET coefficients with Ar as collision partner are largest for $\Delta N = 0$, $\Delta J = \pm 1$ and decrease monotonically with transferred energy, while those for collisions with He exhibit a strong tendency for symmetry conservation; for He, the largest measured RET coefficient occurs for $\Delta N = \Delta J = -2$ transfer.[269] The recent quantum mechanical calculations of Jörg et al.[270] for RET of OH ($A^2\Sigma^+$) with He and of Degli Esposti and Werner[271] for RET of OH ($A^2\Sigma^+$) with Ar are in excellent agreement with these measurements, showing that differences in the interaction potentials are the cause of the variation in the RET behavior.

In subsequent experiments, we have measured RET coefficients at 300 K for OH ($A^2\Sigma^+$, $v' = 0$) and the combustion-relevant collision partners N_2, CO_2 and H_2O[272] and for OH ($A^2\Sigma^+$, $v' = 1$) with He, Ar, N_2, CO_2 and H_2O.[273] Some of the results are displayed in Fig. 10. For two different excited levels, $F_2 4$ and $F_2 5$ in $v' = 0$, the RET coefficients for N_2, CO_2 and H_2O are shown as a function of final state rotational quantum number, N'; the length of each bar corresponds to the magnitude of the specific RET coefficient. For each N', the coefficients for symmetry-conserving collisions ($F_2 \rightarrow F_2$) are displayed on the left and those for symmetry-changing collisions ($F_2 \rightarrow F_1$) on the right. The RET behavior is quite different for the three colliders. On average, RET is most efficient with H_2O as collision partner. Whereas both H_2O and N_2 show a propensity for symmetry conservation, this is not observed for CO_2. Interestingly, the RET coefficients for corresponding transitions in collisions with CO_2 are almost identical with those for Ar.[272] For the five collision partners investigated, the RET coefficients in OH ($A^2\Sigma^+$) $v' = 0$ and $v' = 1$ states are very similar.[273]

Detailed information is also available on the rotational energy transfer of specific levels in the elec-

---

* Here, total RET is the sum of all RET processes from a specific rotational or fine structure level; in contrast, state-specific RET denotes the transfer of energy from a fine structure component of a specific rotational state i to a fine structure component f of the same or a different rotational state.
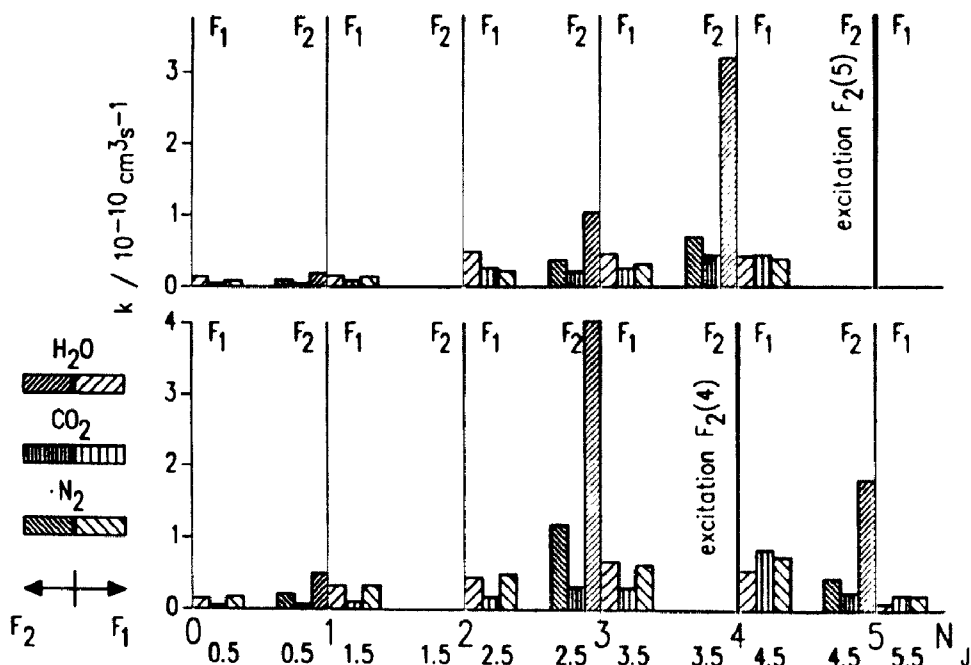
Fig. 10. Rate coefficients for rotational energy transfer of OH $(A^2\Sigma^+, v' = 0)$ at 300 K with colliders N_2, CO_2 and H_2O.[272] Top: excitation of the $F_2 5$ level, bottom: $F_2 4$ excitation.

tronic ground state of the OH radical. Gericke and Comes[274] have measured RET coefficients at 300 K for OH $(X^2\Pi)$ with Ar and H_2O as collision partners. Copeland and Crosley[275] have investigated collisions of OH $(X^2\Pi, v'' = 2)$ with H_2O at 300 K. Wysong *et al.*[276] have reported state-specific RET coefficients at 300 K for OH $(X^2\Pi, v'' = 2)$ with He. In molecular beam experiments, RET of OH $(X^2\Pi)$ has been studied with several collision partners including H_2,[277,278] H_2 and D_2[279] as well as N_2 and CO.[280] Relative parity-resolved RET coefficients for the OH $(X^2\Pi, v'' = 0, J = 3/2^+)$ state have recently been obtained by Schleipen[281] in a molecular beam experiment for He, Ar and H_2 as collision partners. Although some of these results provide a good data base for comparison with recent theoretical work, not all of them are of direct relevance for flame investigations. In a flame experiment, Zizak *et al.*[282] have measured rotational distributions in the OH ground state. They have concluded that for their acetylene flame, RET seems on average to be slightly faster in the OH $(X^2\Pi)$ state than in OH $(A^2\Sigma^+)$. In spite of the considerable experimental complexity demanded in such experiments, further systematic investigations of RET in the OH ground state would be desirable.

4.2.4. Rate equation models

Rate equation models can be used for the analysis of fluorescence signals; they describe the time-dependent populations in all relevant quantum states with a system of ordinary differential equations, accounting for radiative and collisional processes between these states. With the aid of a rate equation model, procedures for the measurement of concentration and

temperature with LIF can be developed and systematically examined with respect to accuracy and reliability. In a first approximation, reduced schemes with 2, 3 or 4 levels are used. These simple models simulate the populations in the two laser-coupled states and in one or two bath levels which may represent rotational or vibrational manifolds. Some of these simple concepts will be discussed with respect to their application in the interpretation of saturated LIF experiments (see Section 4.3).

Considering LIF detection of molecules with a large number of quantum states, it is evident that the validity of such reduced schemes (with a limited number of levels) may only be judged on the basis of more detailed models. Several multi-level approaches have been described in the literature. Chan and Daily[283] have used a set of 31 differential equations for $N' \leq 15$ of the OH $(A^2\Sigma^+, v' = 0)$ state in order to simulate fluorescence spectra. In their model, RET is represented by a relation involving an exponential dependence of the RET coefficient on the transferred energy; a similar version of this function was originally proposed by Crosley in Ref. 15 of Chan and Daily.[283] The parameters used in the model of Chan and Daily[283] are derived from the measured set of coefficients of Lengel and Crosley.[267] With this model, Chan and Daily[284] have determined the flame temperature from fluorescence spectra. Similarly, Crosley and Smith[265] have obtained temperatures from fluorescence spectra using this approach; they stress, however, that the model is not generally applicable. Also, Furuya *et al.*[285] have used the relation of Chan and Daily[283] for the evaluation of temperatures from fluorescence spectra.

Kotlar *et al.*[286] have simulated OH detection in the burnt gas of an atmospheric pressure methane

flame. In their approach, a bath level is introduced which represents all vibrational levels in the electronic ground state with $v'' > 0$. Depending on the choice of the coefficients for the collision processes, a considerable fraction of the population can concentrate in the bath level; using common relations for the interpretation of saturated LIF measurements, this effect would not be taken into account. Lucht et al.[263] have simulated fluorescence spectra measured in low-pressure H_2 O_2 N_2 flames with a multi-level model and determined total RET coefficients for OH $(A^2\Sigma^+, v' = 0)$ under these conditions.

The most detailed rate equation model for the interpretation of LIF experiments has been assembled by Campbell.[287][289] With 232 differential equations, 3 vibrational levels and a manifold of rotational levels in each of the two relevant electronic states $(A^2\Sigma^+$ and $X^2\Pi)$ of the OH radical are represented. With this model, the post-flame conditions of a methane flame have been simulated. Pressure, temperature and laser power density were varied independently, following excitation of a specific rotational level/fine-structure component in the $v' = 0$ or $v' = 1$ state. Different model assumptions on the collision processes have been examined. For electronic quenching, two limiting cases were tested; in one limit, quenching followed radiative selection rules, in the other, quenching to all final states was equally probable. RET was modelled using the relation of Chan and Daily;[283] a single set of coefficients was used for both electronic states. Deviations from a simple two-level model were used as criteria for the applicability of certain measurement procedures, such as narrowband or broadband detection schemes. As a result of the model calculations, support was found for the assumption that experimental schemes which are least sensitive to collisions are most reliable.

Since Campbell's work was published,[287-289] additional information on collisional energy transfer has necessitated improvements in rate equation modelling of LIF experiments. We have followed a similar approach[290,291] for the simulation of OH LIF experiments. The core of our rate equation model is a differential equation solver which has been adapted from a code originally developed for the simulation of large chemical kinetic systems.[292] Time-dependent energy level populations are calculated for the specified input conditions using appropriate radiative and collisional transfer rates. As long as linear excitation is assumed, only the excited electronic state needs to be modelled in detail. Typically, the model includes 51 rotational/fine structure levels (from $J = 0$ to 25) in the OH $(A^2\Sigma^+, v' = 0)$ state and two levels in the $X^2\Pi$ state, the laser-coupled level and a bath level. Collisional processes accounted for in the model include electronic quenching and RET in the excited state. Spectroscopic data have been taken from Coxon[293] and spontaneous emission rates from Trolier.[294]

Since the complete matrix of RET coefficients (on the order of a thousand coefficients for a single temperature and collision partner) is not available from experiments, an adequate numerical relation needs to be found for its representation. An overview of common scaling and fitting laws is given in the review article of Brunner and Pritchard.[295] We have used an energy-corrected sudden (ECS) scaling law, which is an adaptation of the formalisms of Alexander[296] and DePristo et al.[297] Within the ECS scaling approach, the complete set of RET coefficients can be calculated from a smaller set of coefficients (the so-called basis coefficients). For the OH $(A^2\Sigma^+)$ state, these basis coefficients can in many cases be represented by an energy-based power law, leading to the ECS/power (ECS-P) law. The three parameters required by the ECS-P law have been derived separately for each colliding species from our room-temperature RET experiments[269] and from quantum mechanical calculations.[270,271] Figure 11 demonstrates the excellent representation of the measured RET coefficients by this relation, in this case shown for collisions of OH $(A^2\Sigma^+, v' = 0)$ with H_2O at 300 K.[290] Furthermore, total RET rates for H_2O measured in a $H_2/O_2/He$ flame[210] can be accurately represented by this law. Thus, the ECS-P law can be used to model RET in the OH $(A^2\Sigma^+)$ state for a number of colliders and a wide range of temperatures and rotational levels.

In addition to state-specific RET rates, rate equation modelling requires knowledge on state-specific quenching.* Available information on electronic quenching in OH $(A^2\Sigma^+)$ has been reviewed earlier in this section. A key problem with published 'state-specific' effective collisional decay rates at flame temperatures has already been addressed in that context: measured electronic quenching rates are to a certain extent affected by RET and thus represent a weighted average over several quantum states. The rate equation model was applied in this situation to simulate measured decay rates[210] with different level dependences of collisional quenching to estimate true state-specific quenching rates. Similarly, effects caused by the variation of the spontaneous emission rate with rotational level have been examined in detail.[290]

In a further application of the rate model, the influence of the rotational level dependences of quenching and spontaneous emission on the accuracy of two-line LIF thermometry (see Section 4.4) was examined.[159,290] The model permits independent variation of important physical quantities, so that even complex experimental situations can be analyzed. In general, it was observed that RET tends to thermalize the rotational population in the OH $(A^2\Sigma^+)$ state, thus reducing but not eliminating the

---

*State-specific quenching is understood as the isolated electronic quenching process out of a single level, undisturbed by rotational redistribution.
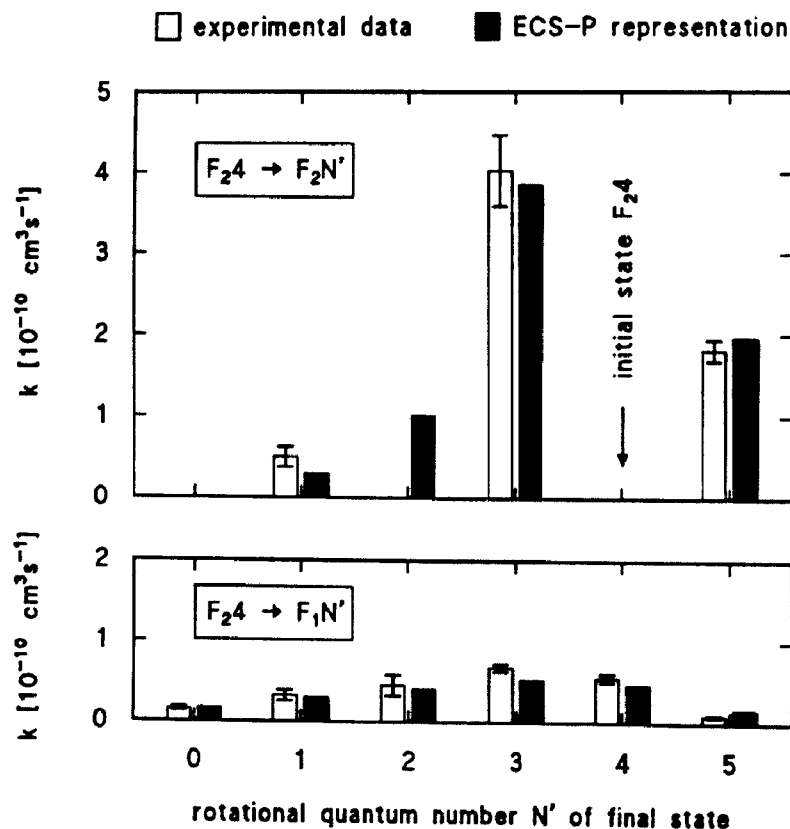
Fig. 11. Measured RET coefficients for OH $(A^2\Sigma^+, v' = 0)$ with H_2O upon F_24 excitation at 300 K, along with their representation by the ECS-P scaling relation discussed in the text.

sensitivity to variations in level-specific quenching. In particular, collisions with N_2 (for which RET is much faster than quenching) enhance this thermalization process.

The model, however, is not limited to the examples discussed here. For instance, it is likely that the RET within the OH $(A^2\Sigma^+, v' = 1)$ state can be represented in a similar fashion as RET in the $v' = 0$ level. However, more information would be desirable on the collision processes of importance, such as state-specific VET at flame temperatures, RET and VET in the ground electronic state, and product state distributions resulting from electronic quenching. With reliable experimental or theoretical data on these quantities, the rate equation model could develop into a more generally applicable and powerful tool for the design and critical examination of linear and saturated LIF experiments.

4.3. Saturated LIF

The saturated LIF technique is based upon the use of very high laser power densities in the excitation process to saturate the absorption transition. A significant fraction of the population is pumped out of the lower laser-coupled level, and stimulated emission becomes the dominant loss mechanism from the excited level. As a consequence, the fluorescence signal no longer increases linearly with increasing laser power density, but exhibits a 'saturation' behavior.

In the limit of infinitely high pump rates, the fluorescence signal becomes independent of laser power density. For the simplest case, with identical degeneracies of the two laser-coupled levels, complete saturation is reached when half of the population of the lower level is pumped to the excited state. Several characteristics of the technique are promising. In particular, the fluorescence signal is independent of collision processes at the limit of complete saturation. Also, the fluorescence signal is very large and is insensitive to variations of the laser power density— valuable features for single-pulse measurements in turbulent flames.

4.3.1. Concepts for the evaluation of saturated LIF experiments

The theoretical background of saturated LIF was originally treated by Piepmeier.[298] In a fundamental series of articles, Daily[299-302] examined the technique in detail. The essential relations have been summarized by Eckbreth.[2] After the first experimental demonstration[303] and further studies, however, it was realized that fully saturated conditions are difficult to achieve in practical experiments.* The reason

---

* In spite of the problems associated with achieving *complete* saturation, the term 'saturated LIF' is used in this article to characterize excitation conditions under which the dependence of the fluorescence intensity on the laser power density is (for single-photon excitation) less than
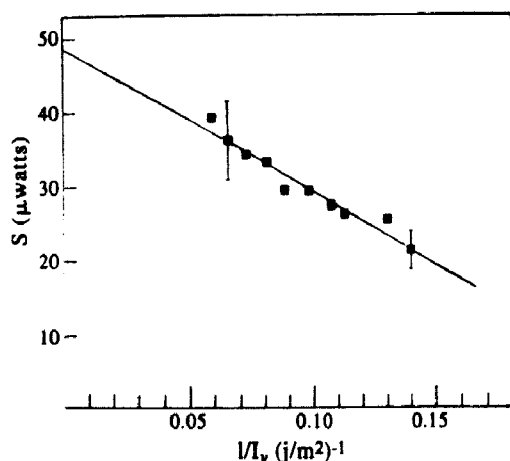
Fig. 12. Saturation curve: fluorescence intensity as a function of inverse laser intensity.[310]

for this are spectral, temporal and spatial variations of the laser intensity (so-called 'wing effects'). Since the laser intensity is not evenly distributed in the space, time and frequency domains, saturation may be achieved in some regions, but not in others, e.g. in the center, but not at the edges of the laser spatial intensity distribution. The measured fluorescence signal is the sum of the fluorescence intensities originating from each of these regions with varying degrees of saturation. Rodrigo and Measures[304] have already discussed the difficulties arising from temporally and spatially inhomogeneous laser intensity profiles.

The early measurements using the saturated fluorescence technique, including those of Sharp and Goldwasser,[305] Daily and Chan,[306] Pasternack et al.[307] and van Calcar et al.[308] aimed at detection of atoms, mainly Na, in atmospheric pressure flames. Two- or three-level rate equation models were used to interpret the results. For molecules with large numbers of quantum states, such models may, however, be inappropriate. Baronavski and McDonald[309,310] have detected the C_2 radical in acetylene flames with saturated fluorescence. They determined the C_2 concentration from a plot of measured fluorescence signal versus inverse laser intensity; an example of this is shown in Fig. 12. The concentration is obtained by extrapolating to infinite laser intensity; the slope of the plot contains information on the effective collision rate. The evaluation procedure is based upon a two-level model, and its accuracy is estimated to be a factor of three in this case.[310] Pasternack et al.[307] have examined the applicability of a two-level model for the detection of MgO in flames. Since this molecule has a low-lying electronic state which could possibly serve as bath level, it was chosen to be an ideal test case. For both Na and MgO detection, the

linear (or less than quadratic for a two-photon process etc.); to avoid confusion with fluorescence following multiphoton excitation, this expression is preferred over 'nonlinear LIF'.

results of saturated LIF and absorption measurements were compared, and they disagreed by about one order of magnitude. Similarly, Bonczyk and Shirley[311] and Verdieck and Bonczyk[312] have found large discrepancies between absorption and saturated LIF results for CH and CN. Lucht and Laurendeau[313] have simulated the detection of OH by saturated LIF with both a two-level model and a multilevel system in order to estimate the fraction of the population that remains in the laser-coupled levels. Using the detailed model, a Boltzmann population distribution (which would allow application of the simpler two-level treatment) was only found under conditions where the coefficient for total RET from the laser-excited level was a factor of 100 larger than that for quenching; this assumption is quite unrealistic for OH. For the measurement of molecular concentrations with saturated LIF in atmospheric pressure flames, the simple two-level approach was therefore abandoned.

Berg and Shackleford[314] have used a four-level model to analyze saturated LIF measurements; two laser-coupled levels and two bath levels which represent the sums of all collisionally populated levels in both electronic states. In their evaluation, a similar plot as that of Baronavski and McDonald[310] results; however, the intercept now yields the concentration in all rotational levels, not only the laser-coupled one. If n levels are populated, the concentration determined with the two-level formalism can thus be in error by up to a factor n. For the same reason, the effective collision rate obtained from the slope may be too high. Berg and Shackleford[314] have reported a quenching coefficient for CH that is a factor of 15 lower than that of Bonczyk and Shirley;[311] this factor approximately corresponds to the number of rotational levels involved.

A modified four-level model, the so-called 'balanced cross-rate model', has been proposed by Lucht et al.[315] for the quantitative interpretation of saturated LIF signals. In contrast to previous studies, they assumed steady state conditions only for the two laser-coupled levels. For typical laser temporal profiles, the time needed for equilibration of the populations in these two levels is a fraction of a nanosecond whereas Kotlar et al.[286] estimate that the population in the entire rotational manifold needs about 30 ns for equilibration in an atmospheric pressure flame. Application of the balanced cross-rate model requires single-line detection. The model furthermore assumes that the RET rates in both electronic states are approximately equal. Under conditions where this assumption holds, a detailed description of the RET processes is not necessary. Recent work by Zizak et al.[282] indicates that, indeed, RET in the electronic ground state of the OH radical is only slightly faster than in the excited state. Lucht et al.[316] have used the balanced cross-rate model for the interpretation of their saturated LIF measurements of the OH concentration in low-pressure

flames. The results agree very well with absorption measurements. Salmon et al.[317] have used the balanced cross-rate model for the measurement of the NH concentration in low-pressure flames; again, their results agree well with those from an absorption experiment. The reliability of the balanced cross-rate model requires, however, verification at higher pressures. Also, broadband detection may become necessary in many experiments. Related studies which address these questions will be described later in this section.

4.3.2. Calibration

Besides rotational redistribution in both electronic states, some other aspects of saturated LIF experiments need consideration, if quantitative information is desired. Among those are polarization effects, the influence of laser-induced chemistry, the contributions to the fluorescence signal of zones with varying degrees of saturation and the efficiency of the detection system.

Altkorn and Zare[131] have pointed out that the fluorescence following excitation with polarized laser light may not necessarily be assumed to be unpolarized, particularly if collisions are of minor importance. Despite collisions, Doherty and Crosley[130] have observed significant polarization in OH LIF experiments in an atmospheric pressure flame. Polarization effects can be reduced, however, if broadband fluorescence is detected or if the laser approaches saturation.[131]

Several groups have observed that laser-induced chemical processes affected quantitative concentration measurements when they used laser pulses of a few microseconds duration. Muller et al.,[318] Iino et al.[319] and van den Wijngaart et al.[320] report the formation of NaOH, NaH or NaO_2 via laser-excited levels when detecting Na.

Varying degrees of saturation caused by spectral, temporal and spatial inhomogeneities in the laser intensity need to be considered in saturated fluorescence experiments. Typically, the laser bandwidth is chosen to be larger than that of the molecular transition so that the spectral laser power density for the excitation process is constant, to a first approximation. Also, the temporal detection interval can often be chosen small enough so that only approximately constant pump rates and correspondingly high saturation degrees contribute to the measured fluorescence signal. However, unless lasers with very homogeneous spatial profiles are available, spatial wing effects will be of influence even with cleverly designed detection geometries. For quantitative measurements, consideration of their contribution is thus essential.

Mailänder[321] has treated the problem of spatially inhomogeneous saturation by introducing a fictitious 'saturated volume'. Every differential element of the detection volume is weighted according to the degree of saturation at this position; volume elements with

high degrees of saturation in the center of the spatial laser intensity distribution thus contribute more to this saturated volume than those in the wings. The saturation degree is evaluated from the measured spatial laser intensity distribution, which is obtained by translation of a pinhole across the laser beam. By integration over all weighted volume elements, the saturated volume is obtained; it is smaller than the detection volume and exhibits complete saturation. Blackburn et al.[322] have measured the fluorescence intensity as a function of laser intensity for different detection geometries and compared the results to calculated saturation curves. In an approach similar to that of Mailänder,[321] van Calcar et al.[323,324] have been able to derive spatially resolved contributions to the fluorescence signal by measuring local laser intensities with a slit. We have followed Mailänder's formalism in our experiments in low-pressure flames.[325-328] Whereas the work of Lucht et al.[316] and Salmon et al.[317] does not adequately account for spatial wing effects, Salmon and Laurendeau[329] in the same group later developed a suitable calibration procedure which relies in part on an Abel inversion. Stepowski and Cottereau[330] and Cottereau[331] have proposed a method which exploits the fact that the two saturated fluorescence signals measured simultaneously in the two detection geometries of Fig. 13 are to different extents affected by zones with low saturation degrees; the ratio of both fluorescence signals is, under certain conditions, independent of collisions. This method, which has become known under the name of "TOPLIF", is especially well-suited for single-pulse concentration measurements with saturated LIF.

Calibration of the optical detection system is also required. The efficiency of the LIF detection system has been measured by Rayleigh scattering,[311,316,333] Raman scattering by H_2[334] and Raman scattering by N_2.[335,176] In addition to Raman scattering by N_2 in room air, we have used scattering of the laser light off a special ground-quartz disk.[326] All these calibration procedures can be applied independently of the radical to be detected; however, great care should be take to determine the efficiency under identical focal conditions and geometrical arrangement, and with the same detection optics and electronics as in the actual LIF experiment.

4.3.3. Quantitative saturated LIF measurements in flames

The applicability of saturated LIF for the quantitative determination of radical concentrations has been investigated by several groups. Lucht et al.[316] and Salmon et al.[317,329,333] have used the saturated LIF technique in low-pressure flames; since the earlier work neglected the spatial wing effects discussed before, their results can in a strict sense only be understood as quantitative after they introduced suit-
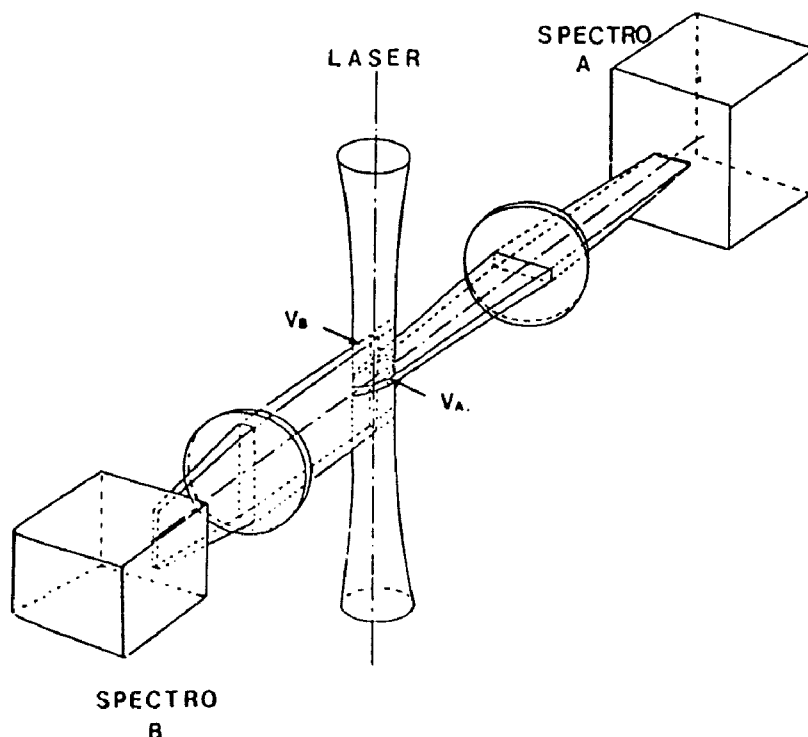
FIG. 13. TOPLIF experiment.[332] Saturated fluorescence signals are simultaneously recorded in geometries A and B which probe different local saturation degrees in the respective observation volumina.

able calibration procedures.[329,333] We have examined the principal sources of systematic errors in a saturated LIF study performed in a 13 mbar C_2H_2/O_2 flame where we measured OH and CH concentrations.[325,326] The influences of rotational redistribution, inhomogeneous spatial laser intensity profile and polarization were investigated systematically. Also, the choice of suitable line pairs for excitation and detection, the use of the rate equation formalism for typical saturation conditions and the calibration of the detection system were discussed. It was shown that especially the calibration procedure demands extreme care. If the necessary calibration steps were properly observed, theoretical saturation curves (calculated for the specific transition, excitation beam profile and observation volume) were in good agreement with experimental values over several orders of magnitude in laser power density. For comparison of the saturated LIF results, we also determined OH concentrations using the evaluation procedure of Baronavski and McDonald[310] as well as linear excitation as described by Stepowski and Cottereau;[134] good agreement of all methods was observed. A subsequent series of experiments[327,328] in hydrogen, methane and acetylene flames at pressures of 40–100 mbar allowed comparison with flame model calculations using a numerical flame code and chemical-kinetic information assembled by Warnatz.[336]

In turbulent H_2 diffusion flames at atmospheric pressure, Lucht et al.[150] have applied the saturated fluorescence technique for single-pulse measurements of the OH concentration. Calibration was provided

by comparison with absorption measurements in a laminar flame. Drake and Pitz[337] have used saturated LIF in the same flames to examine the accuracy of single-shot two-dimensional fluorescence imaging. Lucht et al.[93] have measured the OH concentration in sooting $CH_4/O_2/N_2$ flames at atmospheric pressure by saturated LIF. Under very rich conditions, the OH concentration was too small for detection by laser absorption, so the calibration had to be performed in lean flames. Since the saturated LIF method is insensitive to collisions, this calibration was believed to be quite accurate for the sooting flames, too. Interfering processes which would render the application of saturated LIF to sooting flames difficult, including Mie and Rayleigh scattering, soot incandescence or fluorescence of large hydrocarbon molecules were discussed by Eckbreth et al.[338] According to Lucht et al.,[93] none of these processes seriously affected fluorescence detection, whereas some limitations were imposed by Raman scattering from N_2.

The potential of the saturated fluorescence technique for measurements in high-pressure flames, and in particular the applicability of the balanced cross-rate model for quantitative concentration measurements has been examined by Carter et al.[339] In this numerical study, they have modelled the burnt gas of a H_2/O_2 flame at 2000 K and 1–20 bar with H_2O as collider. They assumed rotational redistribution to be about equally fast in both electronic states. Under these conditions, the reliability of the balanced cross-rate model depends most sensitively on the rates of electronic quenching to high vibrational levels in the
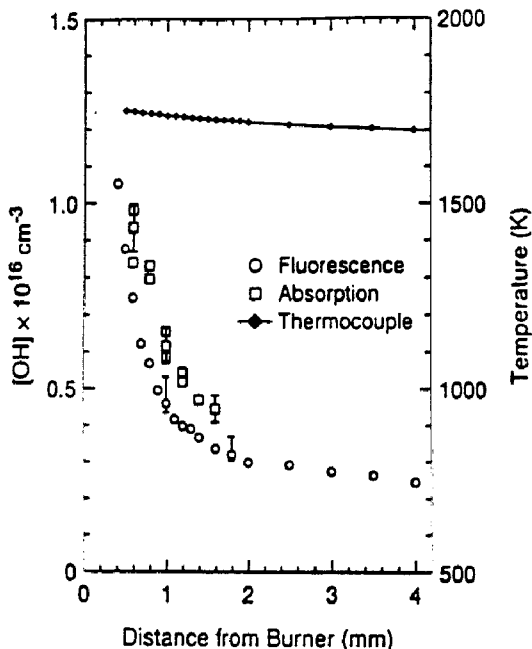
FIG. 14. OH concentration measurement with absorption (squares) and saturated fluorescence (circles) in a $C_2H_6/O_2/N_2$ flame at 6 bar.[342]

electronic ground state and on the rates for subsequent vibrational relaxation in the lower electronic state. There are indications that high vibrational levels are populated upon quenching of the OH $(A^2\Sigma^+)$ state, Crosley and Copeland,[242] an observation that may render the application of the balanced cross rate model problematic. The crucial question is whether the population in the two laser-coupled levels is depleted during the measurement. If this is not the case, the balanced cross-rate model can give quite accurate results at high pressures.

Carter et al.[340-342] have applied the balanced cross-rate model for the evaluation of OH saturated LIF measurements in ethane flames of 1-12 bar. Using—independently of pressure—the calibration factor determined by absorption at 1 bar in the reduction of the saturated LIF experiments at higher pressures, the OH concentration in the 6 bar flame is 25% lower than the concentration measured with absorption in this flame (see Fig. 14). Since both the influences of electronic quenching and line broadening have been considered, this result indicates that a certain fraction of the population leaks into bath levels not represented by the balanced cross-rate model. Carter et al.[342] have estimated that application of the calibration factor determined at 1 bar will cause a systematic error of about 50% in the OH concentration in the 10 bar flame. Considering that the balanced cross-rate model does not include a detailed description of the pertinent collisional energy transfer processes, however, it is remarkably successful for a large range of pressures in spite of these discrepancies.

The TOPLIF method mentioned above has been used to measure OH concentrations in flames of 60-120 mbar and at atmospheric pressure by Des-

groux[343] and Desgroux and Cottereau;[332] the system was calibrated either by absorption or by Rayleigh scattering. The technique has been extended to higher pressures (about 10 bar) by Carter et al.[340,344] and by Desgroux et al.[345] In their study of CH_4/air flames at pressures of 1-9 bar, Desgroux et al.[345] note that the saturation curves for all flames collapse within experimental accuracy, which would be expected using their approach. In addition, the OH concentrations obtained with this method are in reasonable agreement with our own measurements[97] by linear LIF calibrated with absorption in the same flames. Comparing TOPLIF and absorption measurements in high-pressure ethylene flames, Carter et al.[344] noted an increasing disparity between the results of both techniques with increasing pressure, indicating increasing depletion of the laser-coupled levels in the TOPLIF experiment. Since the interpretation of the TOPLIF measurements relies on the balanced cross-rate approach, too, this depletion is not accounted for in the data reduction.

In most saturated LIF experiments, single-line detection has been used so that detailed modelling of the energy transfer in the excited state may at least be avoided in the data evaluation. In general, broadband detection would result in higher fluorescence signals and, accordingly, improved detection sensitivities. In particular for the measurement of NO concentrations with saturated LIF at atmospheric and higher pressures,[346,347] single-line detection is unfeasible because of the dense NO spectrum. Furthermore, with the high power densities available in the UV with excimer lasers, high degrees of saturation can easily also be achieved in two-dimensional applications.[348] Finally, saturated LIF permits the measurement of temperature, as will be discussed further in Section 4.4. For broadband detection typically employed in these applications, in particular at high pressure, suitable formalisms for the quantitative interpretation of saturated LIF are currently being developed.[347]

4.4. Temperature Measurement with LIF

Temperature is one of the most fundamental quantities for the characterization of combustion processes. The temperature distribution in a combustion chamber may reflect design problems and provide clues for the optimization of the construction. Many important reaction rate coefficients depend sensitively on temperature. Therefore, the temperature distribution in a combustion chamber is an indicator of energy released locally from chemical bonds and of local reaction fluxes whch may eventually lead to potentially undesired or harmful products. Furthermore, the temperature distribution is important for the simulation of combustion processes with numerical models and for the comparison of experimental data with the model predictions. For these
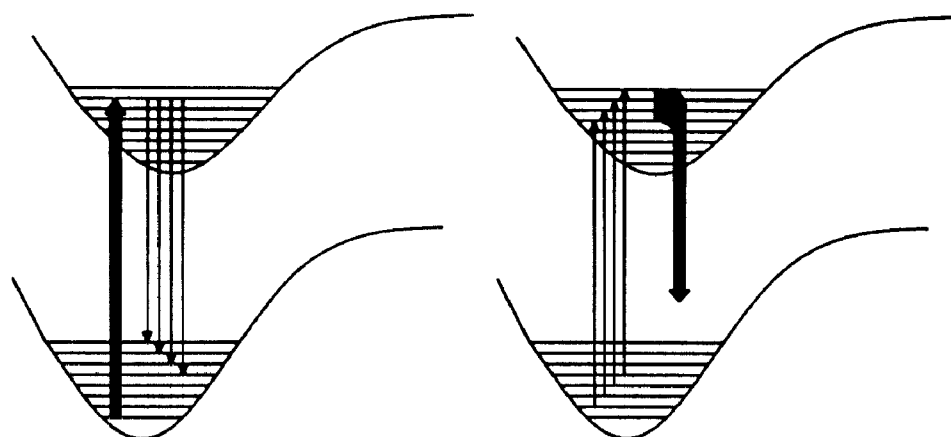
Fig. 15. Schematic energy level diagrams illustrating the principles of fluorescence (left) and excitation
spectra (right) following Crosley.[15]

reasons, the accurate measurement of temperature is one of the essential tasks in combustion diagnostics.

As an excellent introduction to the measurement of temperature with laser-spectroscopic methods, the review of Laurendeau[12] is recommended in combination with the book of Eckbreth.[2] The present article will discuss the measurement of temperature with laser-induced fluorescence. The main reasons for performing temperature measurements with LIF have already been mentioned before. First, it may be advantageous to use the same LIF apparatus for the simultaneous measurement of temperature and reactive species concentrations. Second, LIF offers the potential for instantaneous two-dimensional measurements of the spatial temperature distribution.

Several different approaches for the measurement of temperature with LIF have been described in the literature. Atomic or molecular temperature indicators may be used. For molecular temperature indicators, temperature is usually either derived from the rotational distribution in an electronically excited state, using fluorescence spectra, or from that in the electronic ground state, using excitation spectra. Figure 15 illustrates these two possibilities with the aid of schematic energy level diagrams. Similar to concentration measurements, linear or saturated LIF schemes may be applied. Also, temperature has been evaluated from the population distribution in different vibrational states.[349]

For the measurement of temperature with LIF, the parameters of influence which need to be considered are similar to those for the measurement of concentrations. Polarization effects, absorption of the laser radiation or of the fluorescence by the flame gases, and collisional energy redistribution can lead to substantial systematic errors in the interpretation of the measured fluorescence signals. In contrast to the measurement of concentration, where information on the population in a single quantum state is sufficient, temperature is almost exclusively evaluated

from population distributions in at least two levels. Whereas for a concentration measurement several quantities need to be known in absolute units (including transition probabilities, size of the observation volume, detection solid angle and efficiency, and fluorescence quantum yield), relative values are sufficient for a temperature measurement. Some quantities, such as the geometric ones, are not level-dependent and thus do not enter the data evaluation. In short, the essential information required are the variations of the above quantities with quantum state. Finally, the accuracy of the temperature measurement depends on the temperature sensitivity which is a function of the energy spacing between the two levels and their relative population at different temperatures. Appropriate levels should thus be chosen in view of the temperature range to be measured.

The intensity of a fluorescence line is proportional to the population in the corresponding level (see Section 4.1, Eq. 3). Temperature can be determined by comparison of simulated spectra with measured ones—with temperature and temperature-dependent line-shape as free fit parameters—or from a so-called Boltzmann plot according to

$$\ln(I_{fl}/gB) = -(E/kT) + \text{const.} \qquad (4)$$

Temperature is obtained from the slope of this semilogarithmic plot of the fluorescence intensity I_{fl}, weighted by the Einstein B coefficient and degeneracy g, versus the energy E of the corresponding level. For the interpretation of excitation spectra, energies and degeneracies of the lower state levels enter the evaluation, and for fluorescence spectra, the values for the upper state have to be used. This simple relation, however, ignores variations of the quantum yield with energy level.

4.4.1. Atomic temperature indicators

If metal atoms serve as temperature indicators, these species have in general to be introduced into

the flame of interest in the form of metal salts or complexes; this requirement constitutes the essential disadvantage of this method. The achievable measurement accuracy depends on the assumptions that the metal species can be evenly distributed throughout the flame and leaves the combustion process undisturbed. Besides sodium, atoms with a low-lying metastable state such as indium, gallium, thallium or lead have been primarily used. In a typical experiment, starting from the ground state or the metastable state, a third electronic state is excited and the fluorescence to the respective other lower state is monitored. Bradshaw et al.[48] have discussed the advantages and limitations for several three-level strategies. Kowalik and Kruger[350] have measured temperatures in an acetylene flame using sodium atoms. For temperature measurement with kilohertz repetition rates, Joklik and Daily[351] have proposed a procedure which uses indium atoms as indicators. Aldén et al.[352] have also used indium atoms for the determination of temperature in a methane flame and demonstrated that their technique is capable of one-dimensional temperature mapping. Ambiguities caused by the seeding process may, of course, be avoided by using temperature indicators naturally present in the flame of interest.

4.4.2. Temperature measurement using molecular indicators

Whereas Raman and CARS techniques can rely in many applications on the rather inert nitrogen molecule as a temperature indicator, temperature measurement with LIF is often performed using a reactive species, such as the OH radical, which is present in substantial concentrations in the hot zones of most flames. However, the OH concentration may not be sufficient to permit temperature measurement in cooler regions of unmixed or unburnt gases. Also, the population distribution of a molecule produced by chemical reaction in the flame cannot generally be assumed to be thermal. Several other molecules such as NO or O_2 have been investigated for LIF thermometry. The present discussion, however, will concentrate on temperature measurement using OH rotational spectra; a comparison of the different temperature indicators will be presented at the end of this chapter.

4.4.2.1. OH thermometry using flame emission.
Broida[353] has measured temperatures* in a methane/ air flame by analyzing emission and absorption spectra of the OH radical; the former reflect the population distribution in the excited OH $(A^2\Sigma^+)$ state, the latter correspond to that in the electronic ground state. Typical results are shown in Fig. 16. While the temperatures evaluated from the absorption

_____

*The result of a Boltzmann plot is called 'temperature' in this context, although thermal equilibrium may not necessarily be assured.

spectra appear reasonable, the values determined from the emission spectra exceed the adiabatic flame temperature by several thousand degrees and thus indicate non-thermal distributions. The only contention that non-thermal rotational distributions have been observed in the electronic *ground* state of OH in flames is found in the work of Wang and Davis;[335] their observation, however, is probably the result of inadequate consideration of saturation, absorption or vibrational energy transfer. More recent absorption measurements of the flame temperature, such as those of Lück and Thielen,[100] give no clues for the formation of non-thermal distributions in the electronic ground state of the OH radical.

4.4.2.2. OH thermometry using fluorescence spectra.
Schemes for the determination of temperature from fluorescence spectra are based upon single-line excitation in combination with spectrally-resolved detection. A principal advantage, e.g. for application in turbulent and unsteady flows, is the potential for single-pulse detection of the fluorescence with an optical multi-channel analyzer. However, the evaluation of temperature from the measured spectra may lead to erroneous results. After excitation of an isolated level, rotational energy transfer tends to equilibrate the population in the excited electronic state. The population distribution may, however, be distorted by competing processes with level-dependent cross sections, such as electronic quenching, vibrational relaxation or predissociation. Under these circumstances—which are often met in OH experiments—a non-thermal population is probed see the example in Section 4.2, Fig. 7), and the evaluation according to Eq. 4 does not yield the flame temperature. Quantitative interpretation of the measured fluorescence spectrum in this case requires a model which adequately represents all depopulation and energy transfer processes. The present state of development of these rate equation models has been discussed in detail in Section 4.2.

In spite of incomplete information on both individual transfer rates as well as on the underlying physical principles for collisional energy transfer, several groups have attempted to obtain temperatures from fluorescence spectra with the aid of specific model approaches. Chan and Daily[284] have evaluated temperature measurements in a methane flame at atmospheric pressure with their model. Furuya et al.[285] have analyzed population distributions in OH $(A^2\Sigma^+, v' = 0)$ following excitation of different rotational levels in an atmospheric pressure propane flame; they have observed that the measured spectra can be understood qualitatively using the model of Chan and Daily.[284] The population distribution in rotational levels above the excited one appeared to be almost thermal in their experiments. Similar population distributions have been observed by Zizak et al.[354] In their study, however, even in levels far above the originally excited one, the distributions
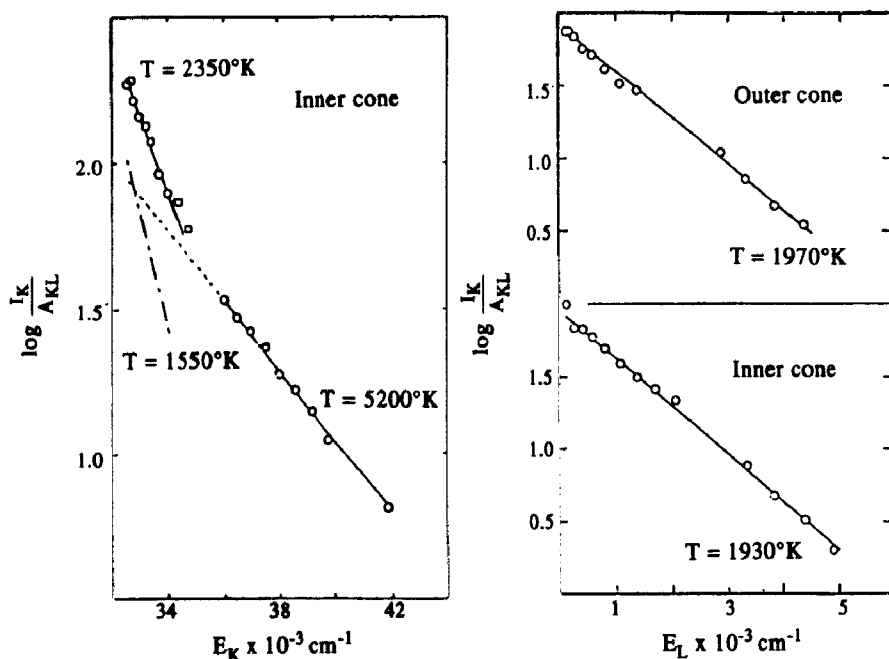
FIG. 16. Comparison of temperatures obtained from rotational spectra of the OH radical measured in emission (left) and absorption (right) in a stoichiometric methane/air flame.[353] From emission spectra, different, too high apparent temperatures are evaluated from low (2350 K) and high (5200 K) rotational levels. Corrections (dash-dotted line, 1550 K) do not lead to the 'true' temperature. In contrast, absorption spectra yield temperatures of 1930–1970 K in accord with the expectations.

were still sensitive to both temperature and chemical composition, and thus this scheme is not generally applicable for OH thermometry.

In our early work on temperature measurement in low-pressure flames,[326-328] we have relied on OH fluorescence spectra which were measured after a substantial delay, following excitation of a single level in the $OH(A^2\Sigma^+, v' = 0)$ state. The necessary delay was defined by monitoring ratios of fluorescence intensities from different collisionally populated levels: when the ratios for selected line pairs approached constant values, the delay was considered to be sufficient. Care was taken to include lines originating from levels adjacent to the laser-excited one as well as some from more distant levels. Delays of about 200 and 60 ns were appropriate for our flames at 13 mbar and 95 mbar, respectively. This method yielded good agreement of the temperatures obtained for different excited transitions in several hydrogen and hydrocarbon flames. Good agreement was also observed between CH and OH temperatures in the limited number of experiments where CH was present in sufficient amounts. However, the general applicability of this technique, especially at more elevated pressure, is questionable.

In conclusion, no satisfactory method for measuring flame temperature from OH fluorescence spectra is presently available; in particular, none of the aforementioned schemes would be generally reliable under typical flame conditions at ambient pressure and above. Computer simulations with rate equation models like the one developed by Kienle et al.,[290]

which includes the most recent information on collisional transfer rates, may be of considerable help in designing suitable measurement procedures.

4.4.2.3. OH thermometry using excitation spectra. The information contained in an excitation spectrum corresponds to that of an absorption spectrum, where fluorescence serves as a monitor for the absorption. Usually, several rotational levels are excited by scanning the laser sequentially across corresponding absorption transitions; the spectral detection interval is kept fixed. For instantaneous two-line thermometry in particular, two transitions are simultaneously excited by two laser wavelengths. Excitation spectra probe the rotational distribution in the electronic ground state, typically in the lowest vibrational level.

As observed by many authors,[104,148,209,265,355] collision processes are again of significant influence. For example, Cattolica and Mataga[209] report systematic temperature errors of up to 10%, if the rotational level dependence of the electronic quenching is neglected in the interpretation of their excitation spectra measured in a low-pressure $H_2/O_2/Ar$ flame. Significant systematic errors may result from variations of the fluorescence quantum yield with rotational level due to level dependences of spontaneous emission, collisional transfer or predissociation rates. The measurement accuracy may depend most sensitively on the choice of excitation transitions and on spectral and temporal detection bandpass. Again, a linear Boltzmann plot does not ensure a correct temperature measurement.
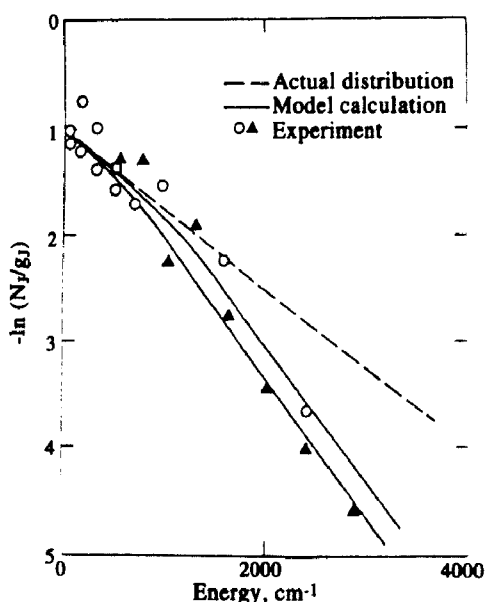
Fig. 17. Influence of the spectral detection interval on the measured temperature,[265] illustrated in a Boltzmann plot. Temperatures obtained using narrowband detection (symbols) were considerably lower than those from broadband excitation spectra, which were found to agree with the actual flame temperature (dashed line). With a model of the energy transfer, the observed narrowband fluorescence intensity distribution could approximately be reproduced (solid line).

Three excitation transitions in the OH (A-X) system have commonly been used to measure OH temperatures: the (0,0) band pumped either by XeCl or dye laser radiation, the (1,0) band for which dye lasers are usually employed, and the (3,0) band* accessible by the KrF laser. Since these three schemes have different advantages and characteristics, they shall be discussed successively.

Some early studies using (0,0), (1,0) or (1,1) excitation may appear contradictory, in particular with regard to their observations on proper spectral gating. Bechtel[356] has measured OH excitation spectra in an atmospheric methane flame and obtained temperatures in good agreement with those measured by Raman spectroscopy under the same conditions. In a burner especially designed to avoid absorption of laser light and radiative trapping, OH was excited in the (0,0) or (1,0) band; the fluorescence detection bandpass is not specified in their paper. Crosley and Smith[265] have measured OH (0,0) excitation spectra in the burnt gas of an atmospheric pressure methane flame and varied the detection interval in the (0,0) band. Whereas broadband detection yielded reasonable temperatures, those obtained with narrow bandpass were low by several hundred degrees, as shown in Fig. 17. With a simulation of the energy transfer, the observed trends could be understood; the model was, however, not designed

---

*With respect to OH concentration measurements, especially at high pressure, these three excitation schemes shall be discussed in more detail in Section 4.5.

for general applicability. Anderson et al.[266] have measured OH temperatures in CH_4/N_2O flames by both exciting and detecting in the (1,1) band. Although they used a relatively narrow detection bandpass, they did not observe any discrepancies between their LIF temperatures and those measured by Raman spectroscopy using N_2 as indicator.

The influence of the spectral and temporal bandpass on the temperature measurement was systematically studied in H_2/O_2 and H_2/N_2O flames at about 10 mbar.[148,355] OH was excited in the (0,0) band and detected with a monochromator whose bandpass was designed to cover the entire (0,0) band with constant efficiency. When the spectral gate was shifted from its optimum position by about 8 nm to the red, resulting in preferential detection of transitions from high rotational quantum numbers, a burnt gas temperature of 3770 K resulted which was high by about 1500 K in comparison with an absorption measurement. The almost perfectly linear Boltzmann plot gave no indication of this dramatic systematic error.[355]

Similarly, the variation of the temporal gate in that experiment had a significant influence on the measured temperature. The broadband fluorescence was detected in the burnt gas of a H_2/N_2O flame using a gate of 10 ns width and a variable delay of 50–250 ns with respect to the laser pulse. With increasing delay, the measured temperature increased by 80–240 K. The fraction of the total population in higher rotational levels which were quenched less effectively[203] became larger, causing the temperatures measured at later times to be higher. Although the rotational level dependence of the quenching of OH ($A^2\Sigma^+$, $v' = 0$) by H_2O, one of the most important quenchers, decreases with increasing temperature,[208] the detection process would be made less sensitive to quenching by using a short gate directly after the laser pulse,[355] thus reducing errors in the temperature measurement. However, besides the variation of quenching with composition, temperature and rotational level, the dependence of the radiative transfer rate (see e.g. Trolier[294]) on quantum state also has to be taken into account; the increase in the radiative decay rate with rotational level tends to counterbalance the effect of the quenching variation to some extent.[159] The reason for this counteractive tendency is the dependence of the quantum yield on the Einstein A coefficient in the numerator and quenching rate in the denominator. Since the influence of the radiative rate is dominant for times directly after the laser pulse, the strategy using prompt, short gates is inappropriate if the level dependence of quenching is small compared to that of the spontaneous emission. Without any independent information or detailed rate equation modelling it is thus difficult to conclude which temporal gate ensures correct temperature measurements.

We have therefore used the rate equation model[290] to simulate the results of our previous study.[355] The

trends observed in the experiment could be reproduced very well, and the model calculations thus enabled us to identify the measurement procedure least sensitive to systematic errors.[357] One proposed scheme appears suitable only for special situations, namely to correct temperature measurements performed with a short gate by the appropriate level-dependent radiative and quenching rates.* As the most generally applicable scheme, temporal (and spectral) integration of the fluorescence signal yields temperatures with reasonable accuracy, although small systematic errors may remain, the magnitude of which depend on chemical environment, on the levels to be pumped and on the temperature to be measured. Residual errors are in the order of 40–50 K at 2300 K in the burnt gas of a low-pressure H_2/N_2O flame and are expected to be similar for the burnt gases of most hydrocarbon/air flames (with temperatures on the order of 2000 K and N_2 and H_2O as the dominant quenchers), at both lower and higher pressures. At temperatures around 1200–1500 K, such as found in the burnt gas regions of low-pressure $H_2/O_2/He$, $H_2/O_2/Ar$ or $H_2/O_2/N_2$ flames (see the studies of Lee et al.,[210] Cattolica and Mataga,[209]† and of Lawitzki et al.,[358] respectively), level-dependences of radiative and quenching rates almost cancel and the error is negligible. Far below 1000 K, where the level-dependent quenching may introduce significant systematic errors, OH is often not present in sufficient amounts for a temperature measurement. The measurement procedure can be optimized further by the proper choice of the excitation transitions. In the high temperature range, it may be advantageous to avoid the lowest rotational levels, thus keeping the level dependence of the radiative rate small while ensuring a large energy spacing. The trade-off between detectable signal (measurable population), high temperature sensitivity (large energy spacing) and minimal systematic error (similar level dependences of radiative and collisional transfer rates) determines the feasibility of a specific measurement scheme for the condition under study.

In our flames at about 10 mbar with OH concentrations on the order of 10^{14} cm^{-3}, absorption in the

(0,0) band was already noticeable over a pathlength of 6 cm.[148] Also, Rea and Hanson[104] have observed a non-negligible influence of laser absorption and radiation trapping in their experiments using rapid laser-wavelength modulation and fluorescence detection in the OH (A-X, 0,0) band to measure the temperature profile throughout the reaction zone of an atmospheric pressure CH_4/air flame. Temperature measurement procedures using excitation of OH to higher levels are significantly less sensitive to absorption and radiation trapping and are therefore better suited for application in combustion systems at high temperatures and pressures. In a systematic study,[358,361] we have investigated the reliability of a temperature measurement strategy which is based upon excitation in the (1,0) band and detection of the combined (0,0) and (1,1) fluorescence. The sensitivity to absorption is about a factor of 4 less and can be decreased further by exciting weak lines, e.g. in the (1,0) S-branch as proposed by Tirgrath[362] and applied by Lawitzki et al.[361] The broadband detection of virtually all emitted fluorescence in both the (1,1) and (0,0) bands is insensitive to polarization as well as to rotational and vibrational energy transfer. This technique was applied in a wide range of temperatures and pressures; experiments included a discharge flow reactor operating at 3000 K and a few mbar, $H_2/O_2/N_2$ flames at about 100 mbar with an accessible temperature range of about 500–1400 K and an atmospheric pressure methane/air flame with a burnt gas temperature of approximately 2050 K. Some measurements were also performed in methane/air flames of 1–10 bar;[97] good agreement was found with CARS results in similar flames.[363,364] In the low-pressure flames, short gates located early after the beginning of the laser pulse were used,‡ and in the flames at ambient pressure and above, time-integrated detection was employed. In addition, the laser intensity was varied and saturated excitation was investigated.[361,362] Comparison with Raman and CARS measurements gave excellent agreement under all flame conditions up to 1 bar.[358] As an example, Fig.18 shows the temperature profiles measured by linear and saturated LIF and N_2 CARS in three low-pressure hydrogen flames at different stoichiometries.

Excitation in the (3,0) branch as described by Andresen et al.,[145] Crosley and Jeffries[365] and Arnold et al.[366] combines several advantages for the

---

*It should be kept in mind that some inconsistencies remain, in particular for low rotational quantum numbers, between level-specific radiative rates derived from theoretical[294] and experimental studies.[359,360] Furthermore, the radiative rate which should be used for a potential correction is not the level-specific one tabulated in these publications, but the effective, ensemble-averaged rate which takes into account that RET has already occurred at the observation time. This ensemble-averaged rate is still level-dependent, but to a lesser extent than the tabulated one. The same caveat applies for the level-dependent quenching rate (an example is given in Lee et al.).[210]

†In view of the discussion in this paragraph and in contrast to the procedure applied by Cattolica and Mataga,[209] the measured fluorescence signals should not be corrected by the level-dependent quenching rates alone.

‡In principle, similar considerations on the appropriate choice of detector timing apply as detailed above. Information on the level dependences of radiative and collision processes is, however, less complete. It appears that level dependences in quenching are of similar magnitude as those for $v' = 0$.[217] Also, RET coefficients are quite similar.[273] The spontaneous emission rate seems to be less level-dependent for $v' = 1$[205,369], however, predissociation significantly influences high rotational levels ($N > 14$). The influence on a particular temperature measurement would have to be modelled in detail.
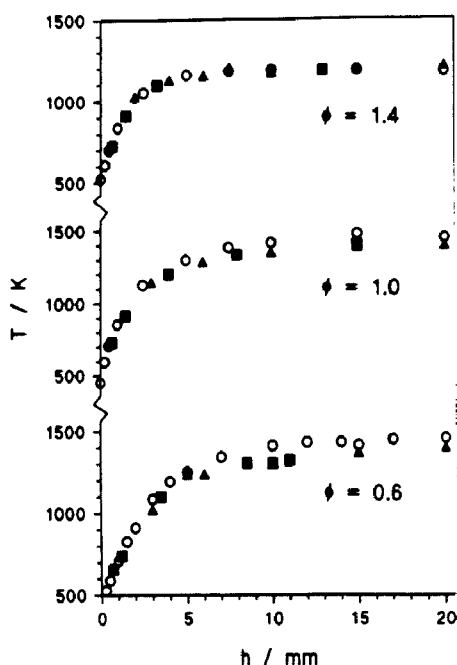
FIG. 18. Temperatures measured by linear (triangles) and saturated LIF (squares) and CARS (circles) in three low-pressure $H_2/O_2/N_2$ flames of different stoichiometry.[358]

measurement of OH temperatures. At atmospheric pressure and below, the signal is almost independent of quenching since the depopulation of the upper state is dominated by predissociation with lifetimes on the order of 100 ps.[367,368,369] At more elevated pressures up to about 10 bar, the sensitivity to collision processes is still less than that of linear LIF. The scheme is also insensitive to absorption and radiative trapping if detection in the (3,3) or (3,2) band is used. A recent comparison of (0,0), (1,0) and (3,0) excitation by Quagliaroli et al.[370] is very instructive in this context. Narrowband detection of radiation originating directly from the $v' = 3$ state also suppresses an adverse effect of vibrational relaxation: since the lower vibrational levels in the OH ($A^2\Sigma^+$) state may radiate with higher efficiencies and are subject to collision processes, detection of the total fluorescence may lead to considerable misinterpretations.[371]

Several limitations need to be addressed, however. First, it has been argued by Gray and Farrow[367] that the high laser intensities which are commonly used for excitation may lead to considerable saturation and thus to a sensitivity to rotational redistribution in the electronic ground state. In their imaging experiment with moderate laser power densities, however, Arnold et al.[366] consider this to be a minor effect. Second, the predissociation lifetime depends on rotational quantum number[367,368,369] and thus—even if collisional processes may be neglected—the fluorescence quantum yield may be level-dependent. Heard et al.[368] and Crosley and Jeffries[365] have shown that this fact may introduce considerable temperature errors. As shown in Fig.19,

the temperature obtained from a (3,0) excitation spectrum taken in the burnt gas of a methane/air flame at 45 mbar deviates by about 700 K from that measured in the (0,0) band, if no correction for level-specific predissociation lifetimes is applied. Since a level dependence of the quenching rate in the opposite direction to that of the predissociation rate is expected, Heard et al.[368] conclude that there is a pressure for each collisional environment at which the influences of both dependences just cancel and where—fortuitously—a correct temperature would result. A significant influence of level-dependent predissociation rates can be avoided if almost neighboring levels with very similar lifetimes are chosen, e.g. excitation of the $Q_1 11$ and $P_2 8$ lines in the experiment of Arnold et al.[366] This strategy suffers from the disadvantage, however, that the energy spacing and, correspondingly, the temperature sensitivity are rather small.

In summary, (3,0) excitation can be very useful in many flame environments at moderate to high pressures and may be the only applicable technique for LIF measurements in situations where high OH number densities occur across a substantial pathlength, such as in high-speed flow facilities.[370] For a reliable temperature measurement, level-dependent predissociation rates should be considered, and saturation (and potential lower state depletion) should be avoided. This may, however, limit achievable signal strength or temperature sensitivity.

4.4.2.4. *Two-line schemes and temperature imaging using OH.* Instantaneous two-dimensional temperature field imaging* in combustion systems requires nearly simultaneous excitation of two transitions. This has implications for the experimental equipment as well as for the measurement procedure. If special laser systems capable of two-line operation (such as that of Ketterle et al.[372]) are not available, two lasers have to be used for excitation, whereas for the detection, two cameras are needed (gated, intensified CCD cameras are typically used). Several two-line excitation schemes avoid problems with level-specific collision rates. Cattolica[373] has proposed excitation of the same fine structure level in the upper electronic state starting from two different levels in the electronic ground state. Thus, the fluorescence quantum yields for both excitations are equal. A similar strategy has been followed by Lucht et al.[374]. Due to the restrictions imposed by selection rules, these schemes suffer from small energy spacing and low temperature sensitivity. Cattolica and Stephenson[375] have refined this approach by exciting the same level in the OH ($A^2\Sigma^+$, $v' = 1$) state using the $Q_1 5$ line in both the (1,0) and (1,1) bands. The energy difference is quite large in this case, allowing for good temperature sensitivity. However, the $v'' = 1$ level is only significantly populated at elevated

---

*Further multi-dimensional applications of LIF are discussed in more detail in Section 6.2.
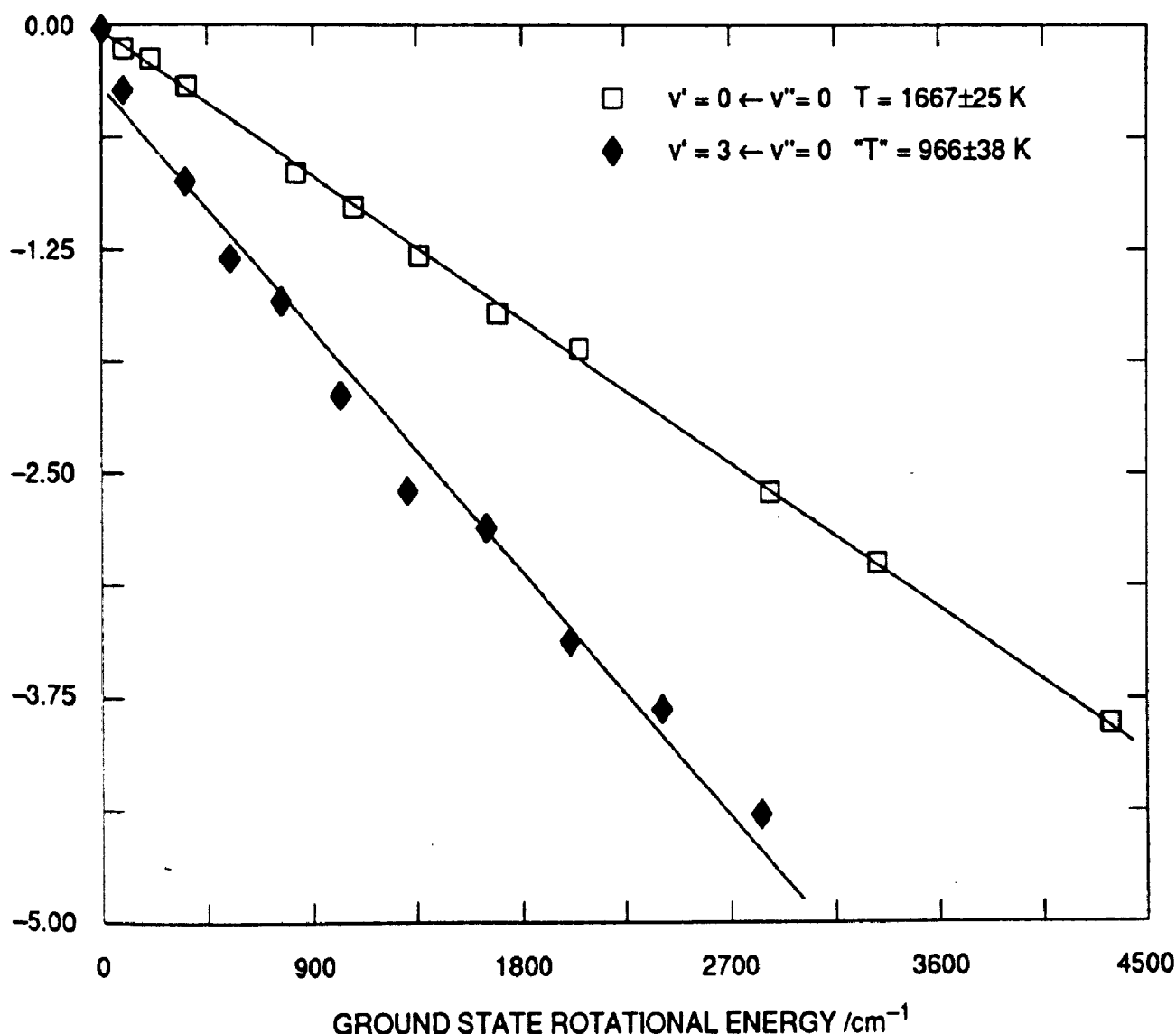
FIG. 19. Boltzmann plots of the relative ground state rotational populations determined from OH excitation spectra in the A-X (3,0) band (diamonds) and in the (0,0) band (squares); no correction for level-dependent predissociation rates was applied in the former experiment.[368]

temperatures above about 1000 K, limiting the applicability of this scheme.

Saturated LIF methods like the ones of Lucht et al.[374] and of Tirgrath[362] and Lawitzki et al.[361] offer a considerable advantage for instantaneous two-dimensional thermometry, besides their relative intensity to collisions; they provide intense fluorescence signals. However, they require an appropriate formalism for the data evaluation which should consider the influence of population depletion and rotational redistribution; also, broadband detection should be described properly. Current theoretical approaches still lack general applicability at moderate to high pressures (see the discussion on concentration measurements with saturated LIF in Section 4.3). Since the crucial problem in single-pulse 2D thermometry experiments may be to obtain a detectable signal, moderate saturation may not be avoidable. We have therefore suggested recently[376] the use of two excitation transitions with almost identical line strengths

in order to achieve similar degrees of saturation for both lines. The saturation terms then cancel to a first approximation in the data evaluation. In general, however, neglect of the saturation terms will lead to considerable temperature errors even for moderate degrees of saturation, as pointed out by Meier et al.[159]

Reliable measurement procedures for instantaneous two-dimensional OH LIF thermometry are currently under development in several laboratories. In addition to the problems mentioned before, limitations imposed by the available dynamic range of the detector systems should not be underestimated in such experiments, especially if zones with steep temperature gradients are probed. Temperature imaging using the predissociative (3,0) transition has been demonstrated recently by Arnold et al.[366] Their measurements in a laminar, premixed ethylene/air flame at atmospheric pressure are, however, not instantaneous in the strict sense, since fluorescence signals
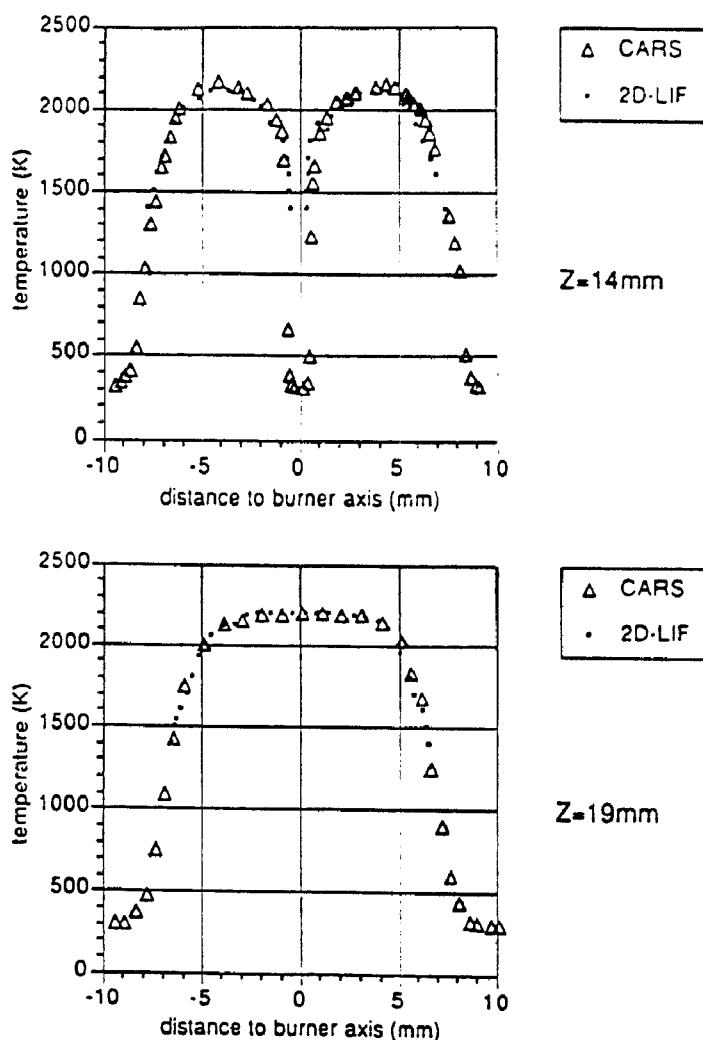
FIG. 20. Comparison of temperature profiles in a laminar, premixed ethylene/air flame from two-dimensional LIF and CARS measurements.[366]

from two consecutive laser pulses were evaluated. The authors state a measurement uncertainty of 7%; the lowest measurable temperature using this scheme is about 1500 K. Excellent agreement with CARS measurements was observed, as illustrated in the one-dimensional profiles from their 2D fields shown in Fig. 20. Instantaneous two-dimensional OH thermometry with a two-laser/ two-camera approach has been reported by Paul et al.[377] and Seitzman et al.[378] At DLR, we have most recently applied a similar scheme based upon excitation in the (1,0) band and broadband detection.[379] Besides using two fully independent laser and camera systems, we have reduced the susceptibility to systematic errors by relying on calibration experiments with a laminar, premixed, flat reference flame of similar chemistry and temperature range. Preliminary results obtained in a turbulent H_2/air diffusion flame appear to be in good agreement—on a statistical basis—with single-pulse point-wise temperature measurements by spontaneous Raman spectroscopy in the same flame.[380]

Although the initial results seem promising, OH thermometry suffers from a severe drawback. Since

none of the OH imaging experiments provides *simultaneous* access to high- and low-temperature regions, this species seems to be of limited value as a temperature indicator for most practical combustion systems, where flame fronts and unburnt fractions of fluid may coexist in close vicinity.

4.4.2.5. *LIF thermometry and temperature imaging using other indicators than OH.* Besides the OH radical, several other molecules have been utilized as indicator species for temperature measurements with LIF. Rensberger et al.[355] compared temperatures derived from spectra of the OH ($A^2\Sigma^+$-$X^2\Pi$), CH $A^2\Delta$-$X^2\Pi$), CH ($B^2\Sigma^-$-$X^2\Pi$), NH ($A^3\Pi_i$-$X^3\Sigma^-$) and CN ($B^2\Sigma^+$-$X^2\Sigma^+$) systems in low-pressure flames. Whereas those obtained with OH, NH and the CH (A-X) transition agree quite well, the results using the CH (B-X) system are systematically lower by 150–200 K and those obtained using CN are higher by about 200 K. Reasons for these discrepancies are unclear; in the case of the CH (B-X) transition, predissociation may be a source of error. CH thermometry using the ($A^2\Delta$-$X^2\Pi$) transition has also been investigated thoroughly in a recent study by Raiche and Jeffries.[381] Since these radical species

are, however, often present only in very low concentrations and occur only in specific regions of most flames, their use as indicator species is restricted to special situations.

Two-dimensional LIF of O_2 has been studied by several groups including Lee et al.,[144] Laufer et al.,[382,383] Miles et al.[384] and Andresen et al.[145] Transitions overlapping with the spectral profile of the ArF excimer laser are strongly predissociative,[385] so that the quenching influence on O_2 LIF measurements is negligible at atmospheric pressure. Thermometry with O_2 as indicator was, however, primarily investigated in non-reacting flows. Lee et al.[144] have excited O_2 with a broadband ArF laser in a flow system using heated air. Since lines originating primarily from excited vibrational levels in the electronic ground state are excited in this scheme, the measurement is limited to temperatures above approximately 800 K. By using narrowband ArF laser radiation, however, transitions from the vibrational ground state may be selected.[383] If reactive flows with changing O_2 concentrations are to be probed, a second measurement of concentration (e.g. with LIF or Raman) is necessary in addition to the temperature measurement itself. Suitable experimental procedures for application in aerodynamic research are under development.[383] Most recently, Pitz et al.[386] have examined the potential of H_2O thermometry using predissociative LIF. In single-pulse measurements, errors were, however, in the order of 10-20% in the range 1000-2000 K.

The most promising temperature indicator for LIF measurements seems to be NO. Since it is quite stable for many flame conditions, it may be seeded into the flame under study. It thus provides access to low-temperature regions where the OH concentration is low. Furthermore, level dependences in quenching of the NO ($A^2\Sigma^+$) state are expected to be small for most combustion gases.[199] An early study of NO thermometry for application in supersonic flows has been performed by Gross and McKenzie.[387] If the NO mole fraction is approximately constant and if its quenching cross section may be assumed to be temperature-independent (which is, however, not true in general, see Section 4.2), the entire temperature field can be determined using a one-line technique, as demonstrated in the first instantaneous two-dimensional temperature measurement.[388] Gross et al.[389] have applied a two-line scheme relying on two dye lasers pumped by the same Nd:YAG laser for a point-wise temperature measurement in a wind tunnel experiment. Non-simultaneous two-dimensional applications of NO two-line techniques using a single laser and camera have been described by McMillin et al.[390] and Palmer et al.[391]

Recent studies of instantaneous two-dimensional LIF thermometry with NO[392,393,394,395] allow a detailed judgement of advantages and limitations. McMillin[392] and McMillin et al.[393] investigated mixing

and combustion in a turbulent supersonic flowfield generated by injection of H_2 fuel (doped with 1% NO and 19% CO) into a high-speed shock-tube flow. Under these conditions, instantaneous temperature fields over the range 300-2000 K were measured with an experimental uncertainty of typically 5-10% for a free stream temperature of 1260 K and 4-22% for a higher free stream temperature of 2200 K. Uncertainties increased when NO was not seeded into the free stream for an in situ calibration; they were also larger for oxidizing free streams due to strong quenching of NO by O_2. Since the largest source of uncertainty was determined to be shot noise, suitable measures should be taken to increase the signal-to-noise ratio. McMillin[392] regards the signal loss from quenching by radicals and H_2O in the reaction zones and burnt gases of combustion flows as the most significant limitation for the technique. Whereas NO was demonstrated to be a good tracer for fuel and unburnt regions, OH might be a superior temperature indicator in the hot zones of flames.

It should be noted, that excitation of the NO (A-X) transition was chosen in the studies mentioned above. An alternative is offered by excitation of the stronger (D-X) transition with the ArF excimer laser.[396] Thus, lower mole fractions of NO can be detected with good sensitivity. However, this excitation scheme may be limited to measurement of higher temperatures since suitable absorption transitions originate from higher vibrational levels in the electronic ground state. Methods for NO thermometry with two-line schemes based upon excimer laser radiation are currently being investigated.[397]

In conclusion, the impression remains that none of the LIF techniques discussed in this section has the potential for general applicability combined with sufficient accuracy, reliability and dynamic range for instantaneous temperature field measurements in all practical combustion systems. For any LIF thermometry experiment to be performed in a combustion environment, it is highly advisable to compare the results under several different conditions with those of other non-invasive methods, including absorption, CARS, Raman or Rayleigh scattering or combinations of those techniques. These methods, which have been characterized in more detail in recent reviews,[2,12] have their own shortcomings, the most essential ones including the limitation to line-of-sight probing for absorption measurements, the restriction to point-wise data collection for CARS applications, the requirement of constant scattering cross section throughout the flame for Rayleigh thermometry, and the low efficiency of the Raman process. More specialized techniques for temperature measurement in combustion, such as degenerate four-wave mixing (see Section 6.3), still require development for these purposes and thus cannot yet be recommended as alternatives.
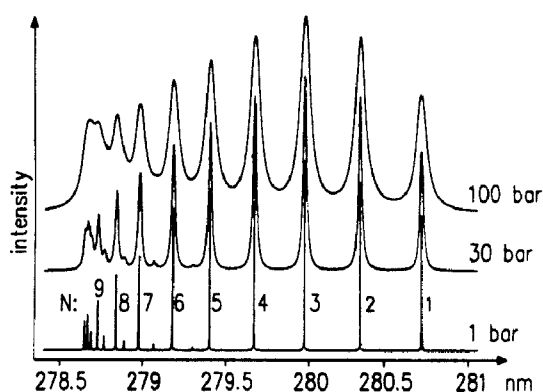
FIG. 21. Simulated spectra of the OH (A-X, 1,0) S branch
for typical flame conditions at 1, 30 and 100 bar.

4.5. LIF and Trace Species Detection at High Pressure

In the overwhelming majority of combustion diagnostics experiments, LIF has been applied at ambient pressure or below; in practical combustion environments, however, pressures far above the atmospheric value may be encountered. In a number of recent studies, several molecules of interest in combustion have been detected by LIF in the pressure range of about 5–35 bar. OH and CN radicals have been monitored in solid propellant flames (see e.g. Edwards et al.[398]), OH and NO have been detected in laminar, premixed high-pressure flames (examples are found in Carter et al.,[341,342,344] Drake et al.,[399] Kohse-Höinghaus et al.,[97] Desgroux et al.[345] and Reisel et al.[346]), and several molecules (including O_2, OH and NO) have been observed in modified high-pressure internal combustion engines (see for example the experiments of Suntz et al.,[400] Becker et al.,[401,402] Arnold et al.,[403,404] Andresen et al.[146,405] and Koch et al.[406]). These pioneering experiments clearly demonstrate that laser-induced fluorescence is well-suited to the characterization of combustion systems at high pressures. In order to interpret the wealth of information that can, in principle, be obtained from combustion processes of practical relevance using LIF, quantitative evaluation of the measured signals, however, becomes increasingly important.

Several aspects of quantitative LIF measurements have been presented in more detail in previous sections. The present section will specifically describe the influence of high pressures on laser-induced fluorescence measurements; also, advantages and limitations of several different LIF strategies will be discussed with respect to their applications at high pressures. Furthermore, a brief comparison with alternative, non-linear techniques, including electronically resonant CARS and degenerate four-wave mixing (see also Section 6.3) will be attempted. Some specific aspects concerning two-dimensional imaging pro-

cedures will be discussed in further detail in Section 6.2.

4.5.1. Linear LIF at high pressure

Collisions restrict the range of application for radical concentration measurements with LIF. As an example, in a flame at atmospheric pressure, not even one of 300 excited OH molecules in the ($A^2\Sigma^+$, $v' = 0$) state will radiate; a natural lifetime on the order of 700 ns compares with an effective lifetime of about 2 ns. At higher pressures, the problem becomes even more acute. Besides increasing collision rates, collisional line broadening becomes important. We have systematically studied this effect in flat, premixed methane/air flames at 1–10 bar.[97] In our experiment, the OH lineshape at 1 bar was dominated by Doppler broadening, whereas collisional broadening essentially determined the lineshape at pressures above 5 bar. With a fixed laser bandwidth of $0.2\ cm^{-1}$, the decreasing spectral overlap of the laser with the absorption line with increasing pressure would lead to a signal loss of about a factor of 2.6 between 1 and 10 bar, in addition to the factor of 10 lost by quenching, providing the OH number density was constant. Extrapolating these experimental results to pressures above 10 bar, an increase of one order of magnitude in pressure would cause a decrease in the fluorescence signal by two orders of magnitude due to quenching and pressure broadening (at pressures above 5 bar, the lineshape is expected to increase linearly with pressure), again assuming the worst case of constant OH number density. Under our conditions, however, the OH number density increased by about a factor of 3 between 1 and 10 bar, the observed signal loss in the burnt gases at 6 mm was thus only about a factor of 6.

Line broadening has an additional, significant effect in LIF experiments at high pressure: the spectral structures which may be well separated at 1 bar tend to merge with increasing pressure. This is illustrated in Fig. 21. With measured collisional broadening coefficients for the burnt gas of a methane/air flame,[407,97] which were found to be in good agreement with individual broadening coefficients determined by Rea et al.,[408,409] spectra of the OH (1,0) S branch were simulated for similar flame conditions at 1, 30 and 100 bar. Whereas in this case, the individual lines appear to be distinguishable even at very high pressures due to the extremely large spacing between the line centers, more dense parts of the OH spectrum would exhibit only small modulations on top of a broad spectral structure. NO spectra in a N_2/CO_2 or He atmosphere at 300 K and 8 bar were observed to be almost unstructured.[410] As a consequence, full spectral modelling of the excitation/emission process may be required. Also, the pressure range for application of two-line temperature meas-

urement procedures (see Section 4.4) appears limited.

Without further systematic studies, it is not easy to predict the influence of collisions for other radicals of interest, or for different flame conditions and pressure ranges. The effects of pressure on measured signal and detection sensitivity will also depend on the experimental equipment and procedure. For these reasons, alternative LIF strategies which are less sensitive to collisional effects have gained increasing attention within the last few years.

4.5.2. Predissociative LIF (LIPF) at high pressure

The principle of LIPF has already been mentioned before: if predissociation is the dominant loss process in the excited state, the fluorescence signal may be reduced (due to the loss of population by predissociation), but insensitive to quenching. For example, in flames at atmospheric pressure, detection of OH with linear LIF is more than an order of magnitude more sensitive than with LIPF; however, the quantum yield for linear fluorescence decreases significantly with increasing pressure, whereas it is about constant for LIPF as long as the predissociation lifetime (which is pressure-independent) is short enough. For variations of the OH quenching rate by a factor of two (typical for turbulent flames), the linear LIF signal varies by the same amount, whereas the LIPF signal changes by only 5%. At 30 bar, the predissociation and quenching rates for OH become approximately equal. Then, LIPF is only about a factor of two less sensitive than linear LIF, and a variation of the quenching rate of a factor of two changes the LIPF signal by more than 50%. Above 30 bar, differences between linear LIF and LIPF disappear for OH measurements. Some comments on the advantages and limitations of LIPF and on its correct application are given by Koch et al.[406] Further considerations are found in articles by Andresen et al.,[146] Seitzman,[411] Seitzman and Hanson[412] and Quagliaroli et al.,[370] and a quantitative comparison of LIF and LIPF detection of OH under identical flame conditions at 1 bar has been performed by Ketterle et al.[413]

Depending on quenching rate and predissociation lifetime, the use of LIPF as a fully quantitative technique is restricted to a certain pressure range; for OH detection in flames, this appears to be the range between about 1–7 bar. This implies, as has been stated before, that a dependence of the LIPF signal on collision processes is not introduced by energy transfer in the excited state (requiring suitable spectral filtering) or in the electronic ground state (saturation should be avoided). Above approximately 7 bar, quenching corrections may become necessary for most flame conditions. Collisional broadening may also affect line-shapes of predissociative transitions, depending on ambient pressure and collisional envi-

ronment, although the lineshape will be dominated by predissociation at 1 bar.

Part of the success of LIPF originates from the use of high-power excimer lasers. Sufficient signals for two-dimensional imaging can be obtained in a research engine under near-realistic combustion conditions, as was demonstrated by Andresen et al.[146,405] Suitable predissociative transitions can be excited with ArF or KrF laser radiation for the detection of O_2 (Wodtke et al.[414]), OH and H_2O (Meijer et al.,[415] Engel et al.[416]). Predissociation lifetimes are in the order of 2–30 ps for O_2 (Lewis et al.,[385] Kim et al.[417]), 2.5 ps for the H_2O $\tilde{C}^1B_1$ state (Meijer et al.[415]) and 100 ps for OH (Gray and Farrow,[367] Heard et al.,[368] Yarkony[369]). With these three important molecules, indicators for several different combustion phases are accessible by LIPF. O_2 and OH LIPF have been applied to high-pressure combustion systems (Andresen et al.[146,405]). H_2O LIPF, however, was initially studied in a low-pressure cell; the $\tilde{C}^1B_1$ state was excited by a two-photon transition with KrF laser radiation and the H_2O fluorescence in the $\tilde{C}^1B_1–\tilde{A}^1B_1$ transition was monitored (Meijer et al.,[415] Engel et al.[416]). There is also the possibility to detect either the OH $(A^2\Sigma^+)$ photofragment by emission (Goss et al.[418]) or, in a more indirect measurement, the OH $(X^2\Pi)$ produced from H_2O photodissociation;[419] both approaches have been used in flow tagging applications. As an alternative, Seitzman[411] suggested single-photon excitation of H_2O to the dissociative $\tilde{A}^1B_1$ state by ArF laser radiation and detection of the resultant OH $(X^2\Pi)$. High-temperature absorption coefficients of H_2O at 193 nm are significant (Davidson et al.,[89] Kessler et al.[420]), and OH is produced very efficiently from vibrationally excited H_2O.[421,422] Although OH originating from H_2O photolysis in a methane/air flame could be detected in a two-dimensional image with high signal levels, this approach is questionable since it does not distinguish between natural OH concentrations in the flame and H_2O. Most recently, Pitz et al.[386] have demonstrated direct detection of H_2O by two-photon LIPF in an atmospheric H_2/air flame. They conclude from their results that H_2O detection by spontaneous Raman scattering is preferable—when applicable—at temperatures above 1000 K, whereas LIPF might be considered as an alternative at lower temperatures.

For quantitative measurements with LIPF, interferences from photodissociation should be avoided. Besides the photolytic formation of OH and H atoms discussed above, irradiation of O_2 with UV laser light may produce significant amounts of oxygen atoms (Goldsmith[423]). In complex chemical environments, photolytic processes can hardly be ruled out; most sources of interference can, however, be detected by systematic absorption/emission spectroscopy over the wavelength range of interest. Rapid measurements of this type using a CCD camera in combination with a spectrometer have recently been

demonstrated by Reckers et al.[424] The use of longer excitation wavelengths such as those proposed by Kim et al.[417] and Dreier et al.,[425] who used stimulated Raman shifting in H_2 or D_2, may assist in avoiding photodissociation; also, they may offer access to less congested spectral regions than, in particular, the ArF laser tuning range.

Spectral signatures of several species are found within the tuning range of excimer lasers, and this can be of great advantage for multi-component investigations. Even if only qualitative concentration distributions are obtained, correlated information on several species is of great value for the characterization of practical combustion systems.

4.5.3. Electronically resonant CARS at high pressure

Although it has not found widespread application due to its complexity in both experimental apparatus and theory, electronically resonant CARS is a very sensitive non-linear technique which is well-suited to applications at high pressure. A short summary of selected experimental work on resonance CARS and of some interesting features of the technique with respect to concentration measurements of minority species in combustion will thus be given.

With CARS, mole fractions of $> 0.5\%$ are typically detectable in flames.[2] In a few special situations, OH has been successfully detected in photolysis experiments by CARS,[426,427] and CARS detection of large O atom mole fractions (3–4%) in flames[428] has also been demonstrated. However, the sensitivity can be greatly enhanced by tuning one or several of the three CARS beams into resonance with electronic transitions. With resonance CARS, several combustion radicals have been detected, including C_2,[429–431] OH,[407,432,433] NH_2[434] and NO_2.[435] A comprehensive theoretical treatment of the technique is given by Attal-Trétout et al.[433,436]

The main feature which makes resonance CARS attractive for combustion diagnostics is its non-linear nature which gives rise to a coherent signal beam. Also, the signal increases with pressure according to a square dependence on the species number density; however, an inverse dependence of the signal on the linewidth for the three molecular transitions involved may offset this effect due to increasing collisional broadening with pressure. As a consequence, the resonance CARS intensity is influenced—in a similarly complex fashion as a LIF signal—by the collisional environment. The sensitivity of both techniques to collisions may, however, be quite different in a given situation.

In methane/air flames at pressures up to 10 bar, Attal-Trétout et al.[407] measured relative OH concentration profiles which were then related to absolute profiles with the aid of the known equilibrium concentration in the burnt gas of the flame at atmospheric pressure. Their results compare favorably with OH concentrations measured by linear LIF

and calibrated by absorption in the same flames.[97] Also, excellent agreement at 1 bar was found with absorption measurements by Cattolica[98] in a very similar flame and with the OH profile predicted by a flame model.[437] For the experimental conditions in this comparative study, linear LIF and resonance CARS offered similar detection sensitivities for the OH radical; based upon signal-to-noise considerations, both techniques would permit detection of OH in similar flames at substantially higher pressures. Attal-Trétout et al.[438] have measured OH concentrations in methane/air flames of up to 20 bar. They have noted that the detection sensitivity was 7 ppm in a stoichiometric flame at 1 bar whereas it degraded to 500 ppm at 20 bar due to the considerable pressure dependence of the resonance CARS signal.

4.5.4. Comparison with saturated LIF and DFWM; further developments

Although it would be premature to judge the quantitative measurement capability of the techniques discussed above at pressures between 20 bar and about 60 bar, some conclusions seem permitted at this stage. It appears highly probable that several important species in combustion can be detected by various LIF strategies in flames at these pressures; either by point-wise measurements—which may, based on suitable calibration procedures, yield absolute number densities—or by single-pulse two-dimensional imaging, which may be less quantitative, but is extremely valuable for capturing important structural features of the flow. Imaging along a line in combination with good spectral resolution will be useful in identifying sources of interference under conditions where spectra tend to be congested or where high-power radiation may lead to unwanted photolytic products. Further investigations of interfering processes, in particular in hydrocarbon flames at high pressures, are recommended if excimer radiation at 248 or 193 nm will be used. Also, systematic studies of collisional broadening as a function of molecular quantum state, collision partner, temperature and pressure (such as the recent experiments of Chang et al.[439] and Kessler et al.[440] will be very valuable for predicting spectral structures and identifying suitable excitation transitions. Finally, measurements of effective fluorescence lifetimes for a range of typical combustion conditions at elevated pressures are urgently needed.

Compared to linear LIF, saturated or predissociative fluorescence may be advantageous if the quenching behavior of the system is not well known or if quenching varies considerably within the observation volume. Saturated LIF, in particular, offers high signal strengths. In Section 4.3, several recent studies were described which reported quantitative, point-wise OH and NO detection in hydrocarbon flames at pressures up to 12 bar.[340,342,344–346,399] For high-pressure applications, it should be kept in mind,

however, that the theory of saturated LIF, especially with respect to broad-band detection, is just developing and is far from being generally applicable. More information on collisional quenching and energy transfer is essential for a quantitative evaluation of high-pressure saturated LIF experiments. Excitation with picosecond laser pulses—provided that sufficient power densities are available—will be preferable to the more traditional nanosecond laser arrangements in order to avoid some of the complications encountered with level-dependent collisional energy transfer and population depletion.

As a prerequisite for LIPF, suitable predissociative transitions must be accessible within the tuning range of pulsed lasers. These conditions are met for a few combustion-relevant species, but not for all (e.g. not for the important NO molecule). LIPF of OH appears well suited for application in high-pressure combustion situations where high number densities may lead to significant absorption of the laser light or to fluorescence trapping. Excitation of predissociative transitions together with detection of fluorescence from high-lying states may be the most attractive method to detect OH in flames of large dimensions, such as that of Versluis et al.[441] or at very high pressures. The quenching-insensitive nature of LIPF, may, however, be invalid at elevated pressure, depending on the relative magnitude of the predissociation and collision rates.

Although it has been demonstrated that resonance CARS is well suited to the measurement of radical concentrations in flames at high pressures, the complexity of both experiment and theory preclude widespread use of this technique. Also, resonance CARS has no imaging capabilities. Thus, it will mainly be attractive as a complementary technique, if the beam-like nature of the signal is an issue (e.g. in combustion facilities with poor optical access).

Degenerate four-wave mixing (DFWM) has many similarities to resonance CARS and, in addition, shares the possibility for performing two-dimensional imaging measurements with LIF. The technique will be described in further detail in Section 6.3. Some preliminary studies at high pressure have been performed, including those on OH detection by Feikema et al.,[442] Bervas et al.[443] and Domingues et al.[444] and on NO by Plath et al.[410] Bervas et al.[443] performed DFWM measurements under the same flame conditions studied before with OH resonance CARS.[407,438] They discussed in detail the signal strengths and noise levels to be expected with both techniques. Whereas the detectivity for OH in an atmospheric methane/air flame was similar, they failed to observe OH DFWM signals above 8 bar, although OH could still be detected with resonance CARS at 20 bar. This was due to beam steering problems in the DFWM experiment, which could, however, in principle be reduced by using a phase-conjugate backward pump beam, such as that demonstrated by Winter et al.[445] Feikema et al.[442] and

Domingues et al.[444] have made similar observations. In their flames of 1–9 bar, they compared absorption, TOPLIF, DFWM and an approach which was analogous to the method employed by Winter et al.,[445] the so-called double phase-conjugate four-wave mixing technique, DPCFWM. They reported increasing problems with beam steering with increasing pressure. Results using all other techniques agreed reasonably well; however, OH LIF was about two orders of magnitude more sensitive than DFWM.[442] Before DFWM (or DPCFWM) can be routinely used at high pressure, further questions have to be systematically addressed, including the effects of collisions on signal intensity and lineshape, the influence of the velocity distribution and the treatment of (incomplete) saturation.

As a final remark, the measurement of temperature in high-pressure combustion systems by the aforementioned techniques deserves further attention. Although a few thorough studies have already demonstrated the potential of some of these methods at moderate pressures, a more generally applicable, well-examined, reliable instrument for the instantaneous measurement of two-dimensional temperature distributions under these conditions has yet to be developed.

5. MULTI-PHOTON SPECTROSCOPY (MPLIF AND REMPI)

Multi-photon techniques, which include multi-photon laser-induced fluorescence (MPLIF) and resonance-enhanced multi-photon ionization (REMPI), provide additional possibilities of detecting minority species in combustion. In particular, these techniques offer excellent alternatives if the frequencies of suitable absorption transitions are difficult to access with conventional laser radiation or if the detected species has no known emission spectrum. MPLIF has mainly served as a means of measuring the concentrations of the light atoms H, O and N in flames, whereas REMPI has provided detection schemes for important hydrocarbon radicals including CH_3, CH_2OH and selected halogenated species as well as for some homonuclear diatomics including H_2 and N_2. In the following, the principles of MPLIF and REMPI will be briefly discussed, and then some recent experimental results will be presented. A more detailed treatment of multi-photon spectroscopy can be found in related books and review articles (see, for example Levenson,[446] Bischel et al.[447] and Halpern et al.[448]).

Some important features of MPLIF and REMPI are illustrated in the schematic energy level diagram in Fig. 22; the corresponding diagram for conventional LIF is included to facilitate a comparison. In this example, excitation of an atomic species is assumed; characteristic radiative and collisional transfer processes are indicated. For the linear, saturated or predissociative LIF measurements discussed
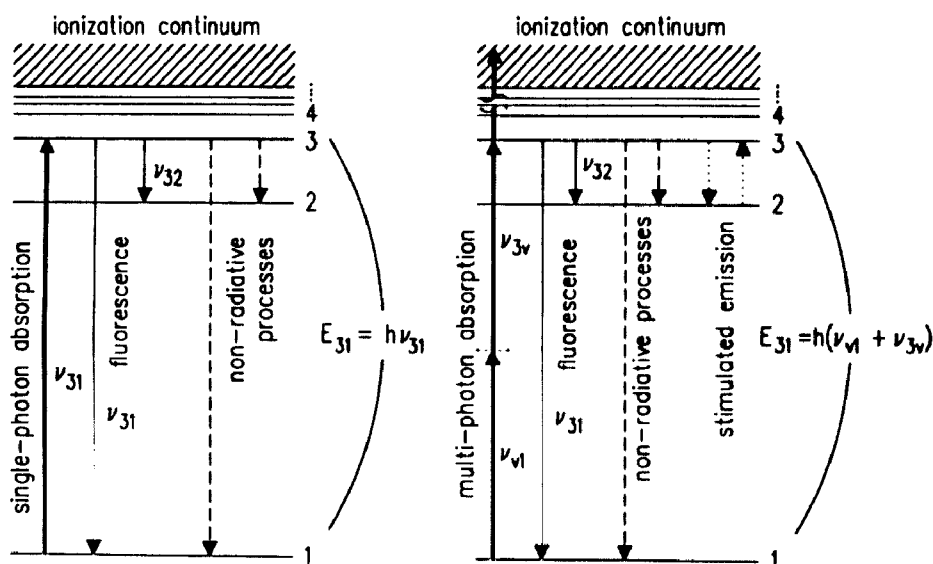
ionization continuum

$E_{31} = h\nu_{31}$

single-photon absorption | ν_{31} | ν_{31} | fluorescence | ν_{32} | non-radiative processes

ionization continuum

$E_{31} = h(\nu_{vl} + \nu_{3v})$

multi-photon absorption | ν_{3v} | ν_{vl} | ν_{31} | fluorescence | ν_{32} | non-radiative processes | stimulated emission

Fig. 22. Schematic energy level diagram illustrating the relevant processes for LIF (left) and multi-photon techniques (right).

before, the atom or molecule under study absorbs one photon. The energy $E_{31} = h\nu_{31}$ of this photon of frequency ν_{31} then matches the energy difference between levels 1 and 3. The excited species in level 3 may emit fluorescence of frequencies ν_{31} and ν_{32} or experience non-radiative deactivation. In MPLIF schemes, the atom or molecule simultaneously absorbs *more than one* photon; two in the example of Fig. 22. In this case, the sum of the energies of both photons corresponds to the energy difference between levels 1 and 3, $E_{31} = h(\nu_{3v} + \nu_{v1})$. As an instructive picture, one can imagine that the first photon excites a 'virtual' level,* and that the second photon then leads to an excitation of level 3. Both frequencies may be the same, so that a single laser may be used, or they may be different. Similarly as in one-photon LIF schemes, the excited state emits fluorescence which may be detected as a measure for the concentration of the species; collisional deactivation needs to be accounted for as usual.

The REMPI approach also starts with an excitation of level 3 by one or by several photons; two in the example of Fig. 22. Upon absorption of one or more additional photons, the excited atom or molecule is then ionized. The electrons or ions created by this process can be detected with very high efficiency. Compared to non-resonant multi-photon ionization, transition probabilities for the REMPI process are typically larger by several orders of magnitude. Furthermore, REMPI spectra exhibit characteristic features of the resonant transition. This is an important prerequisite for selective species detec-

tion and efficient discrimination against a potential background of charged particles. Since REMPI detection requires the use of a probe in the vicinity of the observation volume, this technique cannot be considered truly non-invasive. Therefore, it has been primarily used for monitoring species that fluoresce very weakly or do not emit radiation due to rapid predissociation.

An additional feature of multi-photon absorption is of some interest for combustion diagnostics. Depending on the order m of a multi-photon process (corresponding to the number m of photons required for the absorption step), different selection rules apply. Therefore, accessible excited states are not necessarily the same as for one-photon transitions. For this reason, a population inversion between the excited state 3 and a lower state 2 may occur, if 3 cannot easily be depopulated by emission. Under suitable conditions, stimulated emission of frequency ν_{32} (see Fig. 22) may then be detected. Stimulated emission may be a very effective depopulation process of the upper level and thus may have to be accounted for in quantitative measurements. Also, this stimulated emission scheme has been used in combustion systems for the detection of several atomic and molecular species; it will be briefly described in Section 6.4.

5.1. Specific Considerations for the Application of Multi-photon Techniques

Whereas for one-photon excitation of atoms and small molecules, transition probabilities may be known with sufficient accuracy, this is usually not the case for multi-photon absorption. Also, photoionization cross sections are often not known. If high-lying molecular levels are involved, as, for example

---

* Short-lived 'virtual' energy levels can be understood as a consequence of Heisenberg's uncertainty relation. The transition probability for multi-photon processes is not zero even at considerable distances from 'real' energy levels and it increases in regions with a large density of states.
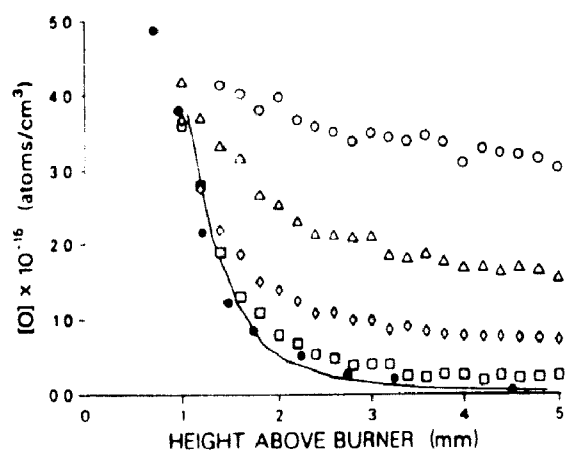
Fig. 23. Influence of the laser power density on the apparent O atom concentration in a lean H_2/O_2 flame at atmospheric pressure.[423] Solid line: O atom concentration calibrated with OH measurements (partial equilibrium assumption); filled circles: REMPI measurement; open symbols: MPLIF measurements; relative intensities: 1 (squares), 10 (diamonds), 30 (triangles) and 300 (circles).

in some REMPI schemes for detection of hydrocarbon radicals, information on molecular constants or spectral structure may also be lacking. In addition, the non-linear dependence of the signal on laser power density may preclude an exact determination of the observation volume (a similar problem was encountered for saturated LIF, see also Section 4.3). It therefore appears that the only reliable procedure which enables quantitative application of multi-photon techniques is a calibration with known concentrations of the investigated species. These may, in special cases, be derived from equilibrium considerations or are, more generally, produced in an independent system.

The transition probability for absorption of more than one photon decreases rapidly with increasing order m of the process. Therefore, considerable laser power densities are required, and these high intensities may cause photolytic generation of unwanted intermediates and products in the system under study. Photodissociation of H_2O and O_2 in flames resulting in the formation of OH, H and O atoms has been observed.[422,423] In addition, with UV laser light, O atoms can be efficiently created in room air from O_2[449] and from other precursor molecules including NO and NO_2.[450] Interferences from photolytic production of C_2 in a wide wavelength range have been reported by Aldén et al.,[451] Goldsmith and Kearsley[452] and Bengtsson and Aldén.[453,454] Any application of multi-photon schemes in combustion systems should therefore be preceded by experimental verification that photolytic processes do not disturb the actual measurement. For this, it may not be sufficient to measure photodissociation probabilities of stable precursors at room temperature, since radicals or vibrationally excited molecules present in flames may offer additional photodissociation channels.

Photolytic interferences may be examined by several strategies. A measurement of the so-called 'power dependence'* is recommended. A power dependence with a slope $> m$ most probably indicates photolytic contributions since photodissociation requires at least one additional photon. However, the slope does not react very sensitively to these processes due to the logarithmic relation involved; also, saturation or photoionization which influence the slope in the opposite direction may simultaneously be present and obscure photolytic interferences. Additional tests may thus be required. Concentration measurements at different laser intensities may reveal photodissociation problems. An example is given in Fig. 23; here, O atoms were detected by two-photon LIF in a H_2/O_2 flame at atmospheric pressure.[423] The laser intensity was varied by a factor of 300. Whereas O atoms detected at the highest laser intensity were almost exclusively laser-created, the O atom concentration naturally present in the flame was obtained with the lowest laser power density. In some cases, two-laser schemes allow simultaneous detection of both photolytic products; for example, in the experiment of Goldsmith,[422] OH was detected while monitoring H atoms, using laser light at 310 and 205 nm, respectively. Thus, H_2O was identified as the most probable precursor for the photolytic production of H atoms.

In conclusion, a good strategy to preclude ambiguities in the application of multi-photon techniques to combustion systems should rely on a compromise between the longest suitable wavelength (minimizing the risk of photolytic fragmentation) and the lowest possible order of the multi-photon excitation process (ensuring sufficient detection sensitivity).

5.2. Detection of Atoms with MPLIF and REMPI

Several atoms including H, O, N and C have been detected in combustion systems with multi-photon techniques. In many flames, H and O atoms are present in quite large concentrations—similar to the OH radical—and they participate predominantly in pyrolysis and oxidation mechanisms. They are involved in radical-producing, chain branching and recombination reactions and thus play a vital role in many combustion processes including ignition, flame propagation, heat release and flame quenching. In addition, H atoms diffuse extremely rapidly in flames, and H atom concentrations may thus be indicative of diffusion processes. A comparison of measured and simulated H atom concentrations can

---

*The dependence of the signal intensity on the laser power density is often represented with a log-log diagram; for a multi-photon process of order m, where the signal depends on the mth power of the laser power density, a straight line with slope m is expected.

be particularly valuable for examining the modelling of diffusion in current flame codes.[455] N and C atoms are very reactive intermediates and are involved in mechanisms producing NO in flames. The detection of these atoms is of significant interest for the investigation of fuel degradation and pollutant formation.

5.2.1. Detection of H atoms

Some of the early multi-photon experiments leading to the detection of H atoms have been performed in cells, including that of Bjorklund et al.,[456] who used (2 + 1) REMPI* with resonant excitation of the 2s state by laser light of 266 and 224 nm and subsequent photoionization with radiation of either wavelength. Two-photon LIF detection of the H atom requires a shorter excitation wavelength since a higher electronic state must be excited.† Bokor et al.[457] have used either two photons of 205 nm or a combination of 193 and 218 nm for the excitation of the $n = 3$ state; (3–2) fluorescence was detected at 656 nm. Goldsmith[458] and Lucht et al.[459] demonstrated the first observations of H atoms in a flame by REMPI and MPLIF, respectively.

Several other schemes have been used for multi-photon detection of H atoms: (3 + 1) REMPI at 365 nm,[460] (2 + 1) REMPI at 243 nm,[461,162] three-photon excitation to the $n = 4$ state with 292 nm radiation and detection of the fluorescence at 486 nm,[462] and two-step excitation with two photons of 243 nm and one of 656 nm.[463,464] In the latter experiment, the second step, exciting the (2–3) transition, was saturated, and (3–2) fluorescence was monitored. Goldsmith[465] compared several detection schemes for H atoms in low-pressure flames and recommended the two-step method as the most reliable one. Its main disadvantage is the need for two lasers. Also, photolytic interferences caused by 243-nm radiation have recently been reported by Goldsmith:[466] in a two-photon process, H_2O may be excited and predissociate to yield H and OH. Due to the higher order of this interfering process, a reliable measurement of H atom concentrations with the two-step method was still possible in rich ethane/air flames, where two-photon LIF with 205-nm excitation failed. Goldsmith and Laurendeau[467] have—in an attempt to reduce the complexity of this scheme—modified the two-step method and instead

saturated the (2–4) transition at 486 nm. Due to particular coincidences in the H atom spectrum, the same laser can then be used for the two-photon transition and the saturation step. However, photodissociation at 243 nm could not be avoided and, in addition, laser-created C_2 radicals which radiate near 486 nm interfered with the H atom fluorescence detection.

These examples illustrate that none of the possible multi-photon excitation/detection schemes can be applied without problems in a flame environment. The relative influence of the undesired processes depends sensitively on experimental parameters as well as on the particular composition at the observation volume. Important quantities in this respect are the excitation and detection wavelengths, the laser power density, the natural atom concentration in the flame and the concentrations of potential precursors. Low-pressure H_2/O_2 flames with comparatively high H atom concentrations are least problematic. With increasing pressure and increasing number of species, the application of multi-photon techniques becomes more difficult, and quantitative measurements may be restricted to a few special combustion situations.

If photolytic interferences are avoided, the H atom concentration can be determined from the measured MPLIF signal. For this, the fluorescence quantum yield must be known. In general, a measurement of the effective fluorescence lifetime provides this information. However, H atom quenching is so fast[450,468] that picosecond time resolution is required for lifetime measurements, even in low-pressure flames. Goldsmith et al.[469] have used laser pulses of 50 ps duration for the determination of effective H atom fluorescence lifetimes in a $H_2/O_2/Ar$ flame at 26 mbar. Effective lifetimes calculated for this flame composition with the measured quenching coefficients of Bittner et al.[468] are in excellent agreement with their results.

Lucht et al.[459] have attempted to minimize the influence of quenching in MPLIF measurements using a scheme which they termed PICLS, photoionization-controlled loss spectroscopy. The idea is—similar to that underlying saturated fluorescence (see Section 4.3) or LIPF (see Section 4.5)—to control the loss of population in the upper state by a process which competes with quenching. For PICLS, the dominant loss process is photoionization, which is induced by a second laser. However, the reduced dependence on quenching must be weighed against the corresponding loss of fluorescence signal. Salmon and Laurendeau[470-472] have used PICLS to measure H atom concentrations in several low-pressure flames. Comparing PICLS and MPLIF results, they have also inferred electronic quenching rates.[473] An application of PICLS in flames at atmospheric pressue would require far higher laser power densities for the ionization step and has thus not been demonstrated to date.

---

*REMPI processes are usually characterized by the number of photons required for the excitation of the resonant intermediate state and for ionization; a (2 + 1) REMPI scheme thus involves two photons for the resonant excitation and one for ionization.

†The very short wavelength corresponding to the only allowed (one-photon) transition from the electronic $n = 2$ state, 2p-1s, cannot usually be detected in flames. Therefore, $n > 2$ has to be excited if fluorescence detection is desired.

A calibration with a known atom concentration allows conversion of the measured—and, if necessary, quenching-corrected—MPLIF signals to an absolute scale. Goldsmith[461] and Salmon and Laurendeau[471] have used an indirect calibration method. They have assumed that in the burnt gas regions of their flames, H and OH concentrations are in partial equilibrium. From independent measurements of temperature and OH concentration, the H atom number density in the burnt gas can be estimated and serves as a reference for the entire H atom profile across the flame front. Whereas the assumption of partial equilibrium for these radicals seems justified for the atmospheric pressure flame of Goldsmith,[461] it may be questionable for low-pressure flames. Also, uncertainties in the temperature and OH concentration measurement influence the H atom determination. We have therefore relied on a different calibration strategy,[450,474,475] which uses a known atom concentration prepared in a discharge flow reactor. Since this technique was also applicable for the measurement of O[476] and N atom concentrations[477,478] in flames, some important features will be described here.

A microwave discharge in N_2 or H_2 with helium as a carrier gas generates N and H atoms; O atoms are produced by the fast reaction of N with NO. By fast gas-phase titration reactions (see, for example, the article of Howard[479] and references therein), the atom concentration in the flow reactor can be determined. The fluorescence signal originating from the unknown atom concentration in the flame is then measured under identical excitation and detection conditions as that produced by the reference concentration in the flow reactor where laser performance, observation volume and detection efficiency remain unchanged. This approach has the advantage that quantities which may not be known precisely, including two-photon excitation rate, ionization rate and laser power density distribution across the observation volume are of minor influence in the evaluation of absolute atom concentrations.

For a quantitative measurement, several parameters of influence need to be considered. First, the collision environment in the flow reactor is different from that in the flame; this variation must be taken into account. This is done using measured temperature profiles, simulated quencher compositions and measured quenching coefficients. Although the temperature dependence of most quenching coefficients is not known at flame temperatures, several important rate coefficients for H and O atom quenching were found to be nearly independent of temperature in the range of 300–700 K;[468] extrapolation to flame temperatures thus seems permitted in a first approximation. The differential equations governing the time-dependent populations in the atomic levels involved (compare with Fig. 22) are solved using effective quenching rates for the flow reactor and flame environment. Fluorescence signals measured in both

systems can thus be related. Since only the ratio of the populations in the flame and the reference system enters the calibration, the atom concentration is not very sensitive to the quenching rate.[475] Besides quenching variations, temperature-dependent ground state populations and absorption lineshapes* may have to be considered for O and H concentration measurements, respectively.

With this calibration procedure, absolute H atom concentrations were measured in 96 mbar $H_2/O_2/Ar$ flames at different stoichiometries. Very low laser power densities (below 5×10^7 W/cm^2) were used. Power dependences and measurements at different laser intensities gave no indications of interferences by photodissociation. This observation was confirmed by the subsequent experiments of Goldsmith[465] in similar flames. In addition, power dependences were simulated using cross sections for two-photon absorption and photoionization calculated by Lambropoulos,[481] the photodissociation rate for H_2O at 205 nm estimated by Goldsmith,[422] experimental laser power densities and measured effective quenching rates. Thus, potential counteracting influences of photoionization, saturation and photodissociation could be detected and the sensitivity of the H atom concentration to a variation of these parameters was determined. Uncertainties in the absolute H atom concentration were in the order of 25–30%. A typical experimental result is presented in the upper panel of Fig. 24, together with the concentration profile simulated by a flame model.[482,336]

Quantitative measurements of H atom concentrations by REMPI were attempted in a series of recent experiments.[162,483,484] The authors have determined relative H atom profiles in a laminar CH_4/air flame at atmospheric pressure. In order to increase the signal-to-noise ratio, the resonant two-photon excitation was performed with counterpropagating laser beams in a so-called 'Doppler-free' arrangement.[483] With this set-up, the thermal velocity distribution of the H atoms was of minor influence on the absorption lineshape. Goldsmith and Rahn[485,486] have used a similar arrangement for the investigation of pressure broadening in flames; in the experiment of Smyth and Tjossem,[483] the increased sensitivity allowed reduction of the laser power density. This was of particular importance in the rich flame zones, where a multitude of interfering photodissociation

---

*The overlap of laser and two-photon absorption lineshapes may decrease with increasing temperature, resulting in a loss of fluorescence intensity; in our experiments, this effect was only significant for the detection of H atoms, which exhibit the largest velocity. The calculation of an appropriate correction factor (in the order of 1.2–1.3 at 1500–2000 K) is detailed in the PhD thesis of Bittner;[475] it is based upon the solution of the density matrix equations in the limit of a weak laser field given by Dai and Lambropoulos.[480]
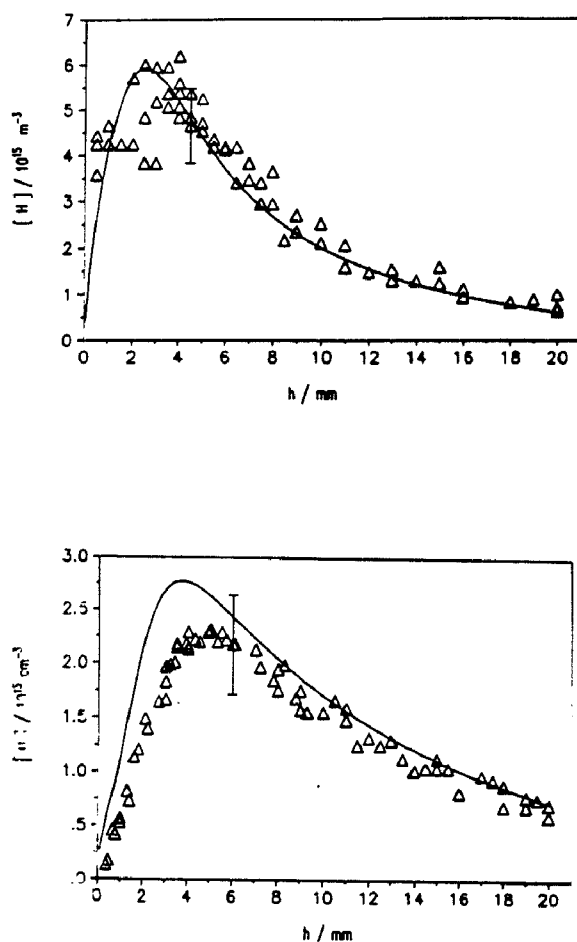
FIG. 24. Absolute H (top) and O atom concentrations (bottom) in a lean $H_2/O_2/Ar$ flame at 95 mbar. [475] Simulations with a flame model (Warnatz)[482, 336] are indicated by the solid lines.

FIG. 25. Efficiency curve for the detection of H atoms by REMPI in a laminar methane/air diffusion flame at 9 mm above the burner. [484] Lower panel: calibration with CO (solid squares), and with Ar (open squares); upper panel: temperature distribution under identical conditions.

and photoionization processes could occur. In contrast, the H atom concentration profile could not be measured under their conditions with the conventional set-up where two photons were absorbed from the same laser beam.

Smyth and Tjossem[484] have developed a calibration procedure for the determination of relative H atom concentrations from measured REMPI signals. The detection efficiency for electrons was obtained in two independent experiments. For this, they have detected Ar by REMPI and mass spectrometry; in addition, REMPI and LIF signals following two-photon excitation of CO were measured simultaneously. Figure 25 shows the detection efficiency measured across the flame by both methods. This calibration curve was then used in the evaluation of relative H atom concentrations under the same flame conditions. The significant dependence of the detection efficiency on the local flame conditions illustrates— as one of the most important results of this study— that an independent calibration is essential for a quantitative application of REMPI. Measured signal intensity distributions will not directly reflect the relative concentrations in most cases. Also, the calibration curve in Fig. 25 is only valid for this particu-
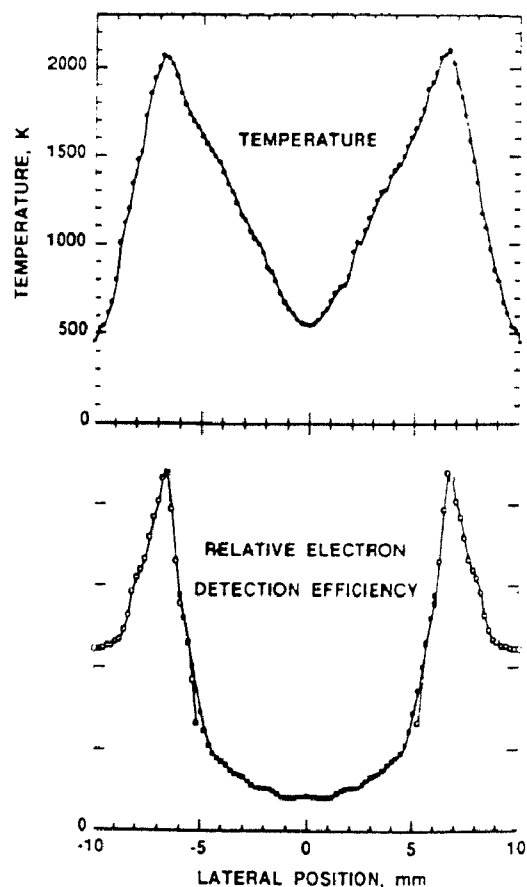
lar flame condition. A REMPI measurement in flames, although it may be more sensitive and less subject to photolytic interferences than the respective MPLIF scheme, can thus be quite tedious. Because of this need for independent calibration and because of the ambiguities introduced by the probe, MPLIF measurements are preferable, if a suitable excitation/detection scheme can be found.

5.2.2. Detection of O Atoms

Oxygen atom concentrations have been determined by multi-photon techniques in a variety of reactive systems. Bischel et al.[487,488] excited the O (3p ^3P) state with two photons of 226 nm and detected the (3p ^3P-2s $^3S^0$) fluorescence at 845 nm. The same scheme was applied by Aldén et al.[489] in the first MPLIF measurement of O atoms in a flame. Laser radiation at 226 nm was also used in a (2 + 1) REMPI process.[490,461] O atoms have been detected by multi-photon techniques in discharges,[491] plasma etching reactors,[492,493] near hot catalytic surfaces[494,495] and in an investigation of ignition processes.[496] Goldsmith[461] determined O atom concen-

trations in a H_2/O_2 flame at atmospheric pressure and used a calibration relying on partial equilibrium assumptions, and Smyth and Tjossem[483] have measured relative O atom distributions in a laminar CH_4/air diffusion flame.

For absolute measurements of O atom concentrations, information on collision rates and on photolytic interferences is required. Photolytic processes capable of generating O atoms in combustion environments have been observed by Miziolek and DeWilde,[449] Meier et al.[450] and Goldsmith.[423] In the latter experiment, vibrationally excited O_2 was identified as a source of laser-created O atoms. Quenching of O atoms with N_2 has been studied by Bischel et al.,[488] and quenching coefficients for a variety of collision partners have been measured by Meier et al.[450] and Bittner et al.[468] Dyer and Crosley[497] have investigated collisional broadening of the absorption lineshape in a Doppler-free arrangement. Miziolek and DeWilde[449] have observed that rapid energy transfer may occur between the neighboring (3p ^{3}P) and (3p ^{5}P) states of the O atoms; they detected fluorescence at 777 nm corresponding to the (3p ^{5}P-2s ^{5}S^0) transition upon excitation of the (3p ^{3}P) state. Dagdigian et al.[498] have measured rate coefficients for the energy transfer between the different fine structure levels in the triplet-quintet system.

Quantitative measurements of oxygen atom concentrations in flames have been performed by Goldsmith,[461] Meier et al.,[476] Bittner[475] and Smyth and Tjossem.[483] Whereas only relative concentration profiles were determined in the latter study, Goldsmith[461] and our own group have used a calibration with a reference concentration. In our experiments, the reference concentration was again produced in a discharge flow system.[476] The laser power density had to be kept extremely low (at about 6×10^6 W/cm^2), since it was evident from both measured power densities as well as measurements with different laser intensities that photolysis—most probably of hot O_2[423]—could interfere with the O atom detection in our low-pressure H_2/O_2/Ar flames. Attempts to estimate the photodissociation cross section from simulations of the measured power dependences were, however, unsuccessful, since this method was too insensitive.

Fluorescence quantum yields were determined directly from lifetime measurements; in contrast to the H atom experiments, nanosecond time resolution was sufficient for the H_2/O_2/Ar flames at 96 mbar. Alternatively, the contributions of the individual quenchers could be summed using calculated flame compositions along with measured room temperature quenching coefficients.[468] Since calculated effective lifetimes were found to be higher than measured ones, it was inferred that the quenching coefficient for O atom collisions with H_2O, the most efficient quencher, is temperature-dependent.[476] With our calibration method, absolute O atom concentrations were obtained in several low-pressure H_2/O_2/Ar flames at 96 mbar. Variations of the quenching efficiency between the flame and the reference system were taken into account as described before. For this, the appropriate differential equations for the time-dependent populations were solved; cross sections for two-photon absorption and photoionization were taken from Bamford et al.[499] and Saxon and Eichler.[500] A typical result is given in the lower panel of Fig. 24. From a sensitivity analysis of the measured atom concentrations with respect to important parameters including two-photon excitation, photoionization and quenching rates, experimental uncertainties were estimated to be in the order of 25–30%.

In a series of related experiments, low-pressure H_2/O_2/Ar flames at different stoichiometries were thoroughly investigated. In addition to the O atom measurements, temperature profiles and the concentrations of the two other most important intermediate species, H and OH, had already been determined in previous experiments.[328,361,474] Experimental results and simulations with a flame model established by Warnatz[482,336] agreed well for most conditions, as was expected for these flames which display rather simple, well-understood chemistry. To illustrate this, model results are shown along with the measured atom concentrations in Fig. 24. It should be noted in this context that an accurate temperature measurement is particularly important for this comparison of experiment and simulation, since temperature influences both the measurements and the model calculations.[475]

Quantitative applications of our calibration technique to hydrocarbon flames proved to be more difficult. First, the number of quenchers is larger. With nanosecond time resolution, effective lifetimes could only be determined for O atoms in several flames at very low pressures.[476] Extrapolations of quenching coefficients to flame temperatures and calculations of the chemical composition are less reliable than for the H_2/O_2 flames. Furthermore, the number of potential photolysis precursors is larger. For example, in an atmospheric pressure CH_4/air flame, the fluorescence signal originated entirely from laser-created O atoms. Also, interfering emissions at the fluorescence wavelengths, which reduced the detection sensitivity, were observed in rich hydrocarbon flames for both H and O atom detection.[474,476] A promising, novel concept was very recently demonstrated by van den Oostendorp et al.[501]; they used a Galilean telescope for shaping the laser beam—which kept the laser power density extremely low (below 0.1 GW/cm^2) while retaining sufficient spatial resolution—and achieved undisturbed O atom detection along a line in a slightly rich, atmospheric pressure methane/air flame. This scheme may be an alternative for reliable MPLIF concentration measurements in complex chemical environments.

5.2.3. Detection of N atoms

N atoms play an important role in the formation of NO in combustion systems. Depending on the particular flame conditions, reactions of N atoms with OH, NO and CH_3 may lead to the production of NO, N_2 or HCN. Also, the N atom is a key intermediate in the combustion of N-containing fuels. Detailed information on the chemistry of nitrogen compounds in combustion is found in the review of Miller and Bowman.[502] Since N atoms are typically formed only in low concentrations, their detection in a flame environment is quite challenging. Results of the few existing investigations appear contradictory. Bian et al.[503] have studied a low-pressure $NH_3/O_2/Ar$ flame with mass spectrometry and failed to observe N atoms due to the limited sensitivity of their apparatus. They assumed that the N atom mole fraction was well below 10 ppm in their flame. Taniguchi et al.[504] have detected N atoms by ESR in an atmospheric pressure methane/air flame doped with NH_3 and reported mole fractions of 5×10^{-8}. In contrast, Miller et al.[505] have estimated N atom mole fractions of 5×10^{-5}–10^{-4} for their HCN-doped $H_2/O_2/Ar$ flame at 33 mbar. In a recent study, Agrup et al.[506] have observed stimulated emission of N atoms in an atmospheric pressure NH_3/O_2 flame; a quantitative interpretation of the measured signals, however, caused considerable difficulties (see also Section 6.4). Also, Westblom et al.[507] have detected N atoms by MPLIF in different atmospheric pressure flames. Due to significant photolytic interferences, they were not able to determine quantitative N atom concentrations.

Motivated by the discrepancies observed in the results of these studies, we have investigated flames doped with different N-containing fuels and attempted to measure absolute N atom concentrations with MPLIF as a function of the dopant. Previously, MPLIF detection of N atoms using two-photon excitation at 211 nm and fluorescence detection around 870 nm had only been performed in flow reactors.[487,488,508,509] Based upon our experience with the calibration in MPLIF experiments for H and O atom detection, a similar approach was used to determine N atom concentrations in several low-pressure $H_2/O_2/N_2$ flames seeded with small amounts of HCN, $(CN)_2$ or NH_3.[477,478] Some of the results shall be summarized here.

In these experiments, typical laser power densities were in the order of 10^8 W/cm². First, $H_2/O_2/N_2$ flames at 96 mbar were studied because temperature profiles had already been determined for these conditions (Lawitzki et al.[358]). However, these investigations were not successful, partly due to interferences at the fluorescence wavelength. In the following experiments, $H_2/O_2/N_2$ flames at 33 mbar doped with 0.6% of N-containing fuels were studied. For calibration purposes, quenching coefficients at room temperature were determined.[478] Quenching co-

efficients for collisions with N_2 and Ar were in good agreement with those of Copeland et al.[508] Effective lifetimes could be measured directly only in the flame seeded with $(CN)_2$; for all other conditions, quenching rates had to be calculated relying on the measured room temperature quenching coefficients and the flame composition obtained from a computer simulation. However, a sensitivity analysis showed that the N atom concentration depended only moderately on the quenching rate, since only the ratios of the respective populations in the reference system and the flame (and not the quenching rate itself) entered the calibration. For an accurate concentration measurement, cross sections for two-photon excitation and for ionization are required; this information is lacking. For the same reason as before, the calibration was, however, not very sensitive to these quantities. The measured concentration profiles in the three flames at 33 mbar are shown in Fig. 26; the overall experimental uncertainty is about a factor of two. Mole fractions in the order of a few ppm are observed. The results demonstrate that the N atom profile depends markedly on the nature of the fuel. Attempts to simulate the measured profiles with a flame model may contribute to a more detailed understanding of some of the mechanisms leading to NO_x formation in combustion systems.

5.2.4. Detection of C atoms

Carbon atoms can be generated from various carbon-containing precursors upon irradiation with UV light. Das et al.[510] have photolyzed C_3O_2 and detected the resulting C atoms by MPLIF, following two-photon excitation at 284 or 287 nm. Sausa et al.[511] have shown that C atoms are formed following photolysis of a variety of carbon-containing molecules by ArF laser radiation. Versluis and Meijer[512] reported that intracavity absorption of C atoms, which most probably originate from photolysis of C-containing impurities in the discharge cavity, is present in many excitation spectra measured with tunable ArF excimer lasers. C atoms have also been detected in the photolysis of CO at 193 nm.[513] Furthermore, Smyth and Taylor[514] and Tjossem and Smyth[515] have observed C atoms as an undesired by-product when monitoring CH_3 or CH with REMPI. To date, it is still questionable whether C atoms naturally present in a flame can be detected in multi-photon experiments.[516]

5.3. Detection of Molecules with MPLIF and REMPI

Multi-photon spectroscopy of molecules is often performed for fundamental reasons. Almost any molecular state is accessible by combination of photons with suitable frequencies. In particular, molecular states near the dissociation limit may be studied with these techniques. A wealth of spectroscopic informa-
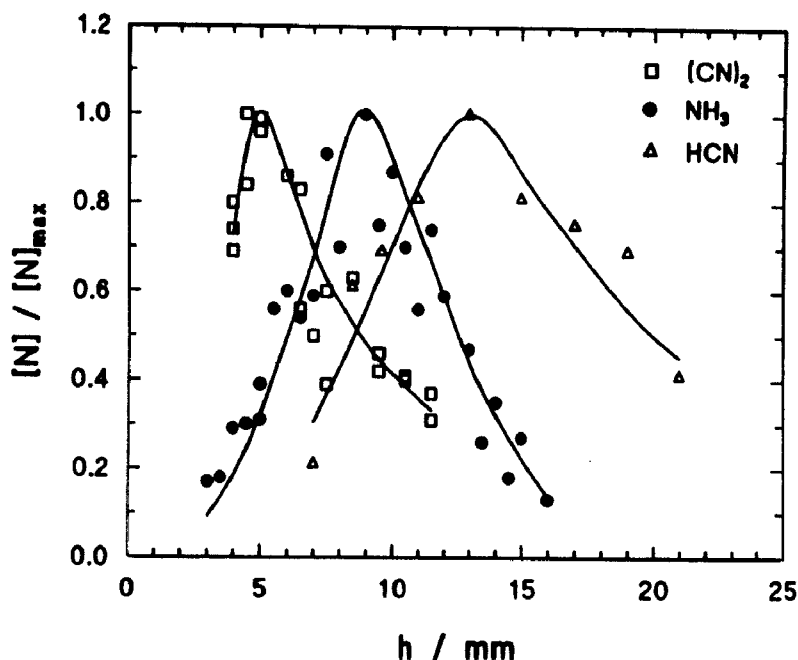
Fig. 26. N atom concentrations in $H_2/O_2/N_2$ flames at 33 mbar as a function of height above the burner for three different N-containing additives (Lawitzki et al.[477]) Squares: 0.6% $(CN)_2$, $[N]_{max}$ 6×10^{12} cm^{-3}; circles: 0.6% NH_3, $[N]_{max}$ 9.2×10^{11} cm^{-3}; triangles: 0.6% HCN, $[N]_{max}$ 1.1×10^{12} cm^{-3}; lines are drawn to guide the eye.

tion has been obtained from REMPI measurements of several diatomics present in combustion systems, including N_2,[517,518] H_2,[519,520] O_2,[521] CO[522,523] and NO.[524–526] Also, MPLIF has been utilized for the detection of combustion-relevant molecules which cannot be excited by one-photon transitions in accessible spectral regions; examples include N_2[527,528,517] and H_2.[529,530] Furthermore, NH_3, a molecule of interest with respect to NO_x formation in flames, was detected by MPLIF.[531] As an alternative to spontaneous Raman spectroscopy or CARS, MPLIF detection may be considered if single-pulse two-dimensional imaging is desired.[532,530] Even for detection of the OH molecule, for which numerous LIF experiments have been reported, two-photon excitation may be of interest. Due to the different selection rules for one- and two-photon transitions, information on the fine structure may be obtained[533] and MPLIF or REMPI signals may be calibrated by comparison with LIF results.[534] Well-suited molecules for calibration purposes are also NO and CO; experimental studies of this type have been performed by Cool[535] and Smyth and Tjossem,[484] respectively.

Many molecules of interest in combustion have been detected by REMPI. The recent review of Hudgens[536] surveys most of the related literature. REMPI is well suited to the detection of non-fluorescing molecules. For example, CH_3 REMPI has been observed in pyrolysis systems[537–540] and flames[163,514,541–543] and REMPI detection of CH_2OH in a flow system has also been reported.[544,545]

Furthermore, REMPI detection can be extremely sensitive. Sirkin and Haas[524] and Sirkin et al.[525]

observed that the detection of NO with REMPI was about a factor of 100 more sensitive than with LIF in their experiments. Rockney et al.[546] have estimated the detection limit for NO with REMPI in a methane/air flame to be approximately 25 ppm. In addition, in the flame experiments of Mallard et al.,[547] the detection sensitivity for NO with REMPI appeared to be considerably higher than with LIF. For these reasons, REMPI has been applied in several combustion-related studies as an alternative to LIF or MPLIF. For example, Tjossem et al.,[548] Bernstein et al.[549] and Cool et al.[542] have detected the HCO radical in flames, Tjossem and Smyth[515] monitored the CH radical, and Tjossem and Cool[550] reported REMPI detection of a number of species including H, O, NO, C_2O and CO. Bernstein et al.[551] have combined LIF (for detection of CH, OH and NO), MPLIF (for H and O atoms and CO) and REMPI (for H, O, CO, CH_3 and HCO) in an investigation of several low-pressure hydrocarbon flames, choosing the most reliable scheme for quantitative measurements in each case.

A most promising line of development appears to be the application of REMPI (in combination with mass spectrometry) to the ultra-sensitive detection of large hydrocarbons, especially chlorinated compounds. Due to their large number of internal energy states, these molecules are not easily detected in the low concentrations present in combustion systems. Pioneering studies have been performed by Rohl-fing,[552] Cool and Williams[553,554] and Williams et al.[555] Although an alternative approach combining photodissociation of chlorinated compounds and subsequent detection of Cl atoms by MPLIF[556] was demonstrated to be suitable as a sensitive monitor of
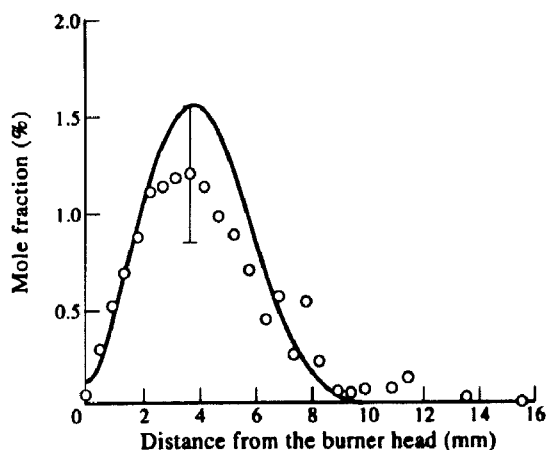
Fig. 27. Experimental and calculated CH_3 mole fractions in a 13 mbar methane/oxygen flame (Etzkorn et al. [559]).

total chlorine concentration, interferences by HCl and Cl_2 could not be excluded. Thus, REMPI-based techniques seemingly offer one of the best chances for continuous, direct monitoring of chlorinated hydrocarbon molecules which may be emitted from hazardous waste incinerators, in particular if suitable surrogate species can be identified.

5.3.1. Detection of CH_3 with REMPI in combustion systems

The CH_3 radical is an important intermediate species in the combustion of CH_4 or higher hydrocarbons. It recombines easily with itself and thus leads to the production of species containing more than one C atom, which may then eventually participate in the formation of soot. Also, it is involved in ignition and flame propagation steps and is thus considered to be one of the most important chain carriers in hydrocarbon combustion; its detection may provide insight into hydrocarbon reaction mechanisms. In addition, it is one of the hydrocarbon intermediates in reburn processes.

CH_3 can be detected by absorption near 216 nm. Glänzer et al.[557] have determined absorption coefficients at high temperature and have studied CH_3 recombination in shock tube experiments. Harvey and Jessen[558] have monitored the CH_3 absorption spectrum in a flame. In most recent experiments, quantitative CH_3 concentration measurements by absorption were successfully demonstrated in shock tubes[81] and low-pressure flames.[559] As an example, Fig. 27 shows measured and calculated CH_3 profiles in a 13 mbar flat, premixed CH_4/O_2 flame reported by the latter group.

As an alternative to absorption, (2 + 1) REMPI detection of CH_3 at 286 nm, (2 + 1) REMPI at 333 nm, or (3 + 1) REMPI at about 450 nm has been used. Detailed spectroscopic investigations of these multi-photon transitions have been performed by DiGiuseppe et al.,[537,538] Hudgens et al.[539] and Black and Powis.[560] Smyth and Taylor[514] were the first to

detect CH_3 REMPI signals in a flame. However, for measurement of the CH_3 distribution, the signal-to-background ratio in their atmospheric pressure CH_4/air diffusion flame was too low. In a very recent experiment in the same flame, a higher sensitivity could be obtained by using a different type of electrode,[163] however, absolute concentrations were not determined. In our investigation of a slightly rich, premixed low-pressure CH_4/O_2 flat flame,[541] the CH_3 signal could be followed as a function of height above the burner surface. Both (2 + 1) REMPI processes were initially studied in a discharge flow reactor, where CH_3 was produced either by reaction of CH_4 with F atoms or of CH_3I with H atoms. A probe similar to that of Cool[535] was employed. In the flame, however, CH_3 REMPI signals at 286 nm could not be detected but were entirely obscured by a regular spectral structure which was later identified by Tjossem and Smyth[515] as a Rydberg transition in molecular oxygen. CH_3 REMPI signals at 333 nm were detected as a function of varying distance of the probe to the excitation volume. Since the measured signal intensity profiles remained constant upon this variation, it was concluded that the probe did not severely disturb the flame. A quantitative interpretation of these results was, however, not possible. In subsequent experiments in low-pressure CH_4/O_2 and C_2H_4/O_2 flames, Cool et al.[542] have measured CH_3 intensity distributions which they interpreted directly as relative CH_3 concentration profiles. However, the influence of variations in the chemical composition on the REMPI detection efficiency—an effect which may be quite significant[484]—was not determined in their study.

Calibration of REMPI measurements in flames has already proved to be extremely difficult for the detection of atomic species. For a polyatomic radical like CH_3, however, the complexity of a quantitative REMPI measurement increases severely due to the many different states involved and their temperature-dependent populations. In this context, attempts to determine absolute CH_3 concentrations in a chemical vapor deposition (CVD) environment shall be briefly reported.

5.3.2. REMPI detection of CH_3 in chemical vapor deposition experiments

Considering that techniques originally developed for detection of intermediate species in combustion systems have increasingly been applied to study the same reactive species, e.g. in chemical vapor deposition of carbon material, especially of diamond, it may be permitted to deviate slightly from the main subject of the paper in order to provide further information on the quantitative detection of a combustion-relevant radical, CH_3, by REMPI. In the experiments that will be described in this section, CH_3 was detected in a chemical environment of much lower complexity than usually encountered in

flames. It is believed that the discussion of the calibration procedures presented below may also assist in the evaluation of the REMPI technique for quantitative application in combustion systems.

Reviews on the gas-phase deposition of diamond are found in recent articles by Yarbrough and Messier,[561] Celii and Butler,[562] Geis and Angus[563] and Bachmann et al.[564] Some of the best-studied systems in this respect are hot filament (HFCVD) reactors and flames, mainly acetylene flames at atmospheric pressure. Detailed reaction kinetic models for diamond deposition in the HFCVD process have recently been reported by Frenklach,[565] Frenklach and Wang,[566] Harris and Weiner,[567] Goodwin and Gavillet,[568] Chu et al.,[569] Harris and Goodwin[570] and Wolden et al.[571] Most mechanistic studies agree on the key role of the H atom; also, it has often been emphasized that CH_3 may be an important diamond precursor (see Harris and Goodwin[570] and references therein and Lee et al.[572]).

In comparison to flames, HFCVD reactors are rather 'clean' systems. Deposition experiments are essentially performed in a low-pressure hydrogen atmosphere at high temperatures, seeded with small amounts of a hydrocarbon species; CH_4 in the majority of experiments. Quantitative applications of multi-photon techniques to these systems may thus appear less challenging. In the pioneering experiment of Celii and Butler,[573] REMPI signal intensity distributions of the H atom have been measured; it is, however, unclear whether the reported profiles reflect relative concentrations. In a few recent studies, including those of our own group, quantitative H atom concentrations have been measured as a function of essential experimental parameters.[574-578]

Similarly, an attempt was made to determine the dependence of the CH_3 concentration on these parameters. For this purpose, CH_3 (2 + 1) REMPI measurements at 333 nm were performed for typical operation conditions as a function of distance from the filament.[579] For a quantitative interpretation of measured REMPI signal intensities, several calibration steps were necessary. First, the detection efficiency had to be determined for each operating condition. Because of the charged particles emitted from the hot filament, the detection efficiency for electrons was strongly position-dependent. In a first approximation, the detection efficiency was inferred from simultaneous MPLIF and REMPI measurements of H atoms under the same operation conditions; the concentrations determined by MPLIF served as a reference. However, since ion mobilities may be involved, the detection efficiency for H atoms is not necessarily the same as for CH_3. Therefore, simultaneous MPLIF and REMPI measurements were also performed with NO as a calibration species, which had, however, to be seeded into the system. Electron detection efficiencies measured with H and NO agreed within a factor of 2, so that an uncertainty of similar

magnitude was assumed for the CH_3 measurements.

A second calibration step required consideration of the temperature-dependent changes in the CH_3 population distribution. With increasing distance from the hot filament, the temperature in the gas phase decreases significantly, as was observed in LIF measurements with (seeded) NO as a temperature indicator. Also, rotational level-dependent predissociation was observed to influence the spectral structure of the probed CH_3 $(3p\,^2A_2''-X^2A_2''\,0_0^0)$ band significantly as a function of temperature. Since spectroscopic constants and predissociation rates were not known well enough for quantitative measurements at high temperatures (where high rotational levels are populated), temperature-dependent REMPI spectra measured in the discharge flow and HFCVD reactors were evaluated to yield this information.[580] As one of the results, Fig. 28 shows the measured CH_3 spectrum at 300 K along with a simulation; different magnitudes of level-dependent predissociation were assumed. At higher temperatures, higher rotational levels in the excited state which predissociate more rapidly are accessible. The spectral envelope at high temperatures (most structural features observed at 300 K are then obscured because of the multitude of overlapping lines) could be well represented by the same set of spectroscopic constants and predissociation parameters. Taking temperature effects in the vibrational and rotational population distributions of the electronic ground state into account, and considering the loss of population by predissociation in the resonant excited state as a function of rotational level, a temperature-dependent calibration factor was determined which allowed comparison of REMPI signals in the HFCVD reactor with known CH_3 concentrations measured in the discharge flow reactor.

The absolute CH_3 concentrations obtained with this calibration procedure are reliable within a factor of 3. The large uncertainty in the electron detection efficiency contributes predominantly to this value; also, experimental uncertainties in the measurement of the temperature profile, of the CH_3 reference concentration—by the fast reaction of CH_3I with H atoms—and in the determination of the level-dependent predissociation were considered. Although this overall level of uncertainty appears rather high, more precise, quantitative, systematic information on CH_3 concentrations in HFCVD systems is not readily available. Besides some indirect[567] and relative[581] determinations of CH_3, Menningen et al.[582] have recently measured the variation of the CH_3 concentration with filament temperature and gas composition using absorption of a Xe lamp at 216 nm; CH_3 profiles as a function of distance from the filament were, however, not given. Hsu[583] has measured the CH_3 concentration as a function of methane content in the vicinity of the substrate with mass spectrometry; again, a direct comparison with our results is not possible due to the different operating
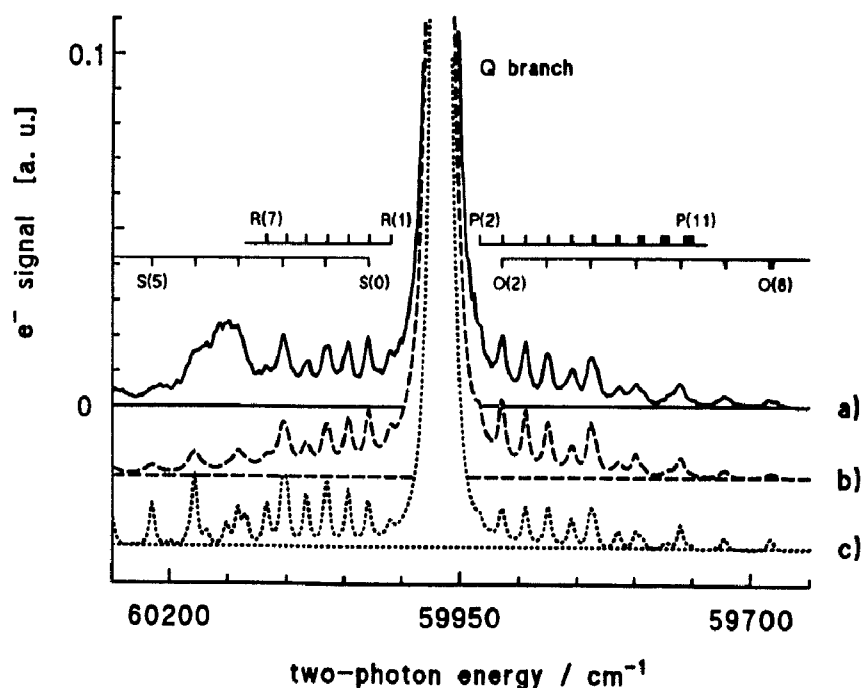
FIG. 28. Measured (a) and simulated (b, c) CH_3 spectrum at 300 K. In contrast to calculation (c), (b) considers level-dependent predissociation (Heinze et al. [580]).

conditions of the two systems. Very recently, Corat and Goodwin[584] have determined relative CH_3 concentrations with REMPI as a function of the substrate temperature. They have calibrated their REMPI probe with Ar (similar to the procedure proposed by Smyth and Tjossem[484]) and have accounted for the dependence of the vibrational ground state population on temperature. However, the variation of rotational population distribution with temperature, including temperature-dependent losses due to state-specific predissociation in the excited state, was not considered. Our experiments show that neglect of these contributions in the evaluation of the REMPI data may lead to an error of about a factor of 2 in the relative CH_3 concentration between 600–1400 K. Also, the gas temperature was not determined but assumed to be equal to the substrate temperature.

The difficulties encountered in performing quantitative CH_3 measurements with REMPI in a HFCVD reactor illustrate some of the problems that may hamper quantitative application of this technique to other, chemically more complex environments such as combustion systems. Potential sources of error associated with multi-photon techniques include, in particular, uncontrolled, composition-dependent photodissociation, for which only a limited number of precursors and channels have been identified. In addition, information on multi-photon excitation, photoionization, collisional quenching and predissociation rates may be incomplete. Furthermore, the presence of a REMPI probe in reactive environments is questionable. In general, REMPI also furnishes information at only a single position in the flame;

although single-pulse imaging is possible with MPLIF, such applications have been scarce. Due to these limitations, MPLIF and REMPI do not appear to play a dominant role in laser diagnostics of combustion systems. Whenever possible, alternative techniques should be applied. For concentration measurements of stable species, spontaneous Raman or CARS, or in some cases LIF or LIPF may be more suitable. For non-fluorescing radicals, absorption measurements may be considered. Since it seems unrealistic to assume that multi-photon techniques will be routinely used in turbulent or high-pressure flames, not to mention practical combustion systems, they should preferentially be applied in situations where no alternatives are available. The detection of some important atomic species, including H, O, N and possibly also C and Cl in flames may remain a domain of MPLIF, and the highly sensitive measurement of certain trace species concentrations, including those of large hydrocarbon and halogenated hydrocarbon molecules, may be an attractive field of application for REMPI in combination with mass spectrometry.

6. FIELDS UNDER DEVELOPMENT

In the preceding sections, several laser-diagnostic techniques for the quantitative detection of intermediate species in combustion systems have been described, including laser absorption, laser-induced fluorescence (in its linear, saturated and predissociative variants), and approaches using multi-photon excitation. Although difficulties and limitations which may

restrict quantitative measurements with these techniques to specific environments have been discussed, examples for their application from a period of more than a decade have typically been given. In contrast, some more recent lines of development will be discussed in the present section. Three aspects may be of particular interest in this respect: simultaneous detection of several species, multi-dimensional single-pulse acquisition of concentration, temperature and velocity distributions, and intermediate species detection with non-linear techniques which provide laser-like signal beams and may be applicable in systems with limited optical access or in media charged with droplets or particulate matter.

6.1. Multi-species Detection

Since the concentrations of combustion species are interlinked through a complex network of chemical reactions, correlations may be revealed by the detection of several key molecules. In special cases, accidental coincidences in the spectra of some atoms and molecules allow simultaneous excitation of more than one species with the same laser. Some suitable schemes have been reported. With a combination of laser radiation in the vicinity of 287 and 226 nm, which may be produced using the same dye laser with frequency doubling and subsequent stimulated Raman shifting, OH (near 287 nm), O_2, O atoms and NO (all near 226 nm) may be excited simultaneously. Figure 29 shows the spectra of these species and the overlap of specific lines.[585] The corresponding fluorescence occurs in different wavelength regions and can be separated by appropriate filtering. In principle, this scheme allows simultaneous measurement of the concentration of an oxidizer, reactive intermediates and a major pollutant. Wysong et al.[586] have demonstrated combined detection of O, O_2 and NO using this approach, and Westblom and Aldén[531,587] have simultaneously measured OH, O and NO. Goldsmith et al.[589] have, however, observed photochemical interferences in flames using N_2O as oxidizer, when O, OH and NO were detected simultaneously. In some regions of the flames where H_2O and N_2O are both present, laser radiation at 226 nm can photodissociate N_2O to generate O ^1D which may rapidly form two OH radicals upon collisions with H_2O, thus leading to misinterpretations of the OH measurement.

Spectral coincidences have also been reported at other wavelengths. Anderson et al.[107] have used a Kr^+ laser in the range of 454–488 nm for the excitation of CH, CN and NCO; the fluorescence of at least two of these radicals could be observed for all chosen Kr^+ lines. Aldén et al.[590] have excited NO (by a two-photon process) and NO_2 simultaneously using laser radiation of 452 nm. Starting with laser light near 615 nm, frequencies for the simultaneous excitation of OH (at 308 nm) and H atoms (at

205 nm) can be produced by doubling and mixing processes.[591] Jeffries et al.[592] have found spectral coincidences near 312 nm which permit simultaneous measurements of OH, NH, CH and CN. Furthermore, OH and O_2 distributions were measured simultaneously[593] with a tunable KrF excimer laser which was modified to operate at two different frequencies.[372]

Probably the number of spectral coincidences which may be useful in a combustion environment is limited. It is certainly advisable to exploit schemes like the ones mentioned above whenever possible, one major advantage being that exactly the same volume is probed for all species. Multi-species detection can, however, also be performed sequentially in laminar flames and, with an increase in experimental complexity, in turbulent and unsteady combustion systems. Two types of typical investigations using multi-species detection are now increasingly being performed: detailed chemical analysis in low-pressure flat flames and flame structure studies in turbulent combustion.

Whereas during the past 12–15 years of LIF experiments in combustion, many groups have— successfully—attempted to measure the concentration of a single species (most often the OH radical) with high reliability, it was always clear that more information is needed for validation of computer models of the flame chemistry. Over the past few years, laser-based techniques have been applied in a similar fashion to the way mass spectrometry had been used before; profiles of many chemically interdependent species are measured and conclusions on chemical pathways are being drawn from comparison with computer simulations. In recent experiments, low-pressure methane and ethane flames with a variety of oxidizers have been investigated, combining LIF, MPLIF and REMPI for the measurement of atoms, radicals and stable species including H, O, OH, CH, CH_3, HCO, CO, CN, NH, NH_2, NO, NO_2 and others. Examples include studies by Zabarnick et al.,[127,128] Branch et al.,[129] Heard et al.,[171] Jeffries et al.,[455] Etzkorn et al.[543] and Bernstein et al.[551]

Multi-species approaches are, however, not limited to flat, premixed low-pressure flames. As a representative example for an extensive series of investigations, the recent article of Norton et al.[163] summarizes information acquired on the chemistry of a CH_4/air diffusion flame. Correlated multi-species diagnostics is essential in turbulent combustion and requires measurements with different diagnostic techniques. Barlow et al.[153] have determined mixture fractions in turbulent H_2 jet flames by a measurement of the majority species concentrations with spontaneous Raman scattering, and simultaneously measured the concentration of OH as a key intermediate by laser-induced fluorescence. More recently, they extended these experiments to the study of NO formation in H_2 jet flames[156,157] and performed simultaneous measurements of the majority species, OH, NO, and
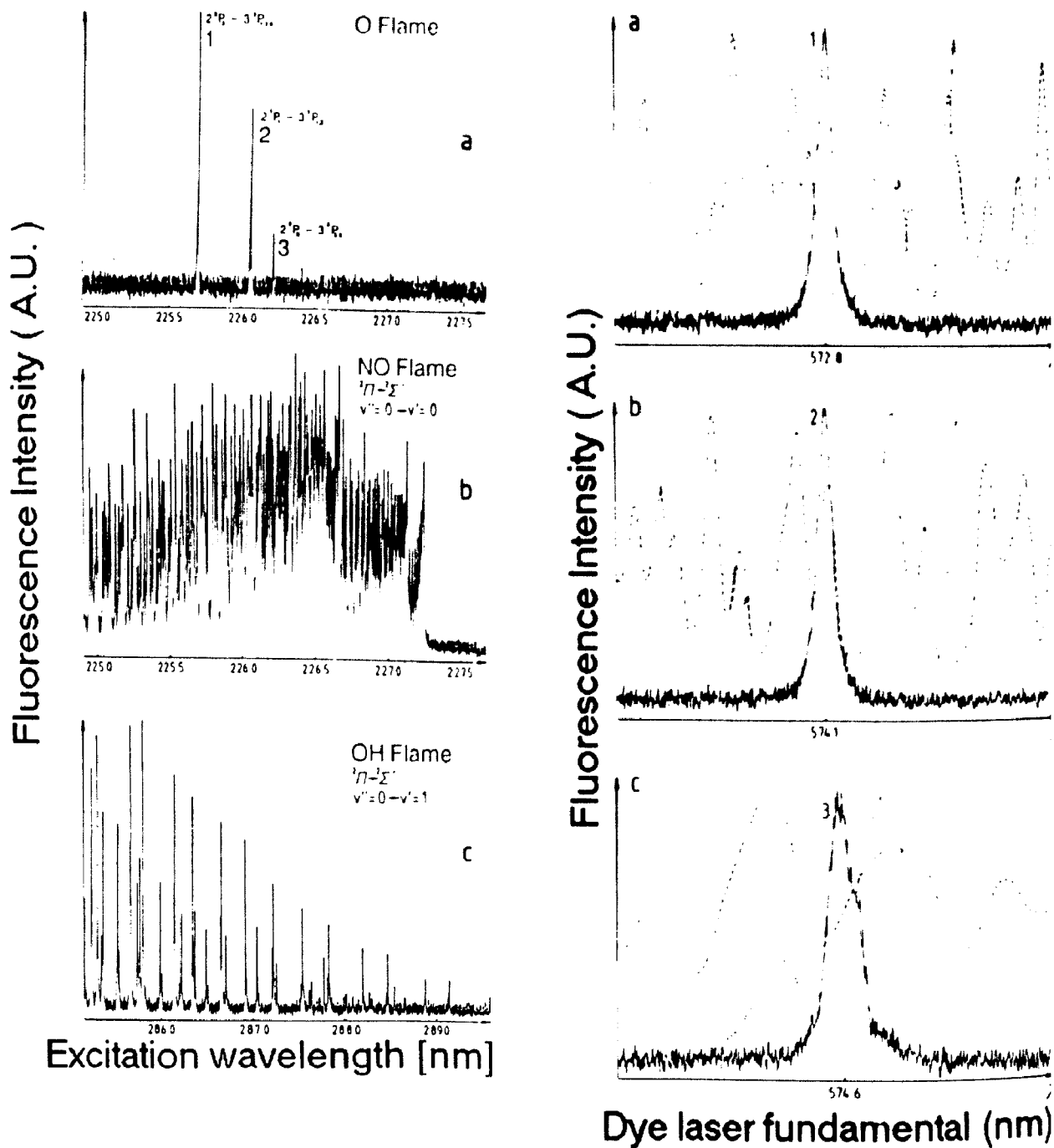
FIG. 29. Spectral region for the simultaneous detection of O, NO and OH (Westblom and Aldén [585]). The left side shows spectra measured in a H_2/N_2O flame, the right side the overlap of suitable lines.

temperature, combining Rayleigh and Raman scattering with LIF. A similar concept was used in an investigation of turbulent CH_4, $CO/CH_4/N_2$ and $CO/H_2/N_2$ diffusion flames near extinction.[594,595] Further applications of the combined Raman/-Rayleigh/LIF technique were reported by Masri et al.[596] for a turbulent non-premixed methanol flame and by Masri et al.[154] for diffusion flames of H_2/CO_2 fuel. Recently, Stårner et al.[158] performed simultaneous imaging of OH and CH in the turbulent methane flame investigated previously in the Raman/-Rayleigh/LIF experiments. Furthermore, a turbulent H_2 jet diffusion flame has been studied with

simultaneous multi-species Raman scattering and OH LIPF using a UV excimer laser.[155] In a very similar H_2 jet flame, single-pulse multi-species Raman measurements[160,380] have been performed in conjunction with simultaneous single-pulse imaging of OH and NO seeded into the flame as a tracer for fuel.[159,291] Similarly, Schefer et al.[597,598] reported simultaneous imaging of OH and CH with LIF and of CH_4 with spontaneous Raman scattering in a lifted, turbulent CH_4 jet flame. Combination of a variety of diagnostic techniques for the simultaneous measurement of several species is also of great importance in the investigation of internal combustion

engines; related studies have been performed by Andresen et al.[146,405] and Koch et al.[406] Most recent approaches provide one-dimensional quantitative, correlated, single-pulse information on composition and temperature in turbulent flames.[599,600]

In view of these studies it may be expected that multi-species approaches combining several diagnostic techniques will provide structural information in practical combustion situations. Important aspects include the characterization of the mixing process by monitoring stable species concentrations—if necessary by adding suitable tracer molecules—and concentration measurements of some key intermediates that may reveal details of the flame structure. The OH radical can easily be monitored and is therefore often chosen for this purpose, although CH appears to be a superior indicator for the flame front. Monitoring several other intermediate and product species, including nitrogen- or carbon-containing molecules, may provide an insight into particular details of reaction mechanisms and may thus assist in the development of strategies for reduction of undesired and hazardous emissions.

Concentration measurement has been emphasized in the preceding discussion; it should, however, not be forgotten that multiple quantities (not only multiple species) are important for the characterization of combustion systems. Measurements of temperature and velocity distributions are also essential for improved understanding of combustion processes. In a pioneering experiment in this respect, Chang et al.[83] and DiRosa et al.[84] have demonstrated simultaneous measurement of velocity, temperature, pressure, density and mass flux in a high speed combustion system using narrowband laser absorption. Although their experiment necessarily yields spatially averaged quantities, which are questionable for characterization of turbulent processes, multi-quantity approaches deserve increased attention. Furthermore, it should be noted that the numerous investigations providing point-wise, correlated species and temperature information have been of great value for a better understanding of combustion chemistry; for the study of practical combustion systems, however, multi-dimensional approaches are preferable.

6.2. Two-Dimensional Imaging

With several laser-optic techniques based upon light scattering processes, including Mie, Rayleigh and Raman scattering as well as LIF and MPLIF, one- or two-dimensional cross sections through a flame, which represent the momentary distribution of certain physical quantities, can be obtained with good spatial resolution. In these experiments, the laser beam is shaped into a sheet, typically 0.1–0.5 mm thick and 1–5 cm wide, which traverses the flame; the scattering signal is collected, in general at

right angles to the laser propagation path, with an appropriate camera. Single-pulse measurements in the nanosecond regime can be performed, thus effectively freezing both flow and chemistry in most atmospheric pressure combustion situations. A typical experimental arrangement is shown in Fig. 30. Two-dimensional imaging shares some common features with regular photography, however, the information that can be obtained is far more detailed, as well as being species-specific and temporally and spatially resolved. In the following, two-dimensional imaging with laser-induced fluorescence, often termed PLIF,* will be emphasized.

The first planar LIF measurements were demonstrated almost simultaneously by two groups;[601-603] 2D imaging of OH and, in addition, NO[602] was reported. Also, the availability of linear detector arrays permitted one-dimensional LIF measurements at about the same time.[604] Since then, particularly in the last 4–5 years, the number of publications in this field has increased enormously. PLIF and other two-dimensional techniques have become an indispensable instrument for the investigation of practical combustion systems. The particular value of single-pulse 2D measurements is evident; a multitude of sequentially acquired, point-wise data cannot be regarded as a true alternative. For example, a point-wise measurement of the CH concentration at an arbitrary position in a rapidly fluctuating, turbulent flame gives no indication where this position was located in relation to the flame front, whereas the concentration measured at the same location within a single-pulse 2D frame is easily related to its surrounding environment.

PLIF is a very versatile technique. Excellent reviews of PLIF measurements, its capabilities and limitations as well as on typical instrumentation have been given by Hanson[16,605] and Hanson et al.[17] Imaging of concentration distributions—not necessarily quantitative—have been performed for a variety of stable molecules including O_2,[144,146,405,593,606-608] CO,[532,590,609] NO,[146,394,441,590,610] NO_2[186,590,611] and H_2.[530] A large number of studies have addressed 2D imaging of radicals, in particular of OH; examples are found in the work of Hertz and Aldén,[612] Kychakoff et al.,[608] Pfefferle et al.,[166] Suntz et al.,[400] Seitzman et al.,[613] Arnold et al.,[593] Becker et al.,[401,402] Sick et al.,[614] Andresen et al.,[146,405] McMillin et al.,[615] Schefer et al.,[597] Schäfer et al.,[348] Smooke et al.,[616,617] Versluis et al.,[441] Stårner et al.,[158] Roberts et al.,[618] Meier et al.[159] and Ketterle et al.[413] Furthermore, planar distributions of CH[158,597,616,617,619-622] and of C_2[620] have been measured. Atomic species including O[501,607,623]
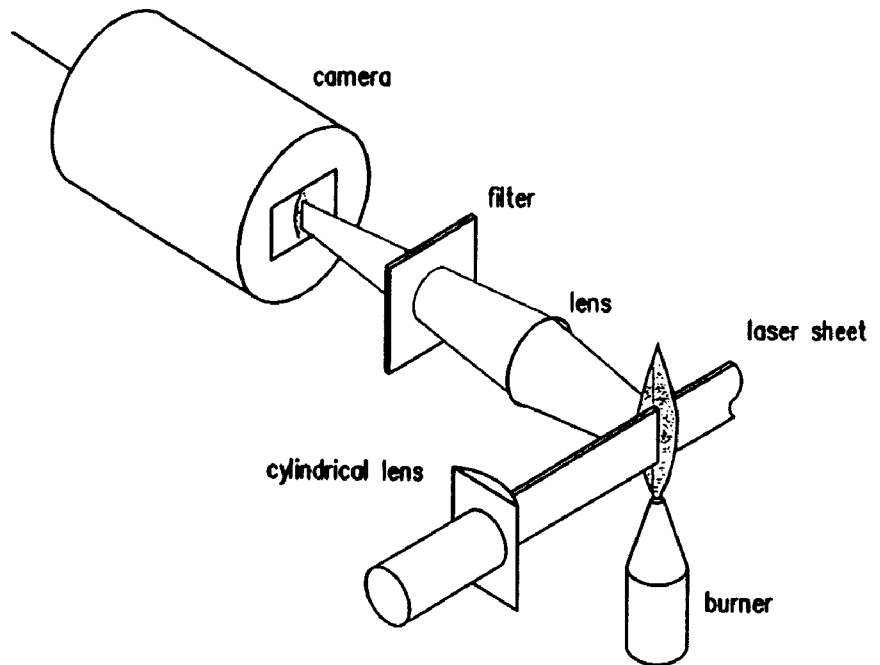
---

* PLIF: Planar Laser-Induced Fluorescence.

Fig. 30. Typical arrangement for two-dimensional imaging.

and H[464] have been detected with one-dimensional MPLIF.

Not only structural or concentration imaging has been performed with PLIF. The measurement of two-dimensional temperature distributions in combustion systems with single-pulse fluorescence techniques has been discussed in Section 4.4; examples using OH, O_2 and NO as temperature indicators have been given therein. Also, PLIF has been applied for 2D pressure imaging[624] and for 2D velocity measurements via the Doppler shift using iodine[588,625-628] or biacetyl (2,3-butanedione)[629] as tracer species. Although seeding with particles was avoided with this technique, the thermal decomposition of both substances limited its application to cold, non-reacting flows. This and several further disadvantages were overcome by using NO as a tracer species.[630,631] Their approach requires only a single, pulsed laser which traverses the flow twice. Images of the fluorescence from both counter-propagating sheets are then evaluated to determine the 2D velocity field. In contrast to previous measurements based upon the use of narrowband cw laser radiation, the laser lineshape controls the accessible range of velocities. Furthermore, short, flow-stopping interrogation times can be used. Palmer et al.[391] and Palmer and Hanson[632,633] have deduced the velocity field from single and averaged images in their studies of high enthalpy flows; both NO and OH were excited by broadband, pulsed lasers.

In a different scheme, Boedeker[419] has measured velocity distributions by photolyzing H_2O with a first laser and detecting the resultant OH radicals using LIF with a second laser. In a more recent study,[634] this technique has been further evaluated for high-speed combustion systems and considered

for use in the exhaust of the space shuttle main engine. Furthermore, O_2 has been examined as a velocity indicator.[635-638] By a technique which combines tagging of the O_2 molecules by vibrational excitation via stimulated Raman scattering and interrogation of the tagged molecules by laser-induced fluorescence,* lines are optically written into the flow and their propagation with the flow is followed. In principle, O_2 is present in many combustion situations; however, it participates in the chemical reactions and its concentration may not be sufficient in rich zones. Limitations may also be imposed by the presence of colliders which may efficiently depopulate the vibrationally excited level and by difficulties in interpreting the resultant velocity data. Most recently, naturally present OH has also been proposed as a velocity indicator for reacting flows.[627] The method is again based on the measurement of the Doppler shift and requires a powerful narrowband UV source, which is in this case a pulse-amplified ring dye laser; first applications to an underexpanded jet have been demonstrated.

In the investigation of combustion systems, characterization of the mixing process, often in the pre-ignition phase, is of crucial importance. Two-dimensional fluorescence and phosphorescence schemes for these purposes are being developed. For many situations, tracer species can be used which mark the fuel in the liquid or vapor phase. Melton[639] has proposed a method which allows discrimination between vapor and liquid; it relies on the formation of exciplex

---

* This approach has become known under the name of RELIEF, which stands for Raman Excitation and Laser-Induced Electronic Fluorescence.

molecules. As typical dopants, unsaturated organic molecules (M) are chosen which can be excited by laser radiation and then interact with a second tracer species (Q). The emission of the resulting exciplex molecule (MQ*) is characteristic for the condensed phase, and the (spectrally distinguishable) emission of the monomer (M*) is seen only in the vapor phase. The general idea was outlined for the tracer system of naphthalene ($=$M) and TMPD ($=$Q)* in cetane; the approach was refined in subsequent work by Melton and Verdieck.[640] Calibration procedures for a quantitative application of the exciplex measurement scheme are given by Rotunno et al.[641] Since the emission of TMPD is rapidly quenched by O_2, this particular tracer combination is unfortunately not suited for studies in combustion systems[642] where the fuel is mixed with air. Quenching of naphthalene fluorescence by O_2 was, however, successfully applied to follow internal circulation in initially oxygen-free n-decane droplets.[643]

Arnold et al.[644] have suggested the use of acetaldehyde as a tracer species for fuel imaging in combustion environments. This molecule is thermally stable up to about 900 K and thus survives the compression phase in internal combustion engines; it is readily excited with 308 nm XeCl excimer radiation and its fluorescence emission may conveniently be monitored in the visible spectral region. Acetaldehyde decomposes rapidly in the flame front which thus can be clearly marked. One of the most important aspects, however, is the almost negligible variation of the fluorescence yield with pressure up to about 7 bar, which makes acetaldehyde well suited for engine studies. Tait and Greenhalgh[645] also emphasize the temperature independence of the acetaldehyde fluorescence yield in the range of 300–800 K, while the emission of acetone which was used as an alternative tracer molecule exhibits a marked temperature dependence in their experiments. Recently, Lozano et al.[646] have examined the suitability of acetone as a fuel tracer in detail; however, they found the acetone fluorescence to be temperature-independent. Some other aldehydes and ketones with similar properties have been investigated, including hexafluoroacetone[646] and 2-butanone.[647] For iso-octane it has been reported that the fluorescence of the fuel itself could be monitored,[146] however, this was later attributed to a potential impurity in the system.[405] Lozano et al.[646] have summarized a number of criteria which should facilitate the choice of tracer species. In a given system, vapor pressure of the tracer species, excitation and emission wavelength, fluorescence yield and its temperature and pressure dependence, quenching of the emission, in particular by oxygen, toxicity and economic aspects must thus be considered. In this respect, acetone seems to be a highly suitable seed molecule for many purposes.

---

*TMPD: TetraMethyl-p-Phenylene Diamine or 1,4-bis(dimethylamino-)benzene.

Recently, attempts have been made to fully characterize a hollow-cone nozzle for fuel intake by a combination of different diagnostic methods including elastic scattering, stimulated Raman scattering, lasing action and fluorescence;[648] for this, the laser dye rhodamine 6G was added as a tracer in some of the experiments. Various constituents of a spray including ligaments and sheets, large and small droplets as well as fuel vapor could be selectively imaged. A combination of Mie and Rayleigh scattering with LIF has been used in an investigation of a utility burner;[649] important features of a standard system and a variant with reduced NO emission could be distinguished in spite of the hostile environment by comparing averaged images both on and off molecular resonances (see one-dimensional traces in Fig. 31).

In addition to the need for pressure-, temperature- and oxygen-insensitive fuel tracers, e.g. for the study of fuel/air mixing in the intake and compression phases of internal combustion engines, concepts are also required for following the mixing process on a molecular scale in heavily turbulent, gaseous systems. The spatial resolution in 2D imaging experiments is typically 0.1–0.5 mm (corresponding to the thickness of the laser sheet) which is usually insufficient to resolve the smallest turbulent length scales. This spatially integrative effect has implications for the experimental investigation of mixing processes. For example, assume that fuel and air stream were doped with two different fluorescent tracers. The measured LIF signal from the observation volume would be identical in two entirely different situations: in the first case, both fuel and air could be completely mixed on a molecular level, and in the opposite case, totally unmixed fluids could each occupy half of the observation volume. For these reasons, systems are being studied which lead to light emission only upon molecular contact between two tracer species. Winter et al.[650] have suggested the use of biacetyl and toluene. Laser excitation at 266 nm excites only toluene; biacetyl emission is only observed if collisional energy transfer between the two species has occurred and thus indicates mixing on a molecular scale. A similar concept has been pursued by Yip et al.,[651] who use acetone in combination with biacetyl; upon collisions of excited acetone molecules with biacetyl, phosphorescence is observed which can be easily distinguished from acetone fluorescence. For a quantitative evaluation which would provide the degree of mixing in the observation volume, rate equation modelling of all contributing processes is recommended. A major problem for application to combustion systems, however, is again the rapid quenching of biacetyl emission by O_2. A different approach which relies on the presence of oxygen quenching has recently been demonstrated by Paul and Clemens.[652] In their experiment, they have exploited the fact that at ambient temperature, NO is efficiently quenched by O_2 whereas quenching is negligible for pure N_2. The
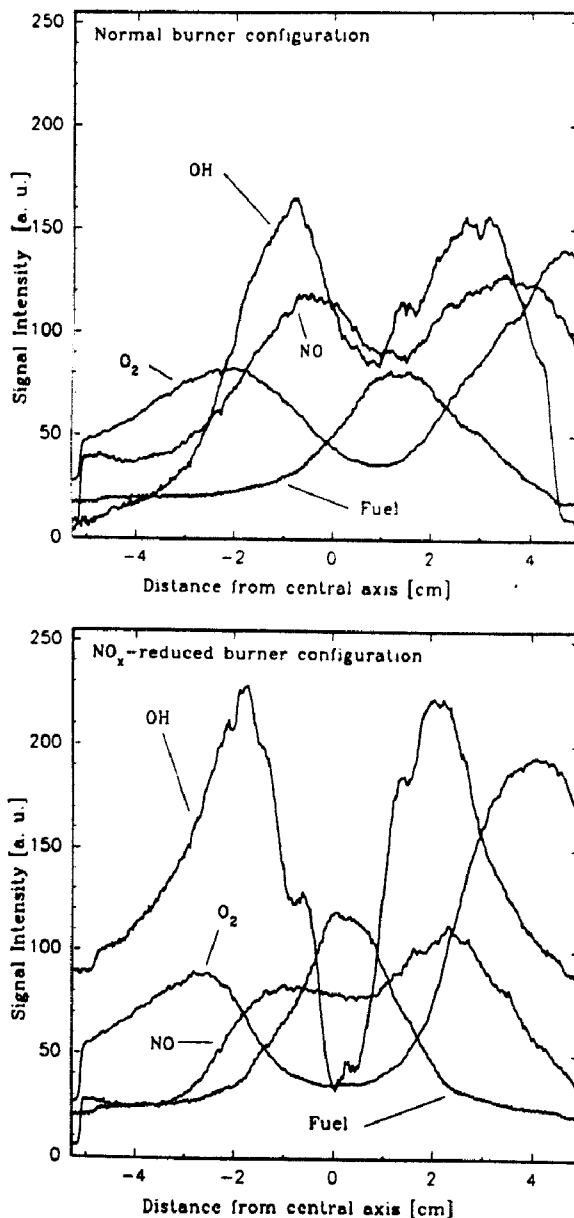
Fig. 31. Fluorescence intensity profiles of several species measured for two variants of a commercial oil spray burner (Koch et al.[649]). The one-dimensional profiles were obtained as cross sections from the respective two-dimensional images; averaged intensity distributions on and off resonance (512 images each) were subtracted. In spite of the turbulent nature of the flame, differences in flame structure are clearly discernible in the averaged distributions.

NO fluorescence intensity was thus used to discriminate between mixed and unmixed states in their investigation of an axisymmetric shear layer produced by a NO-seeded jet of N_2 into coflowing air. Paul and Clemens[652] suggest further use of the NO seeding technique to study differential diffusion in a He/CO_2 system, where CO_2 is a strong quencher while quenching of NO by He is insignificant.

The examples discussed in this section and others not mentioned here demonstrate the immense potential of two-dimensional LIF techniques. However, limitations may be encountered in many cases. In particular, lack of inert indicator species for tempera-

ture measurement, thermal decomposition of some of the tracers for velocity measurement, and oxygen quenching of the emission of some tracers for mixing studies have already been addressed. Furthermore, photochemical interferences may cause problems. In many experiments, C_2 has been created from various precursors upon irradiation with laser light.[451, 454, 532, 609, 653] Strong interferences by fluorescence of polyaromatic hydrocarbons which could cause errors in CH imaging experiments were observed by Norton and Smyth[654] and Raiche and Jeffries.[381] This potential source of interference was not explicitly addressed in recent 2D measurements of the CH concentration by Schefer et al.[597, 598] and Stårner et al.[158]

Two-dimensional LIF intensity distributions do not necessarily provide quantitative results. Although the underlying physics is essentially the same as for point-wise measurements (e.g. information on the influence of collisions may be required) the necessary data may not be readily available on a 2D single-pulse basis. Comments on the present status of 2D LIF temperature measurement have already been given in Section 4.4. In single-pulse 2D concentration imaging with linear LIF, the varying collision efficiency associated with local variations in composition and temperature needs to be accounted for; similar corrections may be necessary for predissociative or saturated LIF measurements at higher pressures. The most general approach would be simultaneous fluorescence and lifetime imaging, in analogy to the concepts proposed by Ni and Melton[655] and Hirano et al.[656] For quantitative imaging of important combustion radicals (e.g. OH, CH, NO) in turbulent atmospheric pressure flames, however, where single-pulse data acquisition and a time resolution of < 1 ns may be required, related lifetime measurements have, to the author's knowledge, not yet been performed.

An estimate of the magnitude of quenching corrections may be provided from point-wise measurements of composition and temperature by using spontaneous Raman scattering and tabulated quenching coefficients. Barlow et al.[152, 153] have reported simultaneous point-wise Raman and OH LIF measurements at various locations in a turbulent flame. Joint two-dimensional Raman and LIF experiments are, however, generally not feasible on a single-pulse basis. Therefore, Barlow and Collignon[657] have proposed a linear LIF detection scheme for OH which is almost insensitive to quenching variations. This is possible due to counteracting tendencies in the thermal population of a particular level and temperature-dependent quenching of fluorescence originating from this level; the quenching efficiency in turn is influenced by temperature dependences in the local collider density and composition as well as in the individual quenching coefficients. From a large data base of single-pulse point-wise measurements of local composition and temperature in a turbulent H_2/air diffusion flame,[160, 380] we have recently ana-

lyzed local variations in effective quenching of OH and NO and assembled quenching 'maps' for these radicals throughout the flame.[658] If the *average* composition and temperature is taken into account, spatial variations in quenching may be very small. For cross sections through the flame at different heights above the nozzle, average quenching variations were found to be in the order of ±10–15% for both radicals,[159,379] although the collisional environment changed drastically from low-temperature unburnt fuel at the jet center core across the high-temperature reaction zone to cooler, air-enriched regions at the outside of the combustion zone. The effective quenching at a single location fluctuated within about a factor of two on a *single-pulse* basis; in many cases, however, a predictable dependence on temperature was observed.[658] If linear single-pulse 2D LIF imaging of OH and NO is performed in conjunction with an instantaneous 2D temperature measurement, quantitative evaluation of the measured intensity distributions in terms of concentrations should be possible in a H_2/air combustion environment with an accuracy of about 30%.

Quantitative information is a necessary prerequisite for comparison of experiment and model predictions. Numerical simulation has advanced in parallel to the efforts devoted to multi-dimensional measurements of intermediate species concentrations. One of the most recent and instructive examples of a detailed comparison of experiment and flame modelling has been given by Smooke et al.,[616,617] who studied an axisymmetric laminar methane air flame. Sequential one-dimensional Raman images averaged over a large number of laser pulses were used to map the chemical composition of the entire flame.[616] In a similar way, OH and CH profiles were assembled in LIF experiments.[617] Potential interferences from broadband fluorescence in the CH measurements were considered by taking images on and off the CH resonance. From the individual radial profiles, the concentration distributions over the entire flame were reconstructed and compared with those obtained from a numerical simulation. Both numerical and experimental results agree remarkably well. Implications of this study for the modelling of turbulent diffusion flames using the flamelet concept warrant further investigation.

For the study of complex, turbulent flow fields, information in more than two dimensions is of interest. In a variety of studies, measurement techniques for 3D imaging or for recording temporal evolutions of 2D structures have been addressed. Dyer and Crosley[659] have measured consecutive 2D distributions of the OH radical. Three-dimensional reconstruction of sequential 2D images at different locations across a reproducible, forced flow were reported by Hanson.[16] Kychakoff et al.[608] have attempted quasi-instantaneous 3D imaging by rapidly acquiring a sequence of 2D cross sections through a turbulent jet flame. In a similar approach, Yip et

al.[660] used a scanning mirror to provide several parallel 2D intersections through the flow. Winter and Long[661] have studied a turbulent H_2/air flame seeded with aerosol which was consumed at the reaction front; using illumination with a 2D sheet of Ar^+ laser radiation, the motion of the flame front was monitored with a sampling rate of 48 kHz. A double-pulse Rayleigh scattering technique has recently been applied by Forkey et al.,[662] who studied the temporal evolution of boundary layer structure and the interaction of a shock wave with the boundary layer.

For the detection of structural and temporal changes, quantitative description of the flow development documented in movies or multi-dimensional images is desirable. Correlation techniques have been used for this purpose. Spatial autocorrelation analysis of 2D OH LIF images has been employed for a wide range of Reynolds numbers by Seitzman et al.[613] in the investigation of a turbulent H_2/air flame. Information on length scales in two dimensions and on a characteristic flame angle was obtained in their study. Miles and Lempert[663] have analyzed spatial correlations in structured flows using double-pulse Rayleigh exposures. In addition, the authors have discussed the application of similar experimental procedures for measuring velocity. A technique for analysis of the temporal development of structures in turbulent flow fields has been applied recently by van Cruyningen et al.[664] For example, sequential 2D images, which were taken in a forced nitrogen jet flow seeded with 5% biacetyl were stacked, and for the complete body of data (in two dimensions in space and one in time), an iso-surface corresponding to 1% biacetyl was calculated which enables the structural development in space and time to be followed.

Yaney et al.[665] have used double-pulse rotational Raman scattering of CO_2 in a turbulent jet flow for the determination of characteristic temporal and spatial scales. Their results agree within a factor of 2 with those estimated from velocity data. Most recently, we have relied on a similar approach in the investigation of a turbulent H_2/air flame.[666] From cross-correlations between two 2D LIF images of OH recorded with a variable delay (see Fig. 32), a characteristic time was determined which is indicative of the combined, interactive development of flow and chemistry, and which, in this case, was close to the time for the movement of large eddies determined by Cheng et al.[155] Smaller segments of the flame can be analyzed to determine time scale 'maps', or additional species with different chemical behavior can be probed for which different characteristic times would be expected. Furthermore, autocorrelation analysis allowed determination of horizontal and vertical length scales.

In summary, many interesting applications of 2D LIF have been demonstrated to date. The further development of multi-dimensional approaches
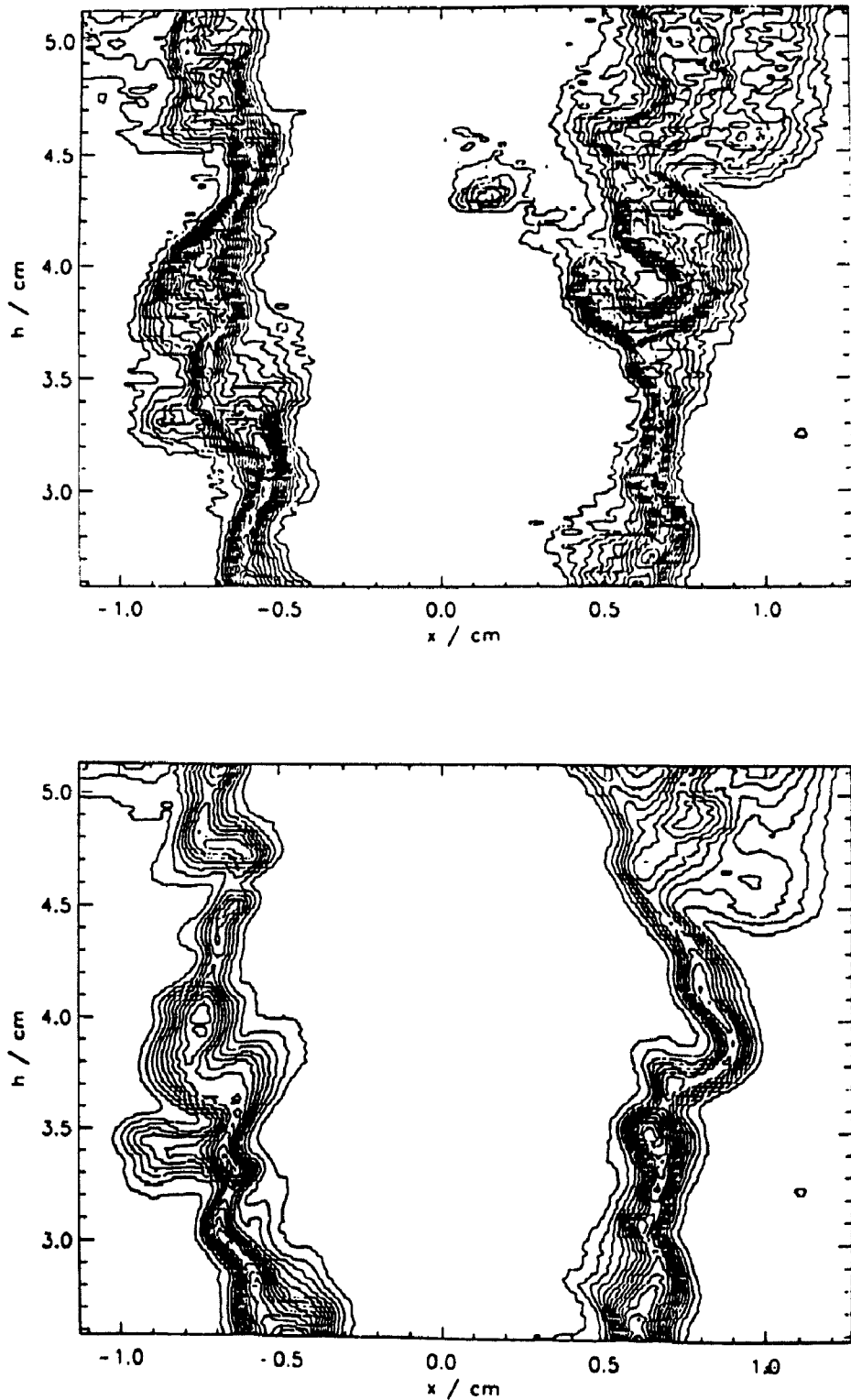
Fig. 32. Consecutive single-pulse two-dimensional OH LIF images in a hydrogen/air diffusion flame (Atakan et al.[666]). The lower image was recorded 0.1 ms after the upper one; some changes in the structure can be recognized. From such an image pair, a characteristic time can be evaluated.

should address several important aspects. For investigations in turbulent combustion systems, combinations of techniques for the simultaneous measurement of several species, including fuel, oxidizer, important intermediates and products, and of several quantities, including composition, temperature and velocity, are particularly desirable. Further effort should also be devoted to the development of schemes which extend these combinative measure-

ments into three spatial dimensions by imaging at least two parallel two-dimensional cross sections through the flow, and which, in addition, provide information on the temporal history of moving or reacting structures through the use of high repetition rates or, as a minimum, double-pulse methods. To avoid spectral or photochemical interferences in systems with complex chemistry, the simultaneous recording of spectra (as an additional dimension) may
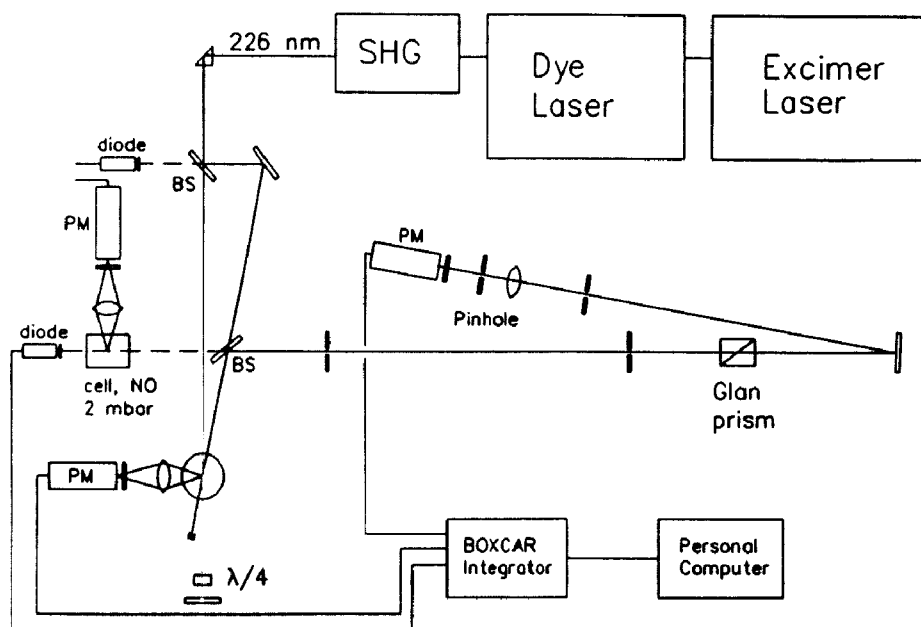
Fig. 33. DFWM arrangement, in this case used for a study of NO in the presence of different colliders (Plath et al.[410]). Forward and backward pump and probe beams are directed through a cell or flow containing NO; DFWM and LIF signals are detected simultaneously. The laser intensity is monitored with a photodiode which detects the reflection off the beam splitter that divides pump and probe beams; this channel also serves as an indicator of absorption by NO caused by two passes through the interaction region. Information on the laser lineshape can be obtained independently from a fluorescence spectrum under linear excitation conditions measured in a reference cell (1% NO in N_2 at 300 K and 2 mbar).

be considered. Furthermore, the issue of suitable spatial resolution deserves attention; here, the molecular mixing concept discussed above may prove helpful. As a key issue for the characterization and potential improvement of combustion systems as well as for the comparison of experimental data with flame model predictions, however, the need for quantitative procedures is again emphasized, without which the qualitative images convey only an unsatisfactory, distorted representation of the combustion process.

6.3. Degenerate Four-wave Mixing (DFWM)

DFWM is a non-linear process which is based upon the interaction of three incoming waves (or laser beams) with the third-order non-linear susceptibility of the medium (the atoms or molecules in a flame) to produce a fourth wave (the signal beam). In a simplified interpretation, the two pump beams create an interference pattern in the medium which is probed by the third beam. The interference pattern or grating corresponds to local variations in the index of refraction as a function of the atomic or molecular density in the observation volume. The grating is interrogated by the probe beam, and the signal beam created during this process thus contains information on species concentration. The theoretical treatment of DFWM has many common features with that of the more widely applied CARS process, since interaction via the third-order non-linear suscep-

tibility is involved in both cases—DFWM can be viewed as a completely degenerate variant of electronic resonant CARS. Therefore, the main characteristics of DFWM closely resemble those of CARS. A detailed description of the technique is beyond the scope of this article; more fundamental information is found in the work of Abrams and Lind[667,668] and Shen.[669]

Before recent applications of DFWM in combustion environments will be discussed, it is instructive to consider some of the characteristic properties of the technique. In contrast to the different pump and probe frequencies required for generation of a CARS signal which is then observed at a third frequency, all four beams in DFWM have the same frequency. Resonance enhancement is achieved by tuning pump and probe beams to an absorption transition instead of probing a Raman line; in this respect, DFWM resembles electronic resonant CARS (see also Section 4.5). In a DFWM experiment, only a single laser is needed; a typical arrangement, like the one shown in Fig. 33, is thus far less complex than that required for resonance CARS. Due to the three-fold electronic resonance, DFWM is extremely sensitive. The detection of very low concentrations can be rendered difficult, however, by interferences from background signals, which may be quite large. In contrast to the background in CARS experiments which is mainly due to non-resonant contributions to the third-order non-linear susceptibility, the background in DFWM experiments is largely caused by diffuse reflection of the laser light off windows and other surfaces which
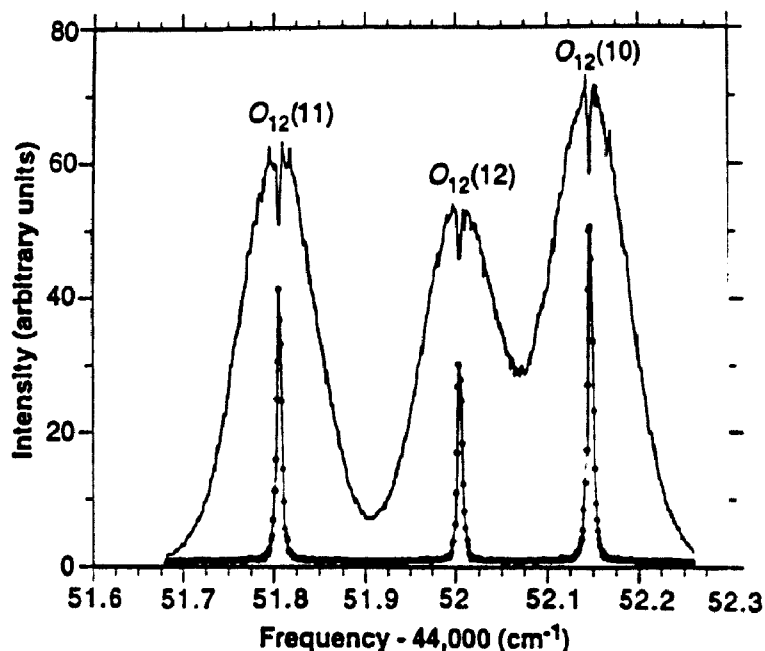
Fig. 34. Comparison between experimental DFWM spectral peaks (connected symbols) and the simultaneously measured fluorescence excitation spectra (solid curve) forming the O_{12} bandhead of the NO A-X transition (Farrow and Rakestraw,[670]).

interferes with the signal detection at the same wavelength. A substantial improvement of the signal-to-noise ratio can be achieved by proper selection of the polarizations of the different laser beams.

DFWM has several advantages for application in combustion systems. Due to the beam-like signal, the technique is well suited to measurements in highly luminous environments. Since only an absorption transition is required, non-fluorescing molecules can, in principle, be detected with good spectral resolution and without the need for probes in the combustion system. DFWM thus offers an excellent alternative to REMPI or conventional absorption experiments. Multi-photon transitions are also accessible for DFWM. Since counterpropagating beams are often used in DFWM schemes, high spectral resolution can be achieved in this Doppler-free arrangement at sufficiently low pressures (i.e. where collisional broadening is insignificant). As an example, Fig. 34 shows the spectral resolution obtained with DFWM in comparison with a LIF excitation spectrum in the O_{12} branch of the NO (A-X) transition;[670] here, the DFWM lineshape is dominated by the laser bandwidth whereas the fluorescence lines exhibit Doppler broadening. If a broadband laser is used, an entire DFWM spectrum can be generated in a single pulse;[671,672] in this feature, DFWM resembles broadband CARS. With the two pump beams expanded to sheets and a probe beam with a large cylindrical cross section, single-pulse 2D imaging can be performed with DFWM; temperature and concentration distributions can be obtained from the intersection volume.[650,673-677] A detailed comparison of essential features of LIF, CARS and DFWM is given by Rakestraw et al.[678]

A rapidly growing field of interest is the application of DFWM to monitor some important combustion species; the related literature has recently been reviewed by Farrow and Rakestraw.[670] In a pioneering study, Ewart and O'Leary[673] have detected the OH radical by DFWM in a methane/air flame. Subsequently, DFWM of OH has been observed by several groups, including Dreier and Rakestraw,[679] Brown et al.[680] and Winter et al.[445] OH concentration profiles in high-pressure flat flames have been measured by DFWM in comparison with other techniques including electronic resonant CARS,[443] DPCFWM,* absorption and TOPLIF†;[442,444] this work was already discussed in Section 4.5. Further applications of the DFWM technique include detection of $NH,$[678,679] $NH_3,$[681] $NO,$[410,682,683] $NO_2,$[677] $H_2,$[684] $HF,$[685] $CH,$[686] $C_2,$[687] CO[684,688] and $HCO.$[689]

In several investigations, temperature has been determined by DFWM. Dreier and Rakestraw[690] measured the flame temperature in a propane/air flame at atmospheric pressure and found good agreement of the DFWM result with a CARS measurement. The temperature obtained from the DFWM spectra was, however, to a certain extent, dependent on pump laser energy. Rakestraw et al.[678] observed good agreement of CARS and DFWM temperature

---

* Double phase-conjugate four-wave mixing, a technique suggested by Winter et al.[445] which reduces beam steering problems by using a phase-conjugate backward pump beam in a four-wave mixing experiment.

† TOPLIF: Saturated laser-induced fluorescence scheme using two detection geometries which are affected differently by zones with low saturation degrees; the ratio of both fluorescence signals may be independent of collisions (see Fig. 13, Section 4.5 and, e.g., Cottereau[331] and Desgroux et al.[345]).

measurements in an atmospheric pressure $NH_3/O_2/N_2$ flame; NH was used as the temperature indicator in the DFWM experiment. The laser intensity was not varied in this case. Further temperature measurements by DFWM in conjunction with the determination of OH concentrations were reported by Feikema et al.[442] and Winter et al.[650] Nyholm et al.[687] recently used the C_2 radical as temperature indicator in their premixed acetylene/oxygen flame. Ewart and Kaczmarek[676] demonstrated 2D temperature imaging with DFWM. In their experiment, two OH transitions in the A-X (0,0) band were probed sequentially, and eight images were averaged for each line to improve the signal-to-noise ratio. The temperature distribution was mapped at two different locations in a laminar premixed methane/air flame and found to be consistent with the expectations. A temperature uncertainty of ±10-15% was estimated for this demonstration experiment.

Whereas in the above studies, temperatures were obtained from spectra acquired by scanning the laser frequency, Jefferies et al.[672] have applied the 'multiplex' broadband DFWM approach of Ewart and Snowdon.[671] DFWM signals from several rotational lines in the OH (A-X, 0,0) band were recorded with a single laser pulse. Since the mode fluctuations of a conventional broadband laser would complicate the interpretation of a multiplex DFWM spectrum, the broadband radiation was provided by a modeless laser[691] with almost constant intensity over about 30 cm^{-1}. Within the laser bandwidth, three separated OH lines in the R_1 branch were probed which exhibited adequate temperature sensitivity. The mean temperature derived from 100 single-pulse measurements was about 10% higher than the adiabatic flame temperature, and the standard deviation was 15% (which may in part be due to changes in the flame conditions). Yip et al.[692] reported a similar multiplex DFWM experiment. They used a standard Nd: YAG/dye laser system with a UV bandwidth of about 1 cm^{-1} to probe two neighboring OH lines in the (A-X, 0,0) band; spectral dispersion of the DFWM signal was achieved using an étalon. Due to random pulse-to-pulse mode fluctuations of the multi-mode laser, DFWM signals of both OH lines were seen in only 15% of the measured single-pulse spectra.

Even though in almost all of the above studies, temperatures measured by DFWM have compared well with adiabatic flame temperatures, thermocouple readings or CARS measurements, most of the results have to be considered as preliminary, and systematic studies are still lacking. The dependence of the measured temperature on laser power density observed by Dreier and Rakestraw[690] may be purely accidental; however, the effect resembles that noted in OH temperature measurements in a flame at atmospheric pressure with saturated LIF.[361] With increasing laser power (and increasing degree of saturation), lower apparent temperatures were obtained; this was attributed to the potential inadequacy of a two-level

model for the interpretation of the saturated LIF signals.

The multiplex DFWM method offers an interesting perspective for the measurement of single-pulse temperatures in turbulent flames. In principle, the technique could be extended to the simultaneous, spatially-resolved determination of the temperature distribution along a line. However, several features would need improvement. Although Yip et al.[692] successfully demonstrated multiplex DFWM with a conventional multi-mode laser system, the modeless laser seems to be a more promising concept. For single-pulse measurements, signal-to-noise considerations limit the attainable accuracy. In the experiment of Jefferies et al.,[672] most of the laser energy within the bandwidth of the modeless laser does not contribute to the DFWM signal. Multiplex DFWM of (seeded) NO as a temperature indicator might overcome some of these difficulties, since the spacing between rotational lines is much lower than for OH. Thus, more lines could be probed within the same bandwidth. As has been discussed in Section 4.4, seeding with NO as tracer might also provide access to low-temperature zones where OH is not present in sufficient amounts.

Quantitative interpretation of DFWM signal intensities in terms of concentrations or temperatures requires that the physical principles be understood in detail. This includes the influences of collisions, molecular motion and saturation on the DFWM signal lineshape and intensity. Most interpretations to date have relied on the theoretical description of Abrams and Lind[667,668] which was derived for an absorbing two-level system driven by monochromatic laser radiation; this approach neglects molecular motion and relaxation within the rovibronic manifold of states. Also, the model assumes two pump beams of equal intensity and a weaker probe beam.

More refined theoretical treatments of the DFWM process are currently being developed and compared with experimental data; they include the effects of pulsed, broadband excitation,[693-695] and of Doppler broadening, quenching, dephasing collisions and saturation on DFWM intensities and lineshapes.[680,696,697] The latter article provides a valuable review of previous theoretical approaches and related experimental results. In their study, the authors perform direct numerical integration of the time- and space-dependent density matrix equations for a two-level system; the approach includes integration over numerous velocity groups and is thus able to treat the case of comparable Doppler and collisional broadening, which is important for the detection of OH and NO by DFWM in typical combustion situations. Furthermore, saturation is considered for both pump and probe laser intensities. Their formalism successfully represents experimental results on DFWM lineshapes for NO in He at different pressures; also, the pressure dependence of the DFWM
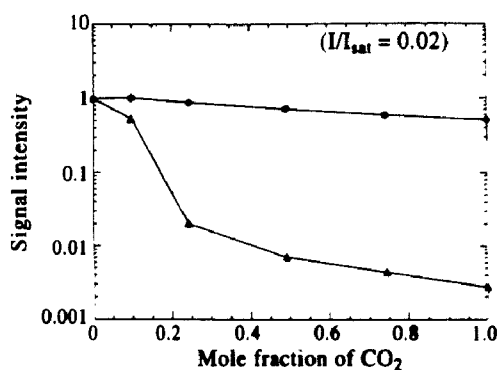
FIG. 35. Nearly unsaturated experimental DFWM (circles) and LIF (triangles) signal intensities versus mole fraction of CO_2 in an N_2/CO_2 mixture (Danehy et al.[696]). The data are normalized to 1.0 at the left axis and are connected by straight lines to guide the eye.

signal at different laser intensities is excellently reproduced.

Several interesting guidelines for further experimental work result from the investigation of Lucht et al.[697] One important recommendation of their work is the operation of both pump and probe lasers with intensities near the saturation intensity in order to minimize the influence of dephasing and quenching collisions, while being insensitive to laser power fluctuations and allowing for adequate signal strength.

Most recently, Danehy et al.[696] have systematically studied the influence of collisional quenching on DFWM intensities in their room temperature investigation of NO. By choosing appropriate mixtures of N_2 and CO_2—a poor and a very efficient quencher of NO, respectively—the collisional dephasing rate was kept constant while the quenching rate was varied by four orders of magnitude. With the quenching rate contributing only as an additive term to the collisional dephasing rate, the coherence decay is in this case dominated by purely elastic dephasing collisions. Considering the population decay, the large variation in the quenching rate is masked by the much less dramatic change in rotational energy transfer rate; for the N_2/CO_2 mixtures under study, the latter varies by about a factor of 2. On the basis of these considerations, the influence of quenching variations on LIF and DFWM intensities was compared under the same conditions. In their experiment, the DFWM signal was observed to be much less sensitive to the variation in quenching rate. For near linear excitation, for example, the LIF signal was attenuated by a factor of 370 when N_2 was replaced by CO_2 while the DFWM intensity decreased only by about a factor of 2, in accordance with expectations (see Fig. 35). As a more general conclusion, DFWM signals will be insensitive to quenching variations if quenching contributes only marginally to homogeneous broadening. This situation may be encountered quite often in typical combustion applications of DFWM, as detailed by the authors.

With the increased understanding of the DFWM

process gained in recent systematic experimental and theoretical investigations, more quantitative applications of the technique can be expected. Several features may be particularly promising for future studies. DFWM using picosecond laser pulses may be advantageous in high-pressure combustion environments. Since the DFWM signal is only present for the duration of the laser pulse, it can be affected by collisions only during that time. Thus, a two-level formalism might still be appropriate at elevated pressures. Furthermore, the formation of so-called thermal gratings—spatial modulations of the refractive index generated as a result of the deposition of energy in the system by collisional energy transfer—may be reduced using shorter pulse lengths. Picosecond DFWM may also be advantageous for the investigation of the dynamics of collision processes. In a pioneering study, Linne and Fiechtner[698] have very recently demonstrated the detection of potassium atoms seeded into a methane/air flame by DFWM using picosecond pulses.

With respect to instrumentation for DFWM experiments, some further aspects deserve attention. Since mode fluctuations can be of critical influence for the DFWM signal, either single-mode or modeless lasers should preferably be used in quantitative experiments, in particular, if single-pulse information is desired. As already discussed in detail, beam steering effects may be reduced using a phase-conjugate backward pump beam.[442,444,445] Complementary to the more commonly applied geometry with two counterpropagating beams, forward scattering with focused excimer lasers has been used by Meijer and Chandler[684] to detect weak absorption features. Using infrared laser radiation to probe rovibrational transitions,[685] the application range of DFWM may be extended significantly to include molecules which are not easily detected with other techniques. In particular, non-fluorescing molecules or species with low fluorescence quantum yields can be probed. In comparison to regular IR absorption, the Doppler-free nature of the DFWM process can be beneficial in resolving spectral structures. Furthermore, the coherent signal may be discriminated very efficiently against background noise, which can be a particular problem in infrared detection. Although DFWM lacks the extreme sensitivity of REMPI, it may be an interesting alternative, especially if the presence of physical probes in the system is not desirable. Further studies in this wavelength regime may examine the potential of DFWM for the detection of polyatomic hydrocarbon species.

In conclusion, it should be kept in mind that DFWM is, in comparison with LIF or CARS, a less mature technique for combustion applications. Many interesting features may make DFWM one of the most versatile diagnostic tools for application in molecular spectroscopy, as well as for the detection of trace species in chemical reactors, flow and combustion systems. As a prerequisite, however, a com-

plete theoretical description of the process should be developed for quantitative measurements. Additional systematic and comparative investigations will undoubtedly contribute to resolving some of the remaining questions.

As an additional note, it should be pointed out that non-resonant four-wave mixing has recently been demonstrated[699] in flow and combustion applications. In preliminary experiments, laser-induced gratings have been used to visualize mixing of He and air without addition of any tracer substance, and also to image the spatial distribution of soot in an acetylene/air diffusion flame. The complex non-linear index of refraction for the different materials gives rise to different signal strengths in this configuration, where a non-resonant, fixed-frequency grating is formed using three beams of 532 nm. The significance of this technique for combustion diagnostics is presently unclear.

6.4. Amplified Spontaneous Emission (ASE)

This technique has primarily been applied for the detection of atoms in combustion systems; for example, H atoms,[700,701] O atoms,[702] C atoms,[516,702,703] N atoms[506,507] and Cl atoms[705] have been detected with ASE. Also, detection of CO[653,706] and NH$_3$[531] have been reported. Stimulated emission is observed as one of the depopulation mechanisms of a level excited by a multi-photon process (see Fig. 22, Section 5). Typically, in the case of two-photon excitation in an atomic system, a level is populated (level 3 in Fig. 22) for which radiative transfer back into the ground state (level 1) is not allowed due to the different selection rules for one- and two-photon transitions. Under favorable conditions, a population inversion can be established between levels 2 and 3, if spontaneous emission to an intermediate energy level (2 in Fig. 22) proceeds efficiently. Spontaneous emission of frequency ν_{32} can thus be amplified. As a prerequisite for the generation of appreciable gain, the population in 3 needs to be quite large, and level 2 must be rapidly depopulated. The inversion is more easily sustained for atoms than for molecules, for which vibrational and rotational energy transfer may contribute to the depopulation of the initially pumped level.

The attraction of the ASE technique results in part from the generation of a coherent signal beam. The ASE signal can be detected in both the forward and backward directions. Quantitative interpretation of the measured intensity is, however, not straightforward, since the amplification depends on both space and time. The ratio of signal to background can be much more favorable for ASE than for MPLIF, so that very small concentrations may be detected. Aldén et al.[653] and Westblom et al.[706] have observed ASE in MPLIF experiments as an extremely intense signal beam which was visible by eye. For the detec-

tion of O atoms, Aldén et al.[704] have noted an ASE intensity which was about a factor of 10^4 higher than the corresponding MPLIF signal. ASE was more successful than MPLIF for the detection of C atoms in flames; N atoms, too, could readily be monitored in flames with ASE, whereas their detection with MPLIF was difficult (see Section 5.2).

Systematic studies of the influence of laser intensity, pressure, collisional environment and other parameters on the ASE intensity have been performed by Westblom et al.[706] in CO experiments in a low-pressure cell, and by Heard and Jeffries[701] in H atom experiments in low-pressure flames. Both groups have simultaneously measured ASE and MPLIF intensities. In general, a decrease of the ASE signal with increasing quenching efficiency was observed. Upon addition of 100 mbar N$_2$, the CO ASE signal disappeared almost completely,[706] while the fluorescence intensity was not too severely affected even at higher N$_2$ pressures. Similar trends were observed in the 10 mbar H$_2$/O$_2$ flames of Heard and Jeffries.[701] As shown in Fig. 36, the ASE intensity decreased most rapidly in the lean flame where the effective quenching was higher.

A typical feature of ASE is the existence of a threshold: the inversion is only created above a certain laser power density. Above threshold, an exponential increase in ASE intensity is noted, so that very high power dependences are observed. Measurement in this regime may lead to strong pulse-to-pulse fluctuations of the ASE signal. On the other hand, intense ASE processes may affect quantitative MPLIF measurements, since stimulated emission can then not be neglected as a depopulation mechanism.

It seems presently unlikely that ASE will play a significant role in combustion diagnostics, in spite of its high sensitivity. Rapid collisional energy transfer will disturb the creation of the necessary population inversion, and therefore, ASE appears, in general, poorly suited for the detection of molecules in flames at atmospheric pressure. Also, a typical ASE experiment does not provide spatial resolution in the direction of the laser beam; arrangements with crossed beams (like the one recently employed by Georgiev et al.[707] for the detection of NH$_3$ and C atoms by two-photon processes) would be required for this purpose. For the detection of small mole fractions of certain atoms, ASE might be advantageous. However, additional effort would be required for quantitative applications. Simulation of typical ASE experiments with coupled differential equations, which describe all relevant processes in space and time, including multi-photon excitation, saturation, spontaneous and stimulated radiative transfer, predissociation, ionization and collisional energy transfer might be a first step towards a thorough understanding of the empirically observed effects.
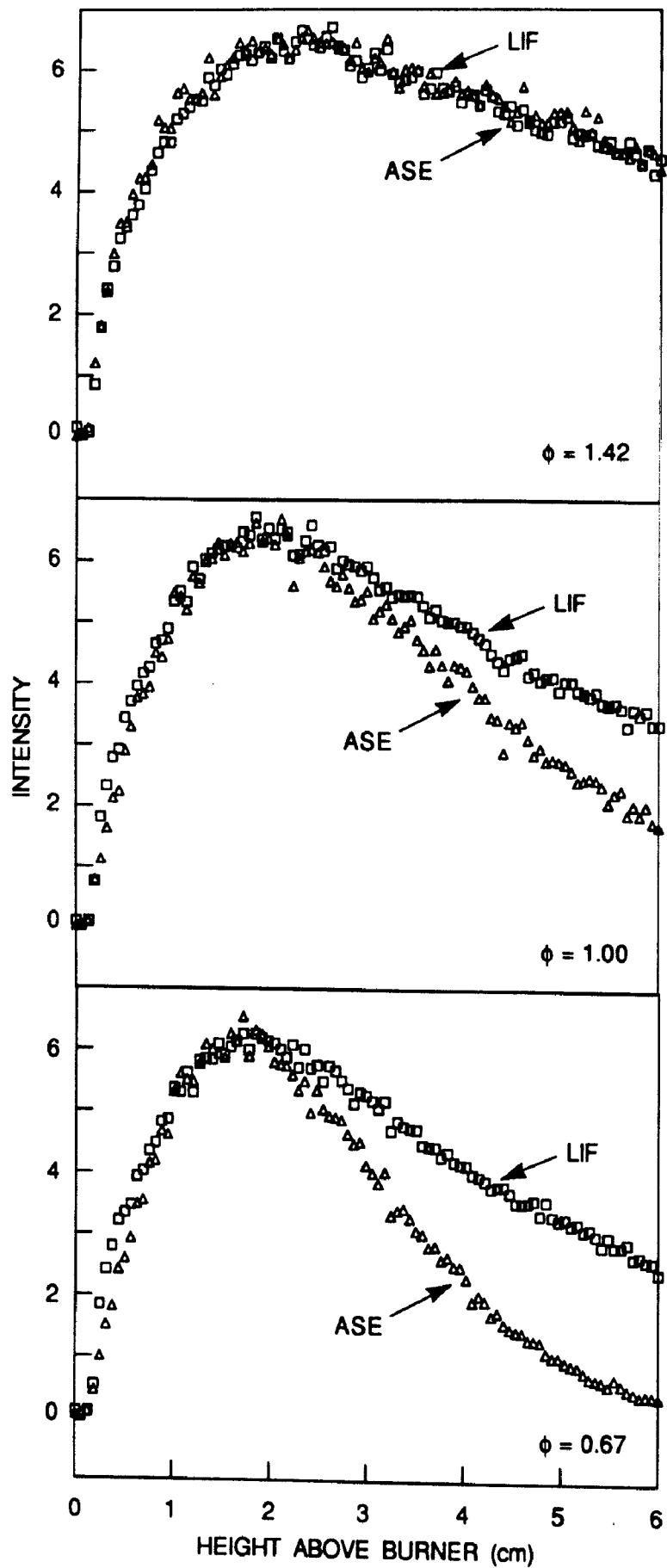
FIG. 36. Comparison of ASE and LIF intensities (scaled to a common maximum) for three hydrogen/oxygen flames at 10 mbar (Heard and Jeffries[701].

7. SUMMARY AND CONCLUSIONS

The primary intention of this article was to give an introduction into recent developments of several laser diagnostic techniques for the measurement of intermediate species concentration and, to some extent, of temperature in combustion systems. Typical applications were described, and it was attempted to characterize the present status and the advantages and limitations of each technique, in particular with respect to quantitative measurements. More attention was devoted to providing the reader with the appropriate references to the technical literature rather than to a general theoretical treatment of each technique with its fundamental equations; for the latter aspect, the reader is referred to the referenced textbooks and review articles. Primarily, laser absorption, laser-induced fluorescence and multi-photon techniques have been discussed. In addition, recent developments have been covered, including multi-dimensional or multi-species applications. Non-linear techniques which offer special features for the detection of intermediate species have also been discussed, including electronically resonant CARS and DFWM.

The importance attributed to individual aspects is inevitably affected by the author's personal opinions. In some cases, digressions into closely related fields were considered helpful in order to elucidate particular properties or inherent difficulties of a technique. Topics which have not been addressed include, for example, polarization spectroscopy,* pump-probe techniques such as ASOPS† or measurements involving particles and droplets. Also, Rayleigh scattering, spontaneous and coherent Raman spectroscopy have not been the subject of this article, because they are typically not suited for the detection of intermediate species. They are, however, most valuable techniques which have found a multitude of applications in combustion diagnostics, and they may be combined with more sensitive techniques such as LIF, REMPI or DFWM for a more complete characterization of specific combustion situations. Examples for such combinations of several diagnostic techniques have been given throughout the article.

In this concluding section, an attempt will be made to give a short general review of the status and potential of the techniques characterized previously, focusing on quantitative concentration and accurate temperature measurement, and to indicate directions for future work. Some more detailed statements, which have already been given at the end of individual sections, will be summarized here. As a condensed, schematic representation of these

comments—although simplified in many respects—Table 1 gives an overview of the techniques, their characteristic features and their predominant regimes of application.

Techniques employing physical probes have lost much of their importance in combustion diagnostics as a consequence of the superior properties of laser-based techniques. In addition, emission and absorption measurements without lasers are no longer widely applied. Laser absorption spectroscopy is one of the most simple and direct diagnostics for the detection of trace species. Based upon the well-understood theory of absorption, quantitative concentration measurements can unambiguously be performed in reactive systems, flows or combustion environments. Laser absorption measurements are therefore often performed for calibration purposes or for studying high-temperature spectroscopy and reaction kinetics. However, absorption is, in general, a line-of-sight technique with limited spatial resolution; its use is restricted to media which exhibit homogeneous absorber density and temperature along the laser beam. Also, the sensitivity may not be sufficient for the detection of very small concentrations.

Laser-induced fluorescence is one of the most widely applied diagnostic methods. Many combustion species can be detected using LIF. In addition to the measurement of molecular concentrations, LIF is also used for the determination of temperature and velocity. With the aid of tracer molecules, LIF provides access to many problems in turbulent mixing and combustion. Applications of LIF have spanned the range from fundamental spectroscopy to the investigation of practical combustion systems, in particular, i.c. engines. One of its most attractive features is the ease of acquiring instantaneous, two-dimensional maps of different process parameters. The most severe drawback of LIF is the sensitivity of the fluorescence signal to collisions. This not only reduces the available signal intensity, but may also complicate quantitative interpretation.

Although a large number of recent studies have been devoted to the measurement of combustion-relevant collision rates, more information on state-selective, high temperature collision processes is needed. State-specific vibrational and rotational energy transfer cross sections, particularly for the electronic ground states of many combustion radicals, are largely lacking. The physical principles which govern the distribution of the available energy among the various accessible energy levels are, in general, almost unexplored; for example, final-state distributions arising from electronic quenching have not yet been studied systematically. Details of the molecular dynamics of most combustion-relevant collision processes are still largely unclear. Further work should include experimental investigations which provide collisional cross sections as a function of initial and

---

*For recent applications of polarization spectroscopy in combustion, see Zizak et al.[708] and Nyholm et al.[709,710]

†ASOPS: Asynchronous Optical Sampling, a pump-probe technique for application in turbulent high-pressure flames described by Fiechtner et al.[711,712] and Kneisler et al.[713]

TABLE 1. Techniques for the determination of intermediate concentrations and temperature in combustion systems

Section	Technique*	Characteristic features	Comments; primary applications
2.	Techniques without lasers		
	ESR, MS, thermocouple	Require physical probes, quantitative applications questionable; low spatial and temporal resolution	Have lost their importance in comparison with laser techniques
	Emission, absorption	Low complexity, low spatial resolution	At present, not of primary importance
3.	Laser absorption	Spatial resolution along a line; low complexity of experiment and theory	Well-suited for calibration purposes; useful in spectroscopic or kinetic context; can yield temperature, pressure and velocity
4.	LIF	Very sensitive; two-dimensional applications and multi-species detection possible; sensitive to collisions	Often applied, very versatile technique; suitable for concentration, temperature and velocity measurements; also used with tracers
4.3.	Saturated LIF	High signal intensity, reduced influence of collisions and laser intensity variations; more complicated theory	Rather seldom applied, potential not fully exploited; broadband and high-pressure applications need refined theory
4.5.	LIPF	Excitation of predissociative states; if predissociation is dominant, lower signal than LIF, but less sensitive to quenching	Mainly applied for O_2 and OH; in the case of OH, suitable at moderate pressures and for high number densities
6.2.	PLIF	Spatially resolved instantaneous two-dimensional image of combustion parameters	Indispensable for practical combustion studies, whenever applicable; species and temperature
5.	Multi-photon techniques	Problems with laser-induced dissociation	Primarily used in chemically simple systems
	MPLIF	Enables detection of several atoms including H, C, N, O, Cl	Practical application e.g. in plasma/CVD* systems
	REMPI	Enables detection of non-fluorescing species; requires physical probe; quantitative interpretation difficult	Potential application for monitoring of polyatomic hydrocarbons and halocarbons
6.3.	DFWM	Laser-like signal beam; sensitive; enables detection of non-fluorescing species; two-dimensional imaging and single-pulse 'multiplex' temperature measurement possible	Promising; primarily feasibility studies available; systematic investigations are being performed; complete theory under development
6.4.	ASE	Laser-like signal beam; very sensitive detection of light atoms and some molecules; in general, spatial resolution along a line	Limited to a few species; quantitative interpretation difficult
4.5.	CARS, resonance CARS	CARS in general too insensitive for radical detection in flames, electronic resonance required; laser-like signal beam; complex experimental arrangement and theory	Limited to special applications

*Abbreviations: MS: Mass spectrometry. LIF: Laser-induced fluorescence. PLIF: Planar laser-induced fluorescence. REMPI: Resonance-enhanced multi-photon ionization. DFWM: Degenerate four-wave mixing. CARS: Coherent anti-Stokes Raman scattering. ESR: Electron spin resonance. LIPF: Laser-induced predissociative fluorescence. MPLIF: Multi-photon laser-induced fluorescence. CVD: Chemical vapor deposition. ASE: Amplified spontaneous emission.

final energy states, collider species and temperature. Furthermore, physically sound extrapolation proce- dures for collisional cross sections with temperature and quantum number should be developed, and, in

addition, quantum mechanical calculations for certain radical–collider pairs have proved extremely supportive in investigations of collisional energy transfer and should be pursued in parallel to experimental studies whenever feasible. In spite of the large number of unknowns in collisional energy transfer, it seems encouraging that detailed rate-equation modelling of all radiative and collisional transfer processes in OH can now successfully reproduce many features observed in LIF experiments, including state-specific fluorescence decay and spectral structure, and that such simulations can be used quantitatively to predict trends in LIF temperature measurement.

Predominantly for measurements at atmospheric and higher pressures, special LIF techniques with reduced sensitivity to quenching are of interest. Saturated LIF generates strong fluorescence signals and can be applied for the detection of many species. Although (partial) saturation is often, even accidentally, achieved in two-dimensional LIF imaging experiments, quantitative measurements with saturated LIF are scarce, since the interpretation of the measured signals is not easy. Theoretical concepts which include energy transfer between multiple states and which treat broadband detection are being developed and verified in high-pressure cells and flames.

Predissociative LIF (LIPF) has attracted attention as a quenching-insensitive alternative for quantitative measurements in high-pressure combustion environments. However, this technique has been demonstrated for only a few species, including OH, O_2 and H_2O. For OH detection, LIPF is almost quenching-insensitive at atmospheric pressure and can be applied with certain precautions at moderately high pressures; above 30 bar, differences between LIF and LIPF disappear. In high-speed flow systems with large OH concentrations, excitation of the predissociative (3,0) transition followed by narrowband detection may be the most attractive measurement scheme. Whereas LIPF of O_2 has been successfully applied in a number of combustion and flow systems, two-photon LIPF of H_2O cannot be fully recommended as an alternative to spontaneous Raman scattering.

To date, coherent techniques are in most cases not (yet) preferred for quantitative radical concentration measurements. The inherent complexity of experiment and theory as well as its restriction to point-wise measurements precludes widespread use of electronically resonant CARS, whereas the potential of degenerate four-wave mixing (DFWM) for quantitative measurements cannot yet be fully assessed. For application of all the aforementioned techniques at elevated pressures, the influence of collisions on spectral lineshapes requires further investigation.

Techniques for the accurate and reliable instantaneous measurement of multi-dimensional temperature distributions are urgently needed. It appears that a LIF technique based upon simultaneous two-line excitation in the linear regime is the most versatile experimental procedure. However, none of the con-

ventional temperature indicator molecules (including OH, O_2, NH, CH and NO) seems to provide the necessary combination of good accuracy, high temperature sensitivity, large dynamic range and general applicability. At present, two-line excitation of (seeded) NO in the A-X system appears to be the most promising scheme for instantaneous two-dimensional LIF temperature mapping. For application in practical combustion systems, single-pulse measurements with CARS or a combination of Raman and Rayleigh scattering may be considered as alternatives, especially for a point-wise, independent verification of two-dimensional LIF results.

Multi-photon spectroscopy enables detection of several combustion-relevant atoms. In addition, non-fluorescing species can be monitored with excellent sensitivity using resonance-enhanced multi-photon ionization (REMPI). A key problem of these multi-photon techniques, however, is their susceptibility to undesired photolytic interferences which restrict their quantitative application primarily to chemically well-understood systems. REMPI also requires the presence of a probe in the vicinity of the observation volume which may cause additional difficulties for quantitative measurements. Although the atomic species can often be detected more sensitively using amplified spontaneous emission (ASE) rather than multi-photon-induced LIF, quantitative applications of this technique are not known to the author.

In general, LIF can be regarded as the most versatile laser diagnostic technique for the detection of reactive intermediates in combustion systems, and it has therefore been established in many laboratories. Reliable, quantitative information can be obtained in many combustion situations. Typical applications range from detailed kinetic studies in flat low-pressure flames to multi-dimensional imaging in turbulent flames and high-pressure engine studies.

The combination of several laser diagnostic techniques, including LIF, Raman and Rayleigh scattering, is one of the most useful instruments of combustion diagnostics. Multi-species detection and simultaneous monitoring of several important quantities enable more detailed and complete investigations of particular combustion situations.

A great deal of research activity in the field of intermediate species detection is currently being devoted to non-linear techniques. Especially for DFWM, a considerable number of experiments have shown the principal applicability of this technique to the measurement of trace species concentrations and temperature. With further systematic studies for various species and combustion environments, it can be anticipated that DFWM will develop into a valuable addition to the present tool of combustion diagnostics.

The accurate measurement of intermediate species concentration (and temperature) in combustion depends to a large extent on intelligent instrumentation. For future applications of laser diagnostics in com-

bustion, several developments can be foreseen, including the use of inexpensive lasers with extended wavelength range (particularly in the infra-red), lasers with short pulse lengths for measurement under collisionally frozen conditions (even at high pressures), and in particular high-energy short-pulse lasers which permit multi-dimensional imaging experiments on these time scales. In parallel, the availability of detectors with extended wavelength characteristics, high efficiency, short gating capability and large dynamic range is desirable.

In conclusion, it should not be overlooked that all applications of laser-diagnostic techniques that were discussed in this article were focused on the quantitative measurement of species concentrations in the gas phase; however, combustion relies to a large extent on liquid or solid fuels. Therefore, methods for the characterization of two-phase combustion environments, including sooting flames, spray combustion and catalytic systems need further development. Also, non-perturbative methods for the quantitative detection of hydrocarbon radicals, which might be involved in chemical pathways leading to engine knock or to the formation of soot, are largely lacking. Furthermore, the development of techniques for the instantaneous measurement of multi-dimensional velocity distributions in turbulent, combusting flows, preferably independent of particle seeding, deserves further attention. With respect to practical combustion, real-time monitoring of potentially hazardous components in complex chemical mixtures, as found in the exhaust gases of waste incinerators or Diesel engines, would be desirable. In summary, quantitative laser diagnostics has contributed significantly to the present knowledge on combustion; the path from laboratory investigations to applications in practical combustion systems, however, is still long and has only begun.

REFERENCES

1. GAYDON, A. G., *The Spectroscopy of Flames*, Chapman and Hall, London (1957).
2. ECKBRETH, A. C., *Laser Diagnostics for Combustion Temperature and Species*, A. K. Gupta and D. G. Lilley (Eds), Abacus Press, Tunbridge Wells (1988).
3. TAYLOR, A. M. K. P., *Instrumentation for Flows with Combustion*, Academic Press, New York (1993).
4. CHIGIER, N. (Ed.), *Combustion Measurements*, Hemisphere, New York (1991).
5. CROSLEY, D. R. (Ed.), *Laser Probes for Combustion Chemistry*, ACS Symposium Series 134, American Chemical Society, Washington (1980).
6. ECKBRETH, A. C., *Eighteenth Symposium (International) on Combustion*, p. 1471, The Combustion Institute, Pittsburgh (1981).
7. BECHTEL, J. H. and CHRAPLYVY, A. R., *Proc. IEEE* 70, 658 (1982).
8. BECHTEL, J. H., DASCH, C. J. and TEETS, R. E., In: *Laser Applications Vol. 5*, p. 129, J. F. Ready and R. K. Erf (Eds), Academic Press, New York (1984).
9. PENNER, S. S., WANG, C. P. and BAHADORI, M. Y., *Twentieth Symposium (International) on Combustion*, p. 1149, The Combustion Institute, Pittsburgh (1984).
10. HARTLEY, D. L., *JQSRT* 40, 291 (1988).
11. STEPOWSKI, D., *Prog. Energy Combust. Sci.* 18, 463 (1992).
12. LAURENDEAU, N. M., *Prog. Energy Combust. Sci.* 14, 147 (1988).
13. SCHOFIELD, K. and STEINBERG, M., *Opt. Eng.* 20, 501 (1981).
14. CROSLEY, D. R., *Opt. Eng.* 20, 511 (1981).
15. CROSLEY, D. R., *J. Chem. Educ.* 59, 446 (1982).
16. HANSON, R. K., *Twenty-First Symposium (International) on Combustion*, p. 1677, The Combustion Institute, Pittsburgh (1986).
17. HANSON, R. K., SEITZMAN, J. M. and PAUL, P. H., *Appl. Phys.* B50, 441 (1990).

18 WOLFRUM, J. (Ed.), *Appl. Phys.* **B50** (No. 6) and **B51** (No. 1) (1990).

19 KOMPA, K., SICK, V. and WOLFRUM, J. (Eds.), *Proceedings of Laser Diagnostics for Industrial Processes*, Heidelberg, Germany: *Ber. Bunsenges. Phys. Chem.* **97** (No. 12) (Dec 1993).

20 FONER, S. N. and HUDSON, R. L., *J. Chem. Phys.* **21**, 1374 (1953).

21 BONNE, U., HOMANN, K. H. and WAGNER, H. GG., *Tenth Symposium (International) on Combustion*, p. 503, The Combustion Institute, Pittsburgh (1965).

22 HOMANN, K. H. and WAGNER, H. GG. *Eleventh Symposium (International) on Combustion*, p. 371, The Combustion Institute, Pittsburgh (1967).

23 FRISTROM, R. M., *Ninth Symposium (International) on Combustion*, p. 560, The Combustion Institute, Pittsburgh (1963).

24 PEETERS, J. and MAHNEN, G., *Fourteenth Symposium (International) on Combustion*, p. 133, The Combustion Institute, Pittsburgh (1973).

25 MILNE, T. A. and GREENE, F. T., *J. Chem. Phys.* **44**, 2444 (1966).

26 LAZZARA, C. P., BIORDI, J. C. and PAPP, J. F., *Combust. Flame* **21**, 371 (1973).

27 BIORDI, J. C., LAZZARA, C. P. and PAPP, J. F., *Combust. Flame* **26**, 57 (1976).

28 BLAUWENS, J., SMETS, B. and PEETERS, J., *Sixteenth Symposium (International) on Combustion*, p. 1055, The Combustion Institute, Pittsburgh (1977).

29 VANDOOREN, J. and VAN TIGGELEN, P. J., *Sixteenth Symposium (International) on Combustion*, p. 1133, The Combustion Institute, Pittsburgh (1977).

30 WESTMORELAND, P. R., HOWARD, J. B. and LONGWELL, J. P., *Twenty-First Symposium (International) on Combustion*, p. 773, The Combustion Institute, Pittsburgh (1986).

31 BASTIN, E., DELFAU, J.-L., REUILLON, M. and VOVELLE, C., *J. Chim. Phys.* **84**, 415 (1987).

32 VANDOOREN, J., *Combust. Sci. Tech.* **84**, 335 (1992).

33 GARO, A., HILAIRE, C., PUECHBERTY, D., *Combust. Sci. Tech.* **86**, 87 (1992).

34 FRISTROM, R. M., *Combust. Flame* **50**, 239 (1983).

35 VOLPONI, J. V., MCLEAN, W. J., FRISTOM, R. M. and MUNIR, Z. A., *Combust. Flame* **65**, 243 (1986).

36 WESTENBERG, A. A. and DE HAAS, N., *J. Chem. Phys.* **40**, 3087 (1964).

37 WESTENBERG, A. A. and FRISTOM, R. M., *Tenth Symposium (International) on Combustion*, p. 473, The Combustion Institute, Pittsburgh (1965).

38 WESTENBERG, A. A., *Progr. Reaction Kinet.* **7**, 23 (1973).

39 NODA, S., MIURA, M. and YOSHIDA, H., *J. Phys. Chem.* **84**, 3143 (1980).

40 NODA, S., DEMISE, H., CLAESSON, O. and YOSHIDA, H., *J. Phys. Chem.* **88**, 2552 (1984).

41 PAUWELS, J.-F., CARLIER, M. and SOCHET, L.-R., *J. Phys. Chem.* **86**, 4330 (1982).

42 JAMES, C. G. and SUGDEN, T. M., *Proc. R. Soc.* **A227**, 312 (1955).

43 BULEWICZ, E. M., JAMES, C. G. and SUGDEN, T. M., *Proc. R. Soc.* **A235**, 89 (1956).

44 MCEWAN, M. J. and PHILLIPS, L. F., *Combust. Flame* **9**, 420 (1965).

45 HALSTEAD, C. J. and JENKINS, D. R., *Combust. Flame* **11**, 362 (1967).

46 GAYDON, A. G. and WOLFHARD, H. G., *Flames*, Chapman and Hall, London (1953).

47 ZEEGERS, P. J. Th. and ALKEMADE, C. Th., *Combust. Flame* **9**, 247 (1965).

48 BRADSHAW, J. D., OMENETTO, N., ZIZAK, G., BOWER, J. N. and WINEFORDNER, J. D., *Appl. Opt.* **19**, 2709 (1980).

49 CARRINGTON, T., *J. Chem. Phys.* **31**, 1418 (1959).

50 KASKAN, W. E., *Combust. Flame* **2**, 229 (1958).

51 BONNE, U. and WAGNER, H. GG., *Ber. Bunsenges. Phys. Chem.* **69**, 35 (1965).

52 EBERIUS, K. H., HOYERMANN, K. and WAGNER, H. GG., *Thirteenth Symposium (International) on Combustion*, p. 713, The Combustion Institute, Pittsburgh (1971).

53 EBERIUS, K. H., HOYERMANN, K. and WAGNER, H. GG., *Fourteenth Symposium (International) on Combustion*, p. 147, The Combustion Institute, Pittsburgh (1973).

54 PORTER, R. P., CLARK, A. H., KASKAN, W. E. and BROWNE, W. E., *Eleventh Symposium (International) on Combustion*, p. 907, The Combustion Institute, Pittsburgh (1967).

55 BULEWICZ, E. M., PADLEY, P. T. and SMITH, R. E., *Proc. R. Soc.* **A315**, 129 (1970).

56 BLEEKRODE, R. and NIEUWPOORT, W. C., *J. Chem. Phys.* **43**, 3680 (1965).

57 JESSEN, P. F. and GAYDON, A. G., *Twelfth Symposium (International) on Combustion*, p. 481, The Combustion Institute, Pittsburgh (1968).

58 LE, Q. N. and VANPEE, M., *Combust. Flame* **62**, 193 (1985).

59 KASKAN, W. E., *J. Chem. Phys.* **31**, 944 (1959).

60 VANDERHOFF, J. A., *Combust. Flame* **84**, 73 (1991).

61 REVET, J. M., PUECHBERTY, D. and COTTEREAU, M. J., *Combust. Flame* **33**, 5 (1978).

62 STEPOWSKI, D., PUECHBERTY, D. and COTTEREAU, M. J., *Eighteenth Symposium (International) on Combustion*, p. 1567, The Combustion Institute, Pittsburgh (1981).

63 SCHOENUNG, S. M. and HANSON, R. K., *Combust. Sci. Tech.* **24**, 227 (1981).

64 CATTOLICA, R. J., YOON, S. and KNUTH E. L., *Combust. Sci. Tech.* **28**, 255 (1982).

65 ZABIELSKI, M. F., DODGE, L. G., COLKET, M. B. and SEERY, D. J., *Eighteenth Symposium (International) on Combustion*, p. 1591, The Combustion Institute, Pittsburgh (1981).

66 SEERY, D. J. and ZABIELSKI, M. F., *Combust. Flame* **78**, 169 (1989).

67 SMITH, O. I. and CHANDLER, D. W., *Combust. Flame* **63**, 19 (1986).

68 DESGROUX, P., GASNOT, L., PAUWELS, J. F. and SOCHET, L. R., *Combust. Sci. Tech.*, submitted for publication (1993).

69 PENNER, S. S., *Quantitative Molecular Spectroscopy and Gas Emissivities*, Addison-Wesley, Reading (1959).

70 MITCHELL, A. C. G. and ZEMANSKY, M. W., *Resonance Radiation and Excited Atoms*, Cambridge University Press (1971).

71 HANSON, R. K., SALIMIAN, S., KYCHAKOFF, G. and BOOMAN, R. A., *Appl. Opt.* **22**, 641 (1983).

72 REA, E. C., Jr., SALIMIAN, S. and HANSON, R. K., *Appl. Opt.* **23**, 1691 (1984).

73 FUJII, N. and SHIN, K. S., *Chem. Phys. Lett.* **151**, 461 (1980).

74 LOUGE, M. Y., HANSON, R. K., REA, E. C. and BOOMAN, R. A., *JQSRT* **32**, 353 (1984).

75 LOUGE, M. Y. and HANSON, R. K., *Twentieth Symposium (International) on Combustion*, p. 665, The Combustion Institute, Pittsburgh (1984).

76 CHANG, A. Y. and HANSON, R. K., *JQSRT* **42**, 207 (1989).

77 DEAN, A. J. and HANSON, R. K., *JQSRT* **42**, 375 (1989).

78 KOHSE-HÖINGHAUS, K., DAVIDSON, D. F., CHANG, A. Y. and HANSON, R. K., *JQSRT* **42**, 1 (1989).

79 DAVIDSON, D. F., DEAN, A. J., DIROSA, M. D. and HANSON, R. K., *Int. J. Chem. Kinet.* **23**, 1035 (1991).

80. WOOLDRIDGE, S. T., HANSON, R. K. and BOWMAN, C. T., *JQSRT* **50**, 19 (1993).
81. DAVIDSON, D. F., CHANG, A. Y., DIROSA, M. D. and HANSON, R. K., *JQSRT* **49**, 559 (1993).
82. CHANG, A. Y., REA, E. C., Jr. and HANSON, R. K., *Appl. Opt.* **26**, 885 (1987).
83. CHANG, A. Y., DIROSA, M. D., DAVIDSON, D. F. and HANSON, R. K., *Appl. Opt.* **30**, 3011 (1991).
84. DIROSA, M. D., CHANG, A. Y. and HANSON, R. K., *Appl. Opt.* **32**, 4074 (1993).
85. DAVIDSON, D. F., CHANG, A. Y., DIROSA, M. D. and HANSON, R. K., *Appl. Opt.* **30**, 2598 (1991).
86. ERNST, J., WAGNER, H. GG. and ZELLNER, R., *Ber. Bunsenges. Phys. Chem.* **82**, 409 (1978).
87. MICHAEL, J. V., SUTHERLAND, J. W. and KLEMM, R. B., *Int. J. Chem. Kinet.* **17**, 315 (1985).
88. DAVIDSON, D. F., CHANG, A. Y. and HANSON, R. K., *Twenty-Second Symposium (International) on Combustion*, p. 1877, The Combustion Institute, Pittsburgh (1988).
89. DAVIDSON, D. F., CHANG, A. Y., KOHSE-HÖINGHAUS, K. and HANSON, R. K., *JQSRT* **42**, 267 (1989).
90. DAVIDSON, D. F. and HANSON, R. K., *Combust. Flame* **82**, 445 (1990).
91. DAVIDSON, D. F., KOHSE-HÖINGHAUS, K., CHANG, A. Y. and HANSON, R. K., *Int. J. Chem. Kinet.* **22**, 513 (1990).
92. BECHTEL, J. H. and TEETS, R. E., *Appl. Opt.* **18**, 4138 (1979).
93. LUCHT, R. P., SWEENEY, D. W. and LAURENDEAU, N. M., *Combust. Sci. Tech.* **42**, 259 (1985).
94. ANDERSON, W. R., DECKER, L. J. and KOTLAR, A. J., *Combust. Flame* **48**, 179 (1982).
95. CHOU, M. S., DEAN, A. M. and STERN, D., *J. Chem. Phys.* **78**, 5962 (1983).
96. KAISER, E. W., MARKO, K., KLICK, D., RIMAI, L., WANG, C. C., SHRINIZADEH, B. and ZHOU, D., *Combust. Sci. Tech.* **50**, 163 (1986).
97. KOHSE-HÖINGHAUS, K., MEIER, U. and ATTAL-TRÉTOUT, B., *Appl. Opt.* **29**, 1560 (1990).
98. CATTOLICA, R. J. *Combust. Flame* **44**, 43 (1982).
99. CHOU, M. S., DEAN, A. M. and STERN, D., *J. Chem. Phys.* **76**, 5334 (1982).
100. LÜCK, K. C. and THIELEN, W., *JQSRT* **20**, 71 (1978).
101. TSATSARONIS, G. and LÜCK, K. C., *J. Non-Equilib. Thermodyn.* **4**, 193 (1979).
102. GREEN, R. M. and MILLER, J. A., *JQSRT* **26**, 313 (1981).
103. JOKLIK, R. G., DAILY, J. W. and PITZ, W. J., *Twenty-First Symposium (International) on Combustion*, p. 895, The Combustion Institute, Pittsburgh (1986).
104. REA, E. C., Jr. and HANSON, R. K., *Appl. Opt.* **27**, 4454 (1988).
105. HARRIS, S. J. and WEINER, A. M., *Opt. Lett.* **6**, 142 (1981).
106. HARRIS, S. J. and WEINER, A. M., *Opt. Lett.* **6**, 434 (1981).
107. ANDERSON, W. R., VANDERHOFF, J. A., KOTLAR, A. J., DEWILDE, M. A. and BEYER, R. A., *J. Chem. Phys.* **77**, 1677 (1982).
108. HARRIS, S. J., *Appl. Opt.* **23**, 1311 (1984).
109. SILVER, J. A., *Appl. Opt.* **31**, 707 (1992).
110. GRABNER, L. and HASTIE, J. W., *Combust. Flame* **44**, 15 (1982).
111. GOLDSMITH, J. E. M., *Opt. Lett.* **6**, 525 (1981).
112. KYCHAKOFF, G., HOWE, R. D. and HANSON, R. K., *Appl. Opt.* **23**, 1303 (1984).
113. STEPOWSKI, D. and GARO, A., *Appl. Opt.* **24**, 2478 (1985).
114. STEPOWSKI, D., *Appl. Opt.* **26**, 1631 (1987).
115. STEPOWSKI, D., *Twenty-Third (International) on Combustion*, p. 1839, The Combustion Institute, Pittsburgh (1990).

116. ALLEN, J. E. Jr, ANDERSON, W. R. and CROSLEY, D. R., *Opt. Lett.* **1**, 118 (1977).
117. TENNAL, K., SALAMO, G. J. and GUPTA, R., *Appl. Opt.* **21**, 2133 (1982).
118. SMITH, G. P., DYER, M. J. and CROSLEY, D. R., *Appl. Opt.* **22**, 3995 (1983).
119. ROSE, A., SALAMO, G. J. and GUPTA, R., *Appl. Opt.* **23**, 781 (1984).
120. KIZIRNIS, S. W., BRECHA, R. J., GANGULY, B. N., GOSS, L. P. and GUPTA, R., *Appl. Opt.* **23**, 3873 (1984).
121. LAWTON, S. A., *Appl. Opt.* **25**, 1263 (1986).
122. ROSE, A. and GUPTA, R., *Opt. Commun.* **56**, 303 (1986).
123. CROSLEY, D. R., *Combust. Flame* **78**, 153 (1989).
124. HACK, W., *Int. Rev. Phys. Chem.* **4**, 165 (1985).
125. WOLFRUM, J., *Appl. Phys.* **B46**, 221 (1988).
126. JEFFRIES, J. B. and CROSLEY, D. R., *Combust. Flame* **64**, 55 (1986).
127. ZABARNICK, S., *Combust. Flame* **85**, 27 (1991).
128. ZABARNICK, S., *Combust. Sci. Tech.* **83**, 115 (1992).
129. BRANCH, M. C., SADEQI, M. E., ALFARAYEDHI, A. A. and VAN TIGGELEN, P. J., *Combust. Flame* **83**, 228 (1991).
130. DOHERTY, P. M. and CROSLEY, D. R., *Appl. Opt.* **23**, 713 (1984).
131. ALTKORN, R. and ZARE, R. N., *Ann. Rev. Phys. Chem.* **35**, 265 (1984).
132. MORLEY, C., *Eighteenth Symposium (International) on Combustion*, p. 23, The Combustion Institute, Pittsburgh (1981).
133. MORLEY, C., *Combust. Flame* **47**, 67 (1982).
134. STEPOWSKI, D. and COTTEREAU, M. J., *Appl. Opt.* **18**, 354 (1979).
135. BERGANO, N. S., JAANIMAGI, P. A., SALOUR, M. M. and BECHTEL, J. H., *Opt. Lett.* **8**, 443 (1983).
136. TAKUBO, U., OKAMOTO, T., KOMINE, N. and YAMAMOTO, M., *Jap. J. Appl. Phys.* **26**, 416 (1987).
137. SCHWARZWALD, R., MONKHOUSE, P. and WOLFRUM, J., *Chem. Phys. Lett.* **142**, 15 (1987).
138. SCHWARZWALD, R., MONKHOUSE, P. and WOLFRUM, J., *Twenty-Second Symposium (International) on Combustion*, p. 1413, The Combustion Institute, Pittsburgh (1988).
139. SCHWARZWALD, R., MONKHOUSE, P. and WOLFRUM, J., *Chem. Phys. Lett.* **158**, 60 (1989).
140. KÖLLNER, M., MONKHOUSE, P. and WOLFRUM, J., *Chem. Phys. Lett.* **168**, 355 (1990).
141. DREIZLER, A., TADDAY, R., MONKHOUSE, P. and WOLFRUM, J., *Appl. Phys.* **B57**, 85 (1993).
142. AGRUP and ALDÉN, M., *Chem. Phys. Lett.* **189**, 211 (1992).
143. MASSEY, G. A. and LEMON, C. J., *IEEE J. Quantum Electron.* **QE-20**, 454 (1984).
144. LEE, M. P., PAUL, P. H. and HANSON, R. K., *Opt. Lett.* **12**, 75 (1987).
145. ANDRESEN, P., BATH, A., GRÖGER, W., LÜLF, H. W., MEIJER, G. and TER MEULEN, J. J., *Appl. Opt.* **27**, 365 (1988).
146. ANDRESEN, P., MEIJER, G., SCHLÜTER, H., VOGES, H., KOCH, A., HENTSCHEL, W., OPPERMANN, W. and ROTHE, E., *Appl. Opt.* **29**, 2392 (1990).
147. LAURENDEAU, N. M. and GOLDSMITH, J. E. M., *Combust. Sci. Tech.* **63**, 139 (1989).
148. KOHSE-HÖINGHAUS, K., JEFFRIES, J. B., COPELAND, R. A., SMITH, G. P. and CROSLEY, D. R., *Twenty-Second Symposium (International) on Combustion*, p. 1857, The Combustion Institute, Pittsburgh (1988).
149. AZZAZY, M. and DAILY, J. W., *AIAA J.* **21**, 1100 (1983).
150. LUCHT, R. P., SWEENEY, D. W., LAURENDEAU, N. M., DRAKE, M. C., LAPP, M. and PITZ, R. W., *Opt. Lett.* **9**, 90 (1984).
151. DRAKE, M. C., PITZ, R. W., LAPP, M., FENIMORE, C.

P., LUCHT, R. P., SWEENEY, D. W. and LAURENDEAU, N. M., Twentieth Symposium (International) on Combustion, p. 327, The Combustion Institute, Pittsburgh (1984).

152. BARLOW, R. S., DIBBLE, R. W. and LUCHT, R. P., Opt. Lett. 14, 263 (1989).

153. BARLOW, R. S., DIBBLE, R. W., CHEN, Y.-Y. and LUCHT, R. P., Combust. Flame 82, 235 (1990).

154. MASRI, A. R., DIBBLE, R. W. and BARLOW, R. S., Combust. Flame 91, 285 (1992).

155. CHENG, T. S., WEHRMEYER, J. A. and PITZ, R. W., Combust. Flame 91, 323 (1992).

156. BARLOW, R. S. and CARTER, C. D., Combust. Flame 97, 261 (1994).

157. CARTER, C. D. and BARLOW, R. S., Opt. Lett. 19, 299 (1994).

158. STÅRNER, S. H., BILGER, R. W., DIBBLE, R. W., BARLOW, R. S., FOURGUETTE, D. C. and LONG, M. B., Twenty-Fourth Symposium (International) on Combustion, p. 341, The Combustion Institute, Pittsburgh (1992).

159. MEIER, U., KIENLE, R., PLATH, I. and KOHSE-HÖINGHAUS, K., Ber. Bunsenges. Phys. Chem. 96, 1401 (1992).

160. PRUCKER, S., MEIER, W., PLATH, I. and STRICKER, W., Ber Bunsenges. Phys. Chem. 96, 1393 (1992).

161. SMYTH, K. C., TJOSSEM, P. J. H., HAMINS, A. and MILLER, J. H., Combust. Flame 79, 366 (1990).

162. SMYTH, K. C. and TJOSSEM, P. J. H., Appl. Phys. B50, 499 (1990).

163. NORTON, T. S., SMYTH, K. C., MILLER, J. H. and SMOOKE, M. D., Combust. Sci. Tech. 90, 1 (1993).

164. PURI, R., MOSER, M., SANTORO, R. J. and SMYTH, K. C., Twenty-Fourth Symposium (International) on Combustion, p. 1015, The Combustion Institute, Pittsburgh (1992).

165. CATTOLICA, R. J. and SCHEFER, R. W., Combust. Sci. Tech. 30, 205 (1983).

166. PFEFFERLE, L. D., GRIFFIN, T. A. and WINTER, M., Appl. Opt. 27, 3197 (1988).

167. PFEFFERLE, L. D., GRIFFIN, T. A., WINTER, M., CROSLEY, D. R. and DYER, M. J., Combust. Flame 76, 325 (1989).

168. GRIFFIN, T. A., CALABRESE, M., PFEFFERLE, L. D., SAPPEY, A., COPELAND, R. A. and CROSLEY, D. R., Combust. Flame 90, 11 (1992).

169. BERGLIND, T. and SUNNER, J., Combust. Flame 63, 279 (1986).

170. FUJIWARA, K., OMENETTO, N., BRADSHAW, J. B., BOWER, J. N., NIKDEL, S. and WINEFORDNER, J. D., Spectrochim. Acta 34B, 317 (1979).

171. HEARD, D. E., JEFFRIES, J. B., SMITH, G. P. and CROSLEY, D. R., Combust. Flame 88, 137 (1992).

172. FILSETH, S. V., ZACHARIAS, H., DANON, J., WALLENSTEIN, R. and WELGE, K. H., Chem. Phys. Lett. 58, 140 (1978).

173. CATTOLICA, R. J., STEPOWSKI, D., PUECHBERTY, D. and COTTEREAU, M. J., JQSRT 32, 363 (1984).

174. PUECHBERTY, D. and COTTEREAU, M. J., Combust. Flame 29, 99 (1977).

175. VANDERHOFF, J. A., BEYER, R. A., KOTLAR, A. J. and ANDERSON, W. R., Appl. Opt. 22, 1976 (1983).

176. VANDERHOFF, J. A., BEYER, R. A., KOTLAR, A. K. and ANDERSON, W. R., Combust. Flame 49, 197 (1983).

177. WONG, K. N., ANDERSON, W. R., VANDERHOFF, J. A. and KOTLAR, A. J., J. Chem. Phys. 86, 93 (1987).

178. COPELAND, R. A., CROSLEY, D. R. and SMITH, G. P., Twentieth Symposium (International) on Combustion, p. 1195, The Combustion Institute, Pittsburgh (1984).

179. MULLER, C. H., SCHOFIELD, K., STEINBERG, M. and BROIDA, H. P., Seventeenth Symposium (International)

on Combustion, p. 867, The Combustion Institute, Pittsburgh (1979).

180. JEFFRIES, J. B., CROSLEY, D. R., WYSONG, I. J. and SMITH, G. P., Twenty-Third Symposium (International) on Combustion, p. 1847, The Combustion Institute, Pittsburgh (1990).

181. SAPPEY, A. D., CROSLEY, D. R. and COPELAND, R. A., Appl. Phys. B50, 463 (1990).

182. HSU, Y.-C., WANG, P.-R., YANG, M.-C., PAPOUSEK, D., CHEN, Y.-T. and CHIANG, W. Y., Chem. Phys. Lett. 190, 507 (1992).

183. BARNES, R. H. and KIRCHER, J. F., Appl. Opt. 17, 1099 (1978).

184. GRIESER, D. R. and BARNES, R. H., Appl. Opt. 19, 741 (1980).

185. COLE, J. B. and SWORDS, M. D., J. Phys. D13, 733 (1980).

186. CATTOLICA, R. J., Twenty-First Symposium (International) on Combustion, p. 1551, The Combustion Institute, Pittsburgh (1986).

187. HARRINGTON, J. E. and SMYTH, K. C., Chem. Phys. Lett. 202, 196 (1993).

188. WILLIAMS, B. A. and FLEMING, J. W., Chem. Phys. Lett. 221, 27 (1994).

189. FUJIWARA, K., OMENETTO, N., BRADSHAW, J. B., BOWER, J. N. and WINEFORDNER, J. D., Appl. Spectrosc. 34, 85 (1980).

190. MILLER, J. H., MALLARD, W. G. and SMYTH, K. C., Combust. Flame 47, 205 (1982).

191. BERETTA, F., CAVALIERE, A. and D'ALESSIO, A., Combust. Sci. Tech. 27, 113 (1982).

192. CIGNOLI, F., BENECCHI, S. and ZIZAK, G., Opt. Lett. 17, 229 (1992).

193. SMITH, G. P. and CROSLEY, D. R., Eighteenth Symposium (International) on Combustion, p. 1511, The Combustion Institute, Pittsburgh (1981).

194. CROSLEY, D. R. and SMITH, G. P., Opt. Eng. 22, 545 (1983).

195. KOHSE-HÖINGHAUS, K., Appl. Phys. B50, 455 (1990).

196. GARLAND, N. L. and CROSLEY, D. R., Twenty-First Symposium (International) on Combustion, p. 1693, The Combustion Institute, Pittsburgh (1986).

197. CROSLEY, D. R., J. Phys. Chem. 93, 6273 (1989).

198. GRAY, J. A., PAUL, P. H. and DURANT, J. L., Chem. Phys. Lett. 190, 266 (1992).

199. DRAKE, M. C. and RATCLIFFE, J. W., J. Chem. Phys. 98, 3850 (1993).

200. WYSONG, I. J., JEFFRIES, J. B. and CROSLEY, D. R., J. Chem. Phys. 92, 5218 (1990).

201. McDERMID, I. S. and LAUDENSLAGER, J. B., J. Chem. Phys. 76, 1824 (1982).

202. COPELAND, R. A. and CROSLEY, D. R., Chem. Phys. Lett. 107, 295 (1984).

203. COPELAND, R. A., DYER, M. J. and CROSLEY, D. R., J. Chem. Phys. 82, 4022 (1985).

204. PAPAGIANNAKOPOULOS, P. and FOTAKIS, C., J. Phys. Chem. 89, 3439 (1985).

205. CLEVELAND, C. B. and WIESENFELD, J. R., Chem. Phys. Lett. 144, 479 (1988).

206. HOOYMAYERS, H. P. and ALKEMADE, C. Th. J., JQSRT 7, 495 (1967).

207. STEPOWSKI, D. and COTTEREAU, M. J., Combust. Flame 40, 65 (1981).

208. JEFFRIES, J. B., KOHSE-HÖINGHAUS, K., COPELAND, R. A., SMITH, G. P. and CROSLEY, D. R., Chem Phys. Lett. 152, 160 (1988).

209. CATTOLICA, R. J. and MATAGA, T. G., Chem. Phys. Lett. 182, 623 (1991).

210. LEE, M. P., KIENLE, R. and KOHSE-HÖINGHAUS, K., Appl. Phys. B58 447 (1994).

211. FAIRCHILD, P. W., SMITH, G. P. and CROSLEY, D. R., Nineteenth Symposium (International) on Combustion, p. 107, The Combustion Institute, Pittsburgh (1982).

212. FAIRCHILD, P. W., SMITH, G. P. and CROSLEY, D. R., J. Chem. Phys. 79, 1795 (1983).
213. SMITH, G. P. and CROSLEY, D. R., J. Chem. Phys. 85, 3896 (1986).
214. COPELAND, R. A. and CROSLEY, D. R., J. Chem. Phys. 84, 3099 (1986).
215. JEFFRIES, J. B., COPELAND, R. A. and CROSLEY, D. R., J. Chem. Phys. 85, 1898 (1986).
216. GERMAN, K. R., J. Chem. Phys. 64, 4065 (1976).
217. COPELAND, R. A., WISE, M. L. and CROSLEY, D. R., J. Phys. Chem. 92, 5710 (1988).
218. BURRIS, J., BUTLER, J. J., McGEE, T. J. and HEAPS, W. S., Chem. Phys. 124, 251 (1988).
219. KENNER, R. D., PFANNENBERG, S., HEINRICH, P. and STUHL, F., J. Phys. Chem. 95, 6585 (1991).
220. HOFZUMAHAUS, A. and STUHL, F., J. Chem. Phys. 82, 3152 (1985).
221. GARLAND, N. L. and CROSLEY, D. R., J. Chem. Phys. 90, 3566 (1989).
222. GARLAND, N. L., JEFFRIES, J. B., CROSLEY, D. R., SMITH, G. P. and COPELAND, R. A., J. Chem. Phys. 84, 4970 (1986).
223. CHAPPELL, E. L., JEFFRIES, J. B. and CROSLEY, D. R., J. Chem. Phys. 97, 2400 (1992).
224. KAES, A. and STUHL, F., J. Chem. Phys. 97, 7362 (1992).
225. KENNER, R. D., ROHRER, F. and STUHL, F., J. Phys. Chem. 93, 7824 (1989).
226. NOKES, C. J. and DONOVAN, R. J., Chem. Phys. 90, 167 (1984).
227. GARLAND, N. L. and CROSLEY, D. R., Chem. Phys. Lett. 134, 189 (1987).
228. GARLAND, N. L. and CROSLEY, D. R., Appl. Opt. 24, 4229 (1985).
229. MEIER, U. E., HUNZIKER, L. E. and CROSLEY, D. R., J. Phys. Chem. 95, 5163 (1991).
230. RAICHE, G. A. and CROSLEY, D. R., J. Chem. Phys. 92, 5211 (1990).
231. CATTOLICA, R. J., MATAGA, T. G. and CAVOLOWSKY, J. A., JQSRT 42, 499 (1989).
232. HEARD, D. E., JEFFRIES, J. B. and CROSLEY, D. R., Chem. Phys. Lett. 178, 533 (1991).
233. BURRIS, J. F., McGEE, T. J. and BARNES, J., Chem. Phys. Lett. 121, 371 (1985).
234. MEIER, U. E., RAICHE, G. A., CROSLEY, D. R., SMITH, G. P. and ECKSTROM, D. J., Appl. Phys. B53, 138 (1991).
235. THOMAN, J. W., Jr, GRAY, J. A., DURANT, J. L. and PAUL, P. H., J. Chem. Phys. 97, 8156 (1992).
236. PAUL, P. H., GRAY, J. A., DURANT, J. L., Jr and THOMAN, J. W., Appl. Phys. B57, 249 (1993).
237. PAUL, P. H., JQSRT 51, 511 (1994).
238. RENSBERGER, K. J., COPELAND, R. A., WISE, M. L. and CROSLEY, D. R., Twenty-Second Symposium (International) on Combustion. The Combustion Institute, Pittsburgh, U.S.A., p. 1867 (1988).
239. RENSBERGER, K. J., DYER, M. J. and COPELAND, R. A., Appl. Opt. 27, 3679 (1988).
240. COPELAND, R. A., WISE, M. L., RENSBERGER, K. J. and CROSLEY, D. R., Appl. Opt. 28, 3199 (1989).
241. BECKER, K. H., HAAKS, D. and TATARCZYK, T., Chem. Phys. Lett. 25, 564 (1974).
242. CROSLEY, D. R. and COPELAND, R. A., Proc. Soc. Photoinstrum. Eng. 742, 6 (1987).
243. MEIER, U. E., HUNZIKER, L. F. and CROSLEY, D. R., European Research Conference on Molecular Energy Transfer (COMET XII), Nijmegen, The Netherlands, July 21-26 (1991).
244. CROSLEY, D. R., personal communication (1994).
245. LENGEL, R. K. and CROSLEY, D. R., Chem. Phys. Lett. 32, 261 (1975).
246. LENGEL, R. K. and CROSLEY, D. R., J. Chem. Phys. 68, 5309 (1978).

247. SMITH, G. P. and CROSLEY, D. R., Appl. Opt. 22, 1428 (1983).
248. RENSBERGER, K. J., JEFFRIES, J. B. and CROSLEY, D. R., J. Chem. Phys. 90, 2174 (1989).
249. RAICHE, G. A., JEFFRIES, J. B., RENSBERGER, K. J. and CROSLEY, D. R., J. Chem. Phys. 92, 7258 (1990).
250. DODD, J. A., LIPSON, S. J. and BLUMBERG, W. A. M., J. Chem. Phys. 92, 3387 (1990).
251. SAPPEY, A. D. and COPELAND, R. A., J. Chem. Phys. 93, 5741 (1990).
252. DAGDIGIAN, P. J., Dynamics and Kinetics of Small Radicals. K. Liu and A. F. Wagner (Eds) (1993).
253. SUDBO, A. S. and LOY, M. M. T., Chem. Phys. Lett. 82, 135 (1981).
254. SUDBO, A. S. and LOY, M. M. T., J. Chem. Phys. 76, 3646 (1982).
255. SMITH, A. V. and JOHNSON, A. W., Chem. Phys. Lett. 93, 608 (1982).
256. IMAJO, T., SHIBUYA, K. and OBI, K., Chem. Phys. Lett. 137, 139 (1987).
257. BROIDA, H. P. and CARRINGTON, T., J. Chem. Phys. 38, 136 (1963).
258. EBATA, T., ANEZAKI, Y., FUJII, M., MIKAMI, N. and ITO, M., Chem. Phys. 84, 151 (1984).
259. JOKLIK, R. G. and DAILY, J. W., Combust. Flame 69, 211 (1987).
260. DIXON, R. N., NEWTON, D. P. and RIELEY, H., J. Chem. Soc. Faraday Trans. 2 83, 675 (1987).
261. DAGDIGIAN, P. J., J. Chem. Phys. 90, 6110 (1989).
262. STEPOWSKI, D. and COTTEREAU, M. J., J. Chem. Phys. 74, 6674 (1981).
263. LUCHT, R. P., SWEENEY, D. W. and LAURENDEAU, N. M., Appl. Opt. 25, 4086 (1986).
264. BURRIS, J., BUTLER, J., McGEE, T. and HEAPS, W., Chem. Phys. 151, 233 (1991).
265. CROSLEY, D. R. and SMITH, G. P., Combust. Flame 44, 27 (1982).
266. ANDERSON, W. R., DECKER, L. J. and KOTLAR, A. J., Combust. Flame 48, 163 (1982).
267. LENGEL, R. K. and CROSLEY, D. R., J. Chem. Phys. 67, 2085 (1977).
268. JÖRG, A., PhD Thesis, DLR Stuttgart, University of Bielefeld, Germany (1991).
269. JÖRG, A., MEIER, U. and KOHSE-HÖINGHAUS, K., J. Chem. Phys. 93, 6453 (1990).
270. JÖRG, A., DEGLI ESPOSTI, A. and WERNER, H.-J., J. Chem. Phys. 93, 8757 (1990).
271. DEGLI ESPOSTI, A. and WERNER, H.-J., J. Chem. Phys. 93, 3351 (1990).
272. JÖRG, A., MEIER, U., KIENLE, R. and KOHSE-HÖING-HAUS, K., Appl. Phys. B55, 305 (1992).
273. KIENLE, R., JÖRG, A. and KOHSE-HÖINGHAUS, K., Appl. Phys. B56, 249 (1993).
274. GERICKE, K. H. and COMES, F. J., Chem. Phys. 65, 113 (1982).
275. COPELAND, R. A. and CROSLEY, D. R., J. Chem. Phys. 81, 6400 (1984).
276. WYSONG, I. J., JEFFRIES, J. B. and CROSLEY, D. R., J. Chem. Phys. 94, 7547 (1991).
277. SCHINKE, R. and ANDRESEN, P., J. Chem. Phys. 81, 5644 (1984).
278. ANDRESEN, P., HÄUSLER, D. and LÜLF, H. W., J. Chem. Phys. 81, 571 (1984).
279. ANDRESEN, P., ARISTOV, N., BEUSHAUSEN, V., HÄUSLER, D. and LÜLF, H. W., J. Chem. Phys. 95, 5763 (1991).
280. SONNENFROH, D. M., McDONALD, R. G. and LIU, K., J. Chem. Phys. 94, 6508 (1991).
281. SCHLEIPEN, J., PhD Thesis, University of Nijmegen, The Netherlands (1992).
282. ZIZAK, G., PETRUCCI, G. A., STEVENSON, C. L. and WINEFORDNER, J. D., Appl. Opt. 30, 5270 (1991).

283. CHAN, C. and DAILY, J. W., *Appl. Opt.* 19, 1357 (1980).
284. CHAN, C. and DAILY, J. W., *Appl. Opt.* 19, 1963 (1980).
285. FURUYA, U., YAMAMOTO, M. and TAKUBO, Y., *Jap. J. Appl. Phys.* 24, 455 (1985).
286. KOTLAR, A. J., GELB, A. and CROSLEY, D. R., In: *Laser Probes for Combustion Chemistry* (D. R. Crosley Ed.), ACS Symposium Series 134, p. 137, American Chemical Society, Washington, 257 (1980).
287. CAMPBELL, D. H., *Appl. Opt.* 21, 2912 (1982).
288. CAMPBELL, D. H., *Appl. Opt.* 23, 689 (1984).
289. CAMPBELL, D. H., *Appl. Opt.* 23, 1319 (1984).
290. KIENLE, R., LEE, M., MEIER, U. and KOHSE-HÖING-HAUS, K., *Third International Symposium on Special Topics in Chemical Propulsion: Non-Intrusive Combustion Diagnostics*, Scheveningen, The Netherlands, May 10–14 (1993).
291. KOHSE-HÖINGHAUS, K., *Third International Symposium on Special Topics in Chemical Propulsion: Non-Intrusive Combustion Diagnostics*, Scheveningen, The Netherlands, May 10–14 (1993).
292. DEUFLHARD, P., BADER, G. and NOVAK, U., Springer series in *Chem. Phys.* 18 (1981).
293. COXON, J. A., *Can. J. Phys.* 58, 933 (1980).
294. TROLIER, M. R., PhD Thesis, Cornell University, U.S.A. (1988).
295. BRUNNER, T. A. and PRITCHARD, D., *Adv. Chem. Phys.* 50, 589 (1982).
296. ALEXANDER, M. H., *J. Chem. Phys.* 76, 3637 (1982).
297. DePRISTO, A. E., AUGUSTIN, S. D., RAMASWAMY, R. and RABITZ, H., *J. Chem. Phys.* 71, 850 (1979).
298. PIEPMEIER, E. H., *Spectrochim. Acta* 27B, 431 (1972).
299. DAILY, J. W., *Appl. Opt.* 15, 955 (1976).
300. DAILY, J. W., *Appl. Opt.* 16, 568 (1977).
301. DAILY, J. W., *Appl. Opt.* 16, 2322 (1977).
302. DAILY, J. W., *Appl. Opt.* 17, 225 (1978).
303. OMENETTO, N., BENETTI, P., HART, L. P., WINEFORD-NER, J. D. and ALKEMADE, C. Th. J., *Spectrochim. Acta* 28B, 289 (1973).
304. RODRIGO, A. B. and MEASURES, R. M., *IEEE J. Quantum Electron.* QE–9, 972 (1973).
305. SHARP, B. L. and GOLDWASSER, A., *Spectrochim. Acta* 31B, 431 (1976).
306. DAILY, J. W. and CHAN, C., *Combust. Flame* 33, 47 (1978).
307. PASTERNACK, L., BARONAVSKI, A. P. and McDONALD, J. R., *J. Chem. Phys.* 69, 4830 (1978).
308. VAN CALCAR, R. A., VAN DE VEN, M. J. M., VAN UITERT, B. K., BIEWENGA, K. J., HOLLANDER, Tj. and ALKEMADE, C. Th. J., *JQSRT* 21, 11 (1979).
309. BARONAVSKI, A. P. and McDONALD, J. R., *J. Chem. Phys.* 66, 3300 (1977).
310. BARONAVSKI, A. P. and McDONALD, J. R., *Appl. Opt.* 16, 1897 (1977).
311. BONCZYK, P. A. and SHIRLEY, J. A., *Combust. Flame* 34, 253 (1979).
312. VERDIECK, J. F. and BONCYZK, P. A., *Eighteenth Symposium (International) on Combustion*, p. 1559, The Combustion Institute, Pittsburgh (1981).
313. LUCHT, R. P. and LAURENDEAU, N. M., *Appl. Opt.* 18, 856 (1979).
314. BERG, J. O. and SHACKLEFORD, W. L., *Appl. Opt.* 18, 2093 (1979).
315. LUCHT, R. P., SWEENEY, D. W. and LAURENDEAU, N. M., *Appl. Opt.* 19, 3295 (1980).
316. LUCHT, R. P., SWEENEY, D. W. and LAURENDEAU, N. M., *Combust. Flame* 50, 189 (1983).
317. SALMON, J. T., LUCHT, R. P., SWEENEY, D. W. and LAURENDEAU, N. M., *Twentieth Symposium (International) on Combustion*, p. 1187, The Combustion Institute, Pittsburgh (1984).
318. MULLER, C. H., SCHOFIELD, K. and STEINBERG, M., *J. Chem. Phys.* 72, 6620 (1980).

319. IINO, M., YANO, H., TAKUBO, Y. and SHIMAZU, M., *J. Appl. Phys.* 52, 6025 (1981).
320. VAN DEN WIJNGAART, C. A., DIJKERMAN, H. A., HOL-LANDER, Tj. and ALKEMADE, C. Th. J., *Combust. Flame* 59, 135 (1985).
321. MAILÄNDER, M., *J. Appl. Phys.* 49, 1256 (1978).
322. BLACKBURN, M. B., MERMET, J.-M., BOUTILIER, G. D. and WINEFORDNER, J. D., *Appl. Opt.* 18, 1804 (1979).
323. VAN CALCAR, R. A., HEUTS, M. J. G., VAN UITERT, B. K., MEIJER, H. A. J., HOLLANDER, Tj. and ALKEMADE, C. Th. J., *JQSRT* 26, 495 (1981).
324. VAN CALCAR, R. A., HEUTS, M. J. G., VAN UITERT, B. K., MEIJER, H. A. J., HOLLANDER, Tj. and ALKEMADE, C. Th. J., *JQSRT* 28, 1 (1982).
325. KOHSE-HÖINGHAUS, K., PERC, W. and JUST, Th., *Ber. Bunsenges. Phys. Chem.* 87, 1052 (1983).
326. KOHSE-HÖINGHAUS, K., HEIDENREICH, R. and JUST, Th., *Twentieth Symposium (International) on Combustion*, p. 1177, The Combustion Institute, Pittsburgh (1984).
327. KOHSE-HÖINGHAUS, K., KOCZAR, P. and JUST, Th., *Twenty-First Symposium (International) on Combustion*, p. 1719, The Combustion Institute, Pittsburgh (1986).
328. KOHSE-HÖINGHAUS, K., KELM, S., MEIER, U., BITTNER, J. and JUST, Th. In: *Complex Chemical Reaction Systems. Mathematical Modelling and Simulation*. J. Warnatz and W. Jäger (Eds), p. 292, Springer, Heidelberg (1987).
329. SALMON, J. T. and LAURENDEAU, N. M., *Appl. Opt.* 24, 1313 (1985).
330. STEPOWSKI, D. and COTTEREAU, M. J., In: *Dynamics of Flames and Reactive Systems*. J. R. Bowen, N. Manson, A. K. Oppenheim and R. I. Soloukhin (Eds), *Prog. Astronaut. Aeronaut.* 95, 642 (1985).
331. COTTEREAU, M. J., *Appl. Opt.* 25, 744 (1986).
332. DESGROUX, P. and COTTEREAU, M. J., *Appl. Opt.* 30, 90 (1991).
333. SALMON, J. T. and LAURENDEAU, N. M., *Appl. Opt.* 24, 65 (1985).
334. BISCHEL, W. K., BAMFORD, D. J. and JUSINSKI, L. E., *Appl. Opt.* 25, 1215 (1986).
335. WANG, C. C. and DAVIS, L. I., Jr, *Phys. Rev. Lett.* 32, 349 (1974).
336. WARNATZ, J. In: *Combustion Chemistry*, W. C. Gardiner, Jr (Ed.), Springer, New York (1984).
337. DRAKE, M. C. and PITZ, R. W., *Exp. Fluids* 3, 283 (1985).
338. ECKBRETH, A. C., BONCZYK, P. A. and VERDIECK, J. F., *Prog. Energy Combust. Sci.* 5, 253 (1979).
339. CARTER, C. D., SALMON, J. T., KING, G. B. and LAURENDEAU, N. M., *Appl. Opt.* 26, 4551 (1987).
340. CARTER, C. D., KING, G. B. and LAURENDEAU, N. M., NASA Contractor Report 185218 (Grant NAG3-351), Purdue University, West Lafayette, Indiana, U.S.A. (1990).
341. CARTER, C. D., KING, G. B. and LAURENDEAU, N. M., *Combust. Sci. Tech.* 71, 263 (1990).
342. CARTER, C. D., KING, G. B. and LAURENDEAU, N. M., *Appl. Opt.* 31, 1511 (1992).
343. DESGROUX, P., PhD Thesis, University of Rouen, France (1988).
344. CARTER, C. D., KING, G. B. and LAURENDEAU, N. M., *Combust. Sci. Tech.* 78, 247 (1991).
345. DESGROUX, P., DOMINGUES, E. and COTTEREAU, M. J., *Appl. Opt.* 31, 2831 (1992).
346. REISEL, J. R., CARTER, C. D. and LAURENDEAU, N. M., *Combust. Flame* 92, 485 (1993).
347. REISEL, J. R., CARTER, C. D., LAURENDEAU, N. M. and DRAKE, M. C., *Combust. Sci. Tech.* 91, 271 (1993).
348. SCHÄFER, M., KETTERLE, W. and WOLFRUM, J., *Appl. Phys.* B52, 341 (1991).

349. CROSLEY, D. R. and SMITH, G. P., *Appl. Opt.* **19**, 517 (1980).

350. KOWALIK, R. M. and KRUGER, C. H., *Combust. Flame* **34**, 135 (1979).

351. JOKLIK, R. G. and DAILY, J. W., *Appl. Opt.* **21**, 4158 (1982).

352. ALDÉN, M., GRAFSTRÖM, P., LUNDBERG, H. and SVANBERG, S., *Opt. Lett.* **8**, 241 (1983).

353. BROIDA, H. P., *J. Chem. Phys.* **19**, 1383 (1951).

354. ZIZAK, G., LANAUZE, J. A. and WINEFORDNER, J. D., *Combust. Flame* **65**, 203 (1986).

355. RENSBERGER, K. J., JEFFRIES, J. B., COPELAND, R. A., KOHSE-HÖINGHAUS, K., WISE, M. L. and CROSLEY, D. R., *Appl. Opt.* **28**, 3556 (1989).

356. BECHTEL, J. H., *Appl. Opt.* **18**, 2100 (1979).

357. KIENLE, R., LEE, M. P. and KOHSE-KÖINGHAUS, unpublished results (1993).

358. LAWITZKI, A., PLATH, I., STRICKER, W., BITTNER, J., MEIER, U. and KOHSE-HÖINGHAUS, K., *Appl. Phys.* **B50**, 513 (1990).

359. GERMAN, K. R., *J. Chem. Phys.* **63**, 5252 (1975).

360. BRZOZOWSKI, J., ERMAN, P. and LYYRA, M., *Phys. Scr.* **17**, 507 (1978).

361. LAWITZKI, A., TIRGRATH, R., MEIER, U., KOHSE-HÖINGHAUS, K., JÖRG, A. and JUST, Th., *Proceedings of the Joint Meeting of the German and Italian Sections of the Combustion Institute*, Ravello, Italy, p. 1.4 (The Combustion Institute, Sezione Italiana, Napoli) (1989).

362. TIRGRATH, R., Poster at the Twenty-Second Symposium (International) on Combustion, Seattle, U.S.A. (1988).

363. WOYDE, M. and STRICKER, W., *Appl. Phys.* **B50**, 519 (1990).

364. WOYDE, M., BERGMANN, V. and STRICKER, W., *Temperature, its Measurement and Control in Science and Industry*. J. F. Schooley (Ed.), Vol. 6 p. 673, American Institute of Physics, New York (1992).

365. CROSLEY, D. R. and JEFFRIES, J. B., *Temperature, its Measurement and Control in Science and Industry*. J. F. Schooley (Ed.), Vol. 6, p. 701, American Institute of Physics, New York (1992).

366. ARNOLD, A., LANGE, B., BOUCHÉ, T., HEITZMANN, T., SCHIFF, G., KETTERLE, W., MONKHOUSE, P. and WOLFRUM, J., *Ber. Bunsenges. Phys. Chem.* **96**, 1388 (1992).

367. GRAY, J. A. and FARROW, R. L., *J. Chem. Phys.* **95**, 7054 (1991).

368. HEARD, D. E., CROSLEY, D. R., JEFFRIES, J. B., SMITH, G. P. and HIRANO, A., *J. Chem. Phys.* **96**, 4366 (1992).

369. YARKONY, D. R., *J. Chem. Phys.* **97**, 1838 (1992).

370. QUAGLIAROLI, T. M., LAUFER, G., KRAUSS, R. H. and McDANIEL, J. C., Jr, *AIAA. Jl.***31**, 520 (1993).

371. STEFFENS, K. L., JEFFRIES, J. B. and CROSLEY, D. R., *Opt. Lett.* **18**, 1355 (1993).

372. KETTERLE, W., ARNOLD, A. and SCHÄFER, M., *Appl. Phys.* **B51**, 91 (1990).

373. CATTOLICA, R. J., *Appl. Opt.* **20**, 1156 (1981).

374. LUCHT, R. P., LAURENDEAU, N. M. and SWEENEY, D. W., *Appl. Opt.* **21**, 3729 (1982).

375. CATTOLICA, R. J. and STEPHENSON, D. A., *Prog. Astronaut. Aeronaut.* **95**, 714 (1985).

376. JÖRRES, V., KOHSE-HÖINGHAUS, K. and MEIER, U., unpublished results (1993).

377. PAUL, P. H., MEIER, U. E. and HANSON, R. K., AIAA Paper 91-0459, 29th Aerospace Sciences Meeting, Reno, U.S.A., January 7-10 (1991).

378. SEITZMAN, J. M., PALMER, J. L., ANTONIO, A. L., HANSON, R. K., DeBARBER, P. A. and HESS, C. F., AIAA Paper 93-0802, 31st Aerospace Sciences Meeting, Reno, U.S.A., January 11-14 (1993).

379. KOHSE-HÖINGHAUS, K. and MEIER, U. E., *Third Inter-*

national Symposium on Special Topics in Chemical Propulsion: Non-Intrusive Combustion Diagnostics, Scheveningen, The Netherlands, May 10-14 (1993).

380. MEIER, W., PRUCKER, S. and STRICKER, W., *Third International Symposium on Special Topics in Chemical Propulsion*, Scheveningen, The Netherlands, May 10-14 (1993).

381. RAICHE, G. A. and JEFFRIES, J. B., *Appl. Opt.* **32**, 4629 (1993).

382. LAUFER, G., McKENZIE, R. L. and HUO, W. M., *Opt. Lett.* **13**, 99 (1988).

383. LAUFER, G., McKENZIE, R. L. and FLETCHER, D. G., *Appl. Opt.* **29**, 4873 (1990).

384. MILES, R. B., CONNORS, J. J., HOWARD, P. J., MARKOVITZ, E. C. and ROTH, G. J., *Opt. Lett.* **13**, 195 (1988).

385. LEWIS, B. R., BERZINS, L., CARVER, J. H. and GIBSON, T. S., *JQSRT* **36**, 187 (1986).

386. PITZ, R. W., CHENG, T. S., WEHRMEYER, J. A. and HESS, C. F., *Appl. Phys.* **B56**, 94 (1993).

387. GROSS, K. P. and McKENZIE, R. L., *Opt. Lett.* **8**, 368 (1983).

388. SEITZMAN, J. M., KYCHAKOFF, G. and HANSON, R. K., *Opt. Lett.* **10**, 439 (1985).

389. GROSS, K. P., McKENZIE, R. L. and LOGAN, P., *Exp. Fluids* **5**, 372 (1987).

390. McMILLIN, B. K., PALMER, J. L., SEITZMAN, J. M. and HANSON, R. K., AIAA Paper 91-1670, 22nd Fluid Dynamics, Plasma Dynamics and Lasers Conference, Honolulu, U.S.A., June 24-26 (1991).

391. PALMER, J. L., McMILLIN, B. K. and HANSON, R. K., AIAA Paper 92-0762, 30th Aerospace Sciences Meeting, Reno, U.S.A., January 6-9 (1992).

392. McMILLIN, B. K., PhD Thesis, HTGL, Stanford University, U.S.A. (1993).

393. McMILLIN, B. K., PALMER, J. L. and HANSON, R. K., *Appl. Opt.* **32**, 7533 (1993).

394. HANSON, R. K., *Third International Symposium on Special Topics in Chemical Propulsion: Non-Intrusive Combustion Diagnostics*, Scheveningen, The Netherlands, May 10-14 (1993).

395. LEE, M. P., McMILLIN, B. K. and Hanson, R. K., *Appl. Opt.* **32**, 5379 (1993).

396. WODTKE, A., HÜWEL, L., SCHLÜTER, H., MEIER, G., ANDRESEN, P. and VOGES, H., *Opt. Lett.* **13**, 910 (1988).

397. BORMANN, F. and ANDRESEN, P., Physics Department, University of Bielefeld, Germany, personal communication (1993).

398. EDWARDS, T., WEAVER, D. P. and CAMPBELL, D. H., *Appl. Opt.* **26**, 3496 (1987).

399. DRAKE, M. C., RATCLIFFE, J. W., BLINT, R. J., CARTER, C. D. and LAURENDEAU, N. M., *Twenty-Third Symposium (International) on Combustion*, p. 387, The Combustion Institute, Pittsburgh (1990).

400. SUNTZ, R., BECKER, H., MONKHOUSE, P. and WOLFRUM, J., *Appl. Phys.* **B47**, 287 (1988).

401. BECKER, H., ARNOLD, A., SUNTZ, R., MONKHOUSE, P., WOLFRUM, J., MALY, R. and PFISTER, W., *Appl. Phys.* **B50**, 473 (1990).

402. BECKER, H., MONKHOUSE, P., WOLFRUM, J., CANT, R. S., BRAY, K. N. C., MALY, R., PFISTER, W., STAHL, G. and WARNATZ, J., *Twenty-Third Symposium (International) on Combustion*, p. 897, The Combustion Institute, Pittsburgh (1990).

403. ARNOLD, A., BECKER, H., HEMBERGER, R., HENTSCHEL, W., KETTERLE, W., KÖLLNER, M., MEIENBURG, W., MONKHOUSE, P., NECKEL, H., SCHÄFER, M., SCHINDLER, K. P., SICK, V., SUNTZ, R. and WOLFRUM, J., *Appl. Opt.* **29**, 4860 (1990).

404. ARNOLD, A., DINKELACKER, F., HEITZMANN, T., MONKHOUSE, P., SCHÄFER, M., SICK, V., WOLFRUM, J., HENTSCHEL, W. and SCHINDLER, K.-P., *Twenty-*

Fourth Symposium (International) on Combustion, p. 1605, The Combustion Institute, Pittsburgh (1992).

405. ANDRESEN, P., SCHLÜTER, H., WOLFF, D., VOGES, H., KOCH, A., HENTSCHEL, W., OPPERMANN, W. and ROTHE, E., *Appl. Opt.* **31**, 7684 (1992).

406. KOCH, A., VOGES, H., ANDRESEN, P., SCHLÜTER, H., WOLFF, D., HENTSCHEL, W., OPPERMANN, W. and ROTHE, E., *Appl. Phys.* **B56**, 177 (1993).

407. ATTAL-TRÉTOUT, B., SCHMIDT, S. C., CRÉTÉ, E., DUMAS, P. and TARAN, J. P., *JQSRT* **43**, 351 (1990).

408. REA, E. C., Jr., CHANG, A. Y. and HANSON, R. K., *JQSRT* **37**, 117 (1987).

409. REA, E. C., Jr, CHANG, A. Y. and HANSON, R. K., *JQSRT* **41**, 29 (1989).

410. PLATH, I., MEIER, U., KOHSE-HÖINGHAUS, K. and ATTAL-TRÉTOUT, B., In: *Proceedings of the Eleventh European CARS Workshop: Coherent Raman Spectroscopy: Applications and New Developments* F. Castellucci, R. Righini and P. Foggi (Eds.), World Scientific Publishing, Singapore (1992).

411. SEITZMAN, J. M., PhD Thesis, Stanford University, U.S.A. (1991).

412. SEITZMAN, J. M. and HANSON, R. K., *AIAA Jl.* **31**, 513 (1993).

413. KETTERLE, W., SCHÄFER, M., ARNOLD, A. and WOLFRUM, J., *Appl. Phys.* **B54**, 109 (1992).

414. WODTKE, A., HÜWEL, L., SCHLÜTER, H., VOGES, H., MEIJER, G. and ANDRESEN, P., *J. Chem. Phys.* **89**, 1929 (1988).

415. MEIJER, G., TER MEULEN, J. J., ANDRESEN, P. and BATH, A., *J. Chem. Phys.* **85**, 6914 (1986).

416. ENGEL, V., MEIJER, G., BATH, A., ANDRESEN, P. and SCHINKE, R., *J. Chem. Phys.* **87**, 4310 (1987).

417. KIM, G. S., HITCHCOCK, L. M., ROTHE, E. W. and RECK, G. P., *Appl. Phys.* **B53**, 180 (1991).

418. GOSS, L. P., CHEN, T. H., TRUMP, D. D., SARKA, B. and NEJAD, A. S., AIAA Paper 91-0355, *29th Aerospace Sciences Meeting*, Reno, U.S.A., January 7–10 (1991).

419. BOEDEKER, L. R., *Opt. Lett.* **14**, 473 (1989).

420. KESSLER, W. J., CARLETON, K. L. and MARINELLI, W. J. *JQSRT* **50**, 39 (1993).

421. ANDRESEN, P., BEUSHAUSEN, V., HÄUSLER, D., LÜLF, H. W. and ROTHE, E. W., *J. Chem. Phys.* **83**, 1429 (1985).

422. GOLDSMITH, J. E. M., *Opt. Lett.* **11**, 416 (1986).

423. GOLDSMITH, J. E. M., *Appl. Opt.* **26**, 3566 (1987).

424. RECKERS, W., HÜWEL, L., GRÜNEFELD, G. and ANDRESEN, P., *Appl. Opt.* **32**, 907 (1993).

425. DREIER, T., DREIZLER, A. and WOLFRUM, J., *Appl. Phys.* **B55**, 381 (1992).

426. DREIER, T. and WOLFRUM, J., *J. Chem. Phys.* **80**, 957 (1984).

427. GERMANN, G. J. and VALENTINI, J. J., *Chem. Phys. Lett.* **157**, 51 (1989).

428. TEETS, R. E. and BECHTEL, J. H., *Opt. Lett.* **6**, 458 (1981).

429. GROSS, K. P., GUTHALS, D. M. and NIBLER, J. W., *J. Chem. Phys.* **70**, 4673 (1979).

430. GREENHALGH, D. A., *Appl. Opt.* **22**, 1128 (1983).

431. ATTAL, B., DEBARRE, D., MÜLLER-DETHLEFS, K. and TARAN, J. P. E., *Rev. Phys. Appl.* **18**, 39 (1983).

432. VERDIECK, J. F., HALL, R. J. and ECKBRETH, A. C., AIAA Paper 83-1477, *18th Thermophysics Conference*, Montreal, Canada (1983).

433. ATTAL-TRÉTOUT, B., BERLEMONT, P. and TARAN, J. P., *Molec. Phys.* **70**, 1 (1990).

434. DREIER, T. and WOLFRUM, J., *Appl. Phys.* **B33**, 213 (1984).

435. GUTHALS, D. M., GROSS, K. P. and NIBLER, J. W., *J. Chem. Phys.* **70**, 2393 (1979).

436. ATTAL-TRÉTOUT, B., MONOT, P. and MÜLLER-DETHLEFS, K., *Molec. Phys.* **73**, 1257 (1991).

437. WARNATZ, J., *Eighteenth Symposium (International) on Combustion*, p. 369, The Combustion Institute, Pittsburgh (1981).

438. ATTAL-TRÉTOUT, B., BOUCHARDY, P., MAGRE, P., PÉALAT, M. and TARAN, J. P., *Appl. Phys.* **B51**, 17 (1990).

439. CHANG, A. Y., DIROSA, M. D. and HANSON, R. K., *JQSRT* **47**, 375 (1992).

440. KESSLER, W. J., ALLEN, M. G. and DAVIS, S. J., *JQSRT* **49**, (1993).

441. VERSLUIS, M., BOOGAARTS, M., KLEIN-DOUWEL, R., THUS, B., DE JONGH, W., BRAAM, A., TER MEULEN, J. J., MEERTS, W. L. and MEIJER, G., *Appl. Phys. B* **55**, 164 (1992).

442. FEIKEMA, D. A., DOMINGUES, E. and COTTEREAU, M. J., *Appl. Phys.* **B55**, 424 (1992).

443. BERVAS, H., ATTAL-TRÉTOUT, B., LE-BOÎTEUX S. and TARAN, J. P., *J. Phys.* **B25**, 949 (1992).

444. DOMINGUES, E., COTTEREAU, M. J. and FEIKEMA, D. A., *Third International Symposium on Special Topics in Chemical Propulsion: Non-Intrusive Combustion Diagnostics*, Scheveningen, The Netherlands, 10–14 May (1993).

445. WINTER, M., RADI, P. P. and STAMPANONI, A., *Twenty-Fourth Symposium (International) on Combustion*, p. 1645, The Combustion Institute, Pittsburgh (1992).

446. LEVENSON, M. D., *Introduction to Nonlinear Laser Spectroscopy*, Academic Press, New York (1982).

447. BISCHEL, W. K., BOKOR, J., KLIGLER, D. J. and RHODES, C. K., *IEEE J. Quantum Electron.* **QE-15**, 380 (1979).

448. HALPERN, J. B., ZACHARIAS, H. and WALLENSTEIN, R., *J. Molec. Spectrosc.* **79**, 1 (1980).

449. MIZIOLEK, A. W. and DEWILDE, M. A., *Opt. Lett.* **9**, 390 (1984).

450. MEIER, U., KOHSE-HÖINGHAUS, K. and JUST, Th., *Chem. Phys. Lett.* **126**, 567 (1986).

451. ALDÉN, M., EDNER, H. and SVANBERG, S., *Appl. Phys.* **B29**, 2207 (1982).

452. GOLDSMITH, J. E. M. and KEARSLEY, D. T. B., *Appl. Phys.* **B50**, 371 (1990).

453. BENGTSSON, P. E. and ALDÉN, M., *Combust. Flame* **80**, 322 (1990).

454. BENGTSSON, P. E. and ALDÉN, M., *Combust. Sci. Tech.* **77**, 307 (1991).

455. JEFFRIES, J. B., SMITH, G. P., HEARD, D. E. and CROSLEY, D. R., *Ber. Bunsenges. Phys. Chem.* **96**, 1410 (1992).

456. BJORKLUND, G. C., AUSSCHNITT, C. P., FREEMAN, R. R. and STORZ, R. H., *Appl. Phys. Lett.* **33**, 54 (1978).

457. BOKOR, J., FREEMAN, R. R., WHITE, J. C. and STORZ, R. H., *Phys. Rev.* **A24**, 612 (1981).

458. GOLDSMITH, J. E. M., *Opt. Lett.* **7**, 437 (1982).

459. LUCHT, R. P., SALMON, J. T., KING, G. B., SWEENEY, D. W. and LAURENDEAU, N. M., *Opt. Lett.* **8**, 365 (1983).

460. TJOSSEM, P. J. H. and COOL, T. A., *Chem. Phys. Lett.* **100**, 479 (1983).

461. GOLDSMITH, J. E. M., *Twentieth Symposium (International) on Combustion*, p. 1331, The Combustion Institute, Pittsburgh (1984).

462. ALDÉN, M., SCHAWLOW, A. L., SVANBERG, S., WENDT, W. and ZHANG, P.-L., *Opt. Lett.* **9**, 211 (1984).

463. GOLDSMITH, J. E. M., *Opt. Lett.* **10**, 116 (1985).

464. GOLDSMITH, J. E. M. and ANDERSON, R. J. M., *Appl. Opt.* **24**, 607 (1985).

465. GOLDSMITH, J. E. M., *Twenty-Second Symposium (International) on Combustion*, p. 1403, The Combustion Institute, Pittsburgh (1988).

466. GOLDSMITH, J. E. M., *Appl. Opt.* **28**, 1206 (1989).

467. GOLDSMITH, J. E. M. and LAURENDEAU, N. M., *Opt. Lett.* **15**, 576 (1990).

468. BITTNER, J., KOHSE-HÖINGHAUS, K., MEIER, U. and JUST, TH., Chem. Phys. Lett. 143, 571 (1988).

469. GOLDSMITH, J. E. M., ANDERSON, R. J. M. and WILLIAMS, L. R., Opt. Lett. 15, 78 (1990).

470. SALMON, J. T. and LAURENDEAU, N. M., Opt. Lett. 11, 419 (1986).

471. SALMON, J. T. and LAURENDEAU, N. M., Appl. Opt. 26, 2881 (1987).

472. SALMON, J. T. and LAURENDEAU, N. M., Combust. Flame 74, 221 (1988).

473. SALMON, J. T. and LAURENDEAU, N. M., JQSRT 43, 155 (1990).

474. BITTNER, J., KOHSE-HÖINGHAUS, K., MEIER, U., KELM, S. and JUST, TH., Combust. Flame 71, 41 (1988).

475. BITTNER, J. PhD Thesis, DLR Stuttgart, University of Heidelberg, Germany (1989).

476. MEIER, U., BITTNER, J., KOHSE-HÖINGHAUS, K. and JUST, Th., Twenty-Second Symposium (International) on Combustion, p. 1887, The Combustion Institute, Pittsburgh (1988).

477. LAWITZKI, A., BITTNER, J. and KOHSE-HÖINGHAUS, K., Chem. Phys. Lett. 175, 429 (1990).

478. BITTNER, J., LAWITZKI, A., MEIER, U. and KOHSE-HÖINGHAUS, K., Appl. Phys. B52, 108 (1991).

479. HOWARD, C. J., J. Phys. Chem. 83, 3 (1979).

480. DAI, B. and LAMBROPOULOS, P., Phys. Rev. A34, 3954 (1986).

481. LAMBROPOULOS, P. Unpublished results (1987).

482. WARNATZ, J., Ber. Bunsenges. Phys. Chem. 82, 834 (1978).

483. SMYTH, K. C. and TJOSSEM, P. J. H., Twenty-Third Symposium (International) on Combustion, p. 1829, The Combustion Institute, Pittsburgh (1990).

484. SMYTH, K. C. and TJOSSEM, P. J. H., Appl. Opt. 29, 4891 (1990).

485. GOLDSMITH, J. E. M. and RAHN, L. A., J. Opt. Soc. Am. B5, 749 (1988).

486. GOLDSMITH, J. E. M. and RAHN, L. A., Opt. Lett. 15, 814 (1990).

487. BISCHEL, W. K., PERRY, B. E. and CROSLEY, D. R., Chem. Phys. Lett. 82, 85 (1981).

488. BISCHEL, W. K., PERRY, B. E. and CROSLEY, D. R., Appl. Opt. 21, 1419 (1982).

489. ALDÉN, M., EDNER, H., GRAFSTRÖM, M. and SVANBERG, S., Opt. Commun. 42, 244 (1982).

490. GOLDSMITH, J. E. M., J. Chem. Phys. 78, 1610 (1983).

491. WALKUP, R. E., SÄNGER, K. L. and SELWYN, G. S., J. Chem. Phys. 84, 2688 (1986).

492. DiMAURO, L. F., GOTTSCHO, R. A. and MILLER, T. A., J. Appl. Phys. 56, 2007 (1984).

493. SELWYN, G. S., J. Appl. Phys. 60, 2771 (1986).

494. PFEFFERLE, L. D., GRIFFIN, T. A., DYER, M. J. and CROSLEY, D. R., Combust. Flame 76, 339 (1989).

495. DYER, M. J., PFEFFERLE, L. D. and CROSLEY, D. R., Appl. Opt. 29, 111 (1990).

496. FORCH, B. E. and MIZIOLEK, A. W., Combust. Sci. Tech. 52, 151 (1987).

497. DYER, M. J. and CROSLEY, D. R., Opt. Lett. 14, 12 (1989).

498. DAGDIGIAN, P. J., FORCH, B. E. and MIZIOLEK, A. W., Chem. Phys. Lett. 148, 299 (1988).

499. BAMFORD, D. J., JUSINSKI, L. E. and BISCHEL, W. K., Phys. Rev. A34, 185 (1986).

500. SAXON, R. P. and EICHLER, J., Phys. Rev. A34, 199 (1986).

501. VAN den OOSTENDORP, D. L., LEVINSKY, H. B., der MEIJ, C. E., JACOBS, R. A. A. M. and BORGHOLS, W. T. A., Appl. Opt. 32, 4636 (1993).

502. MILLER, J. A. and BOWMAN, C. T., Prog. Energy Combust. Sci. 15, 287 (1989).

503. BIAN, J., VANDOOREN, J. and VAN TIGGELEN, P. J., Twenty-First Symposium (International) on Combustion, p. 953, The Combustion Institute, Pittsburgh (1986).

504. TANIGUCHI, M., NODA, S. and YOSHIDA, H., Bull. Chem. Soc. Japan 60, 785 (1987).

505. MILLER, J. A., BRANCH, M. C., McLEAN, W. J., CHANDLER, D. W., SMOOKE, M. D. and KEE, R. J., Twentieth Symposium (International) on Combustion, p. 673, The Combustion Institute, Pittsburgh (1984).

506. AGRUP, S., WESTBLOM, U. and ALDÉN, M., Chem. Phys. Lett. 170, 406 (1990).

507. WESTBLOM, U., AGRUP, S., ALDÉN, M. and CEDERBALK, P., Appl. Opt. 30, 2990 (1991).

508. COPELAND, R. A., JEFFRIES, J. B., HICKMAN, A. P. and CROSLEY, D. R., J. Chem. Phys. 86, 4876 (1987).

509. JEFFRIES, J. B., COPELAND, R. A. and CROSLEY, D. R., J. Chem. Phys. 91, 2200 (1989).

510. DAS, P., ONDREY, G., van VEEN, N. and BERSOHN, R., J. Chem. Phys. 79, 724 (1983).

511. SAUSA, R. C., ALFANO, A. J. and MIZIOLEK, A. W., Appl. Opt. 26, 3588 (1987).

512. VERSLUIS, M. and MEIJER, G., J. Chem. Phys. 96, 3350 (1992).

513. FORCH, B. E. and MERROW, C. N., J. Chem. Phys. 95, 3252 (1991).

514. SMYTH, K. C. and TAYLOR, P. H., Chem. Phys. Lett. 122, 518 (1985).

515. TJOSSEM, P. J. H. and SMYTH, K. C., Chem. Phys. Lett. 144, 51 (1988).

516. WESTBLOM, U., BENGTSSON, P.-E. and ALDÉN, M., Appl. Phys. B52, 371 (1991).

517. LYKKE, K. R. and KAY, B. D., J. Chem. Phys. 95, 2252 (1991).

518. LAUFER, G., KRAUS, R. H. and GRINSTEAD, J. H., Opt. Lett. 16, 1037 (1991).

519. HITCHCOCK, L. M., KIM, G. S., ROTHE, E. W. and RECK, G. P., Appl. Phys. B52, 27 (1991).

520. PINDZOLA, M. S. and DÖRR, M., Phys. Rev. A43, 439 (1991).

521. PRATT, S. T., DEHMER, J. L. and DEHMER, P. M., J. Chem. Phys. 93, 3072 (1990).

522. LOGE, G. W., TIEE, J. J. and WAMPLER, F. B., J. Chem. Phys. 79, 196 (1983).

523. HINES, M. A., MICHELSON, H. A. and ZARE, R. N., J. Chem. Phys. 93, 8557 (1990).

524. SIRKIN, E. R. and HAAS, Y., Appl. Phys. 25, 253 (1981).

525. SIRKIN, E. R., ASSCHER, M. and HAAS, Y., Chem. Phys. Lett. 86, 265 (1982).

526. ROBIE, D. C., BUCK, J. D. and BISCHEL, W. K., Appl. Opt. 29, 3961 (1990).

527. van VEEN, N., BREWER, P., DAS, P. and BERSOHN, R., J. Chem. Phys. 77, 4326 (1982).

528. ALDÉN, M. and WENDT, W., Opt. Commun. 69, 31 (1988).

529. OKADA, T., MAEDA, M., KAJIKI, Y., MURAOKA, K. and AKAZAKI, M., Appl. Phys. B43, 113 (1987).

530. LEMPERT, W., DISKIN, G., KUMAR, V., GLESK, I. and MILES, R., Opt. Lett. 16, 660 (1991).

531. WESTBLOM, U. and ALDÉN, M., Appl. Spectrosc. 44, 881 (1990).

532. HAUMANN, J., SEITZMAN, J. M. and HANSON, R. K., Opt. Lett. 11, 776 (1986).

533. CROSLEY, D. R. and SMITH, G. P., J. Chem. Phys. 79, 4764 (1983).

534. GOLDSMITH, J. E. M. and LAURENDEAU, N. M., Appl. Opt. 25, 276 (1986).

535. COOL, T. A., Appl. Opt. 23, 1559 (1984).

536. HUDGENS, J. W., Advances in Multi-Photon Processes and Spectroscopy, Vol. 4, p. 171, World Scientific, Singapore, (1988).

537. DiGIUSEPPE, T. G., HUDGENS, J. W. and LIN, M. C., J. Chem. Phys. 76, 3337 (1982).

538. DiGiuseppe, T. G., Hudgens, J. W. and Lin, M. C., *J. Phys. Chem.* **86**, 36 (1982).
539. Hudgens, J. W., DiGiuseppe, T. G. and Lin, M. C., *J. Chem. Phys.* **79**, 571 (1983).
540. Chou, M. S., *Chem. Phys. Lett.* **114**, 279 (1985).
541. Meier, U. and Kohse-Höinghaus, K., *Chem. Phys. Lett.* **142**, 498 (1987).
542. Cool, T. A., Bernstein, J. S., Song, X.-M. and Goodwin, P. M., *Twenty-Second Symposium (International) on Combustion*, p. 1421, The Combustion Institute, Pittsburgh (1988).
543. Etzkorn, T., Muris, S., Wolfrum, J., Dembny, C., Bockhorn, H., Nelson, P. F., Attia-Shahin, A. and Warnatz, J., *Twenty-Fourth Symposium (International) on Combustion*, p. 925, The Combustion Institute, Pittsburgh (1992).
544. Dulcey, C. S. and Hugdens, J. W., *J. Phys. Chem.* **87**, 2296 (1983).
545. Dulcey, C. S. and Hudgens, J. W., *J. Chem. Phys.* **84**, 5262 (1986).
546. Rockney, B. H., Cool, T. A. and Grant, E. R., *Chem. Phys. Lett.* **87**, 141 (1982).
547. Mallard, W. G., Miller, J. H. and Smyth, K. C., *J. Chem. Phys.* **76**, 3483 (1982).
548. Tjossem, P. J. H., Goodwin, P. M. and Cool, T. A., *J. Chem. Phys.* **84**, 5334 (1986).
549. Bernstein, J. S., Song, X.-M. and Cool, T. A., *Chem. Phys. Lett.* **145**, 188 (1988).
550. Tjossem, P. J. H. and Cool, T. A., *Twentieth Symposium (International) on Combustion*, p. 132, The Combustion Institute, Pittsburgh (1984).
551. Bernstein, J. S., Fein, A., Choi, J. B., Cool, T. A., Sausa, R. S., Howard, S. L., Locke, R. J. and Miziolek, A. W., *Combust. Flame* **92**, 85 (1993).
552. Rohlfing, E. A., *Twenty-Second Symposium (International) on Combustion*, p. 1843, The Combustion Institute, Pittsburgh (1988).
553. Cool, T. A. and Williams, B. A., *Hazardous Waste and Hazardous Materials* **7**, 21 (1990).
554. Cool, T. A. and Williams, B. A., *Combust. Sci. Tech.* **82**, 67 (1992).
555. Williams, B. A., Tanada, T. N. and Cool, T. A., *Twenty-Fourth Symposium (International) on Combustion*, p. 1587, The Combustion Institute, Pittsburgh (1992).
556. Jeffries, J. B., Raiche, G. A. and Jusinski, L. E., *Appl. Phys.* **B55**, 76 (1992).
557. Glänzer, K., Quack, M. and Troe, J., *Sixteenth Symposium (International) on Combustion*, p. 949, The Combustion Institute, Pittsburgh (1977).
558. Harvey, R. and Jessen, P. F., *Nature* **241**, 102 (1973).
559. Etzkorn, T., Fitzer, J., Muris, S. and Wolfrum, J., *Chem. Phys. Lett.* **208**, 307 (1993).
560. Black, J. F. and Powis, I., *J. Chem. Phys.* **89**, 3986 (1988).
561. Yarbrough, W. A. and Messier, R., *Science* **247**, 688 (1990).
562. Celii, F. G. and Butler, J. E., *Ann. Rev. Phys. Chem.* **42**, 643 (1991).
563. Geis, M. W. and Angus, J. C., *Sci. Am.* **267**, 64 (1992).
564. Bachmann, P. K., Leers, D. and Wiechert, D. U., *Ber. Bunsenges. Phys. Chem.* **95**, 1390 (1992).
565. Frenklach, M., *J. Appl. Phys.* **65**, 5142 (1989).
566. Frenklach, M. and Wang, H., *Phys. Rev.* **B43**, 1520 (1991).
567. Harris, S. J. and Weiner, A. M., *J. Appl. Phys.* **67**, 6520 (1990).
568. Goodwin, D. G. and Gavillet, G. G., *J. Appl. Phys.* **68**, 6393 (1990).
569. Chu, C. J., D'Evelyn, M. P., Hauge, R. H. and Margrave, J. L., *J. Appl. Phys.* **70**, 1695 (1991).
570. Harris, S. J. and Goodwin, D. G., *J. Phys. Chem.* **97**, 23 (1993).
571. Wolden, C., Gleason, K. K. and Howard, J. B., *Combust. Flame* **96**, 75 (1994).
572. Lee, S. S., Minsek, D. M., Vestyck, D. J. and Chen, P., *Science* **263**, 1596 (1994).
573. Celii, F. G. and Butler, J. E., *Appl. Phys. Lett.* **54**, 1031 (1989).
574. Meier, U., Kohse-Höinghaus, K., Schäfer, L. and Klages, C.-P., *Appl. Opt.* **29**, 4993 (1990).
575. Schäfer, L., Bringmann, U., Klages, C.-P., Meier, U. and Kohse-Höinghaus, K., In: *Diamond and Diamond-like Films and Coatings*, NATO/ASI Series B, Vol. 266 p. 643 (1991).
576. Schäfer, L., Klages, C.-P., Meier, U. and Kohse-Höinghaus, K., *Appl. Phys. Lett.* **58**, 571 (1991).
577. Tankala, K. and DebRoy, T., *J. Appl. Phys.* **72**, 712 (1992).
578. Chen, K.-H., Chuang, M.-C., Penney, C. M. and Banholzer, W. M., *J. Appl. Phys.* **71**, 1485 (1992).
579. Heberle, N., Heinze, J., Meier, U. and Kohse-Höinghaus, K., unpublished results (1993).
580. Heinze, J., Heberle, N. and Kohse-Höinghaus, K., *Chem. Phys. Lett.*, **223**, 305 (1994).
581. Celii, F. G. and Butler, J. E., *J. Appl. Phys.* **71**, 2877 (1992).
582. Menningen, K. L., Childs, M. A., Chevako, P., Toyoda, H., Anderson, L. W. and Lawler, J. E., *Chem. Phys. Lett.* **204**, 573 (1993).
583. Hsu, W. L., *Appl. Phys. Lett.* **59**, 1427 (1991).
584. Corat, E. J. and Goodwin, D. G., *J. Appl. Phys.* **74**, 2021 (1993).
585. Westblom, U. and Aldén, M., *Appl. Opt.* **29**, 4844 (1990).
586. Wysong, I. J., Jeffries, J. B. and Crosley, D. R., *Opt. Lett.* **14**, 767 (1989).
587. Westblom, U. and Aldén, M., *Appl. Opt.* **28**, 2592 (1989).
588. Westblom, U. and Aldén, M., *Opt. Lett.* **14**, 9 (1989).
589. Goldsmith, J. E. M., Aldén, M. and Westblom, U., *Appl. Opt.* **29**, 4852 (1990).
590. Aldén, M., Edner, H. and Wallin, S., *Opt. Lett.* **10**, 529 (1985).
591. Goldsmith, J. E. M., *Appl. Opt.* **29**, 4841 (1990).
592. Jeffries, J. B., Copeland, R. A., Smith, G. P. and Crosley, D. R., *Twenty-First Symposium (International) on Combustion*, p. 1709, The Combustion Institute, Pittsburgh (1986).
593. Arnold, A., Ketterle, W., Becker, H. and Wolfrum, J., *Appl. Phys.* **B51**, 99 (1990).
594. Stärner, S. H., Bilger, R. W., Dibble, R. W. and Barlow, R. S., *Combust. Sci. Tech.* **72**, 255 (1990).
595. Stärner, S. H., Bilger, R. W., Dibble, R. W. and Barlow, R. S., *Combust. Flame* **83**, 63 (1991).
596. Masri, A. R., Dibble, R. W. and Barlow, R. S., *Combust. Flame* **89**, 167 (1992).
597. Schefer, R. W., Namazian, M. and Kelly, J., *Twenty-Third Symposium (International) on Combustion*, p. 669, The Combustion Institute, Pittsburgh (1990).
598. Schefer, R. W., Namazian, M. and Kelly, J., *Opt. Lett.* **16**, 858 (1991).
599. Nandula, S. P., Brown, T. M., Pitz, R. W. and DeBarber, P. A., *Opt. Lett.* **19**, 414 (1994).
600. Brockhinke, A., Andresen, P. and Kohse-Höinghaus, K., *Twenty-Fifth Symposium (International) on Combustion*, Irvine, U.S.A., 31 July–5 August, Poster presentation and manuscript in preparation (1994).
601. Dyer, M. J. and Crosley, D. R., *Opt. Lett.* **7**, 382 (1982).
602. Kychakoff, G., Knapp, K., Howe, R. D. and Hanson, R. K., Western States Section of the Combustion Institute, Fall Meeting, Paper No. 82–60 (1982).

603. Kychakoff, G., Howe, R. D., Hanson, R. K. and McDaniel, J. C., Appl. Opt. 21, 3225 (1982).
604. Aldén, M., Edner, H., Holmstedt, G., Svanberg, S. and Högberg, T., Appl. Opt 21, 1236 (1982).
605. Hanson, R. K., JQSRT 40, 343 (1988).
606. Lee, M. P., Paul, P. H. and Hanson, R. K., Opt Lett. 11, 7 (1986).
607. Goldsmith, J. E. M. and Anderson, R. J. M., Opt Lett. 11, 67 (1986).
608. Kychakoff, G., Paul, P. H., van Cruyningen, I. and Hanson, R. K., Appl. Opt. 26, 2498 (1987).
609. Seitzman, J. M., Haumann, J. and Hanson, R. K., Appl. Opt. 26, 2892 (1987).
610. Kychakoff, G., Knapp, K., Howe, R. D. and Hanson, R. K., AIAA Jl. 22, 153 (1984).
611. Cattolica, R. J. and Vosen, S. R., Twentieth Symposium (International) on Combustion, p. 1273, The Combustion Institute, Pittsburgh (1984).
612. Hertz, H. M. and Aldén, M., Appl. Phys. B42, 97 (1987).
613. Seitzman, J. M., Üngüt, A., Paul, P. H. and Hanson, R. K., Twenty-Third Symposium (International) on Combustion, p. 637, The Combustion Institute, Pittsburgh (1990).
614. Sick, V., Arnold, A., Diessel, E., Dreier, T., Ketterle, W., Lange, B., Wolfrum, J., Thiele, K. U., Behrendt, F. and Warnatz, J., Twenty-Third Symposium (International) on Combustion, p. 495, The Combustion Institute, Pittsburgh (1990).
615. McMillin, B. K., Lee, M. P., Paul, P. H. and Hanson, R. K., Twenty-Third Symposium (International) on Combustion, p. 1909, The Combustion Institute, Pittsburgh (1990).
616. Smooke, M. D., Lin, P., Lam, J. K. and Long, M. B., Twenty-Third Symposium (International) on Combustion, p. 575, The Combustion Institute, Pittsburgh (1990).
617. Smooke, M. D., Xu, Y., Zurn, R. M., Lin, P., Frank, J. H. and Long, M. B., Twenty-Fourth Symposium (International) on Combustion, p. 813, The Combustion Institute, Pittsburgh (1992).
618. Roberts, W. L., Driscoll, J. F., Drake, M. C. and Ratcliffe, J. W., Twenty-Fourth Symposium (International) on Combustion, p. 169, The Combustion Institute, Pittsburgh (1992).
619. Dyer, M. J. and Crosley, D. R., Lasers '84, STS Press, p. 211 (1985).
620. Allen, M. G., Howe, R. D. and Hanson, R. K., Opt. Lett. 11, 126 (1986).
621. Namazian, M., Schmitt, R. L. and Long, R. B., Appl. Opt. 27, 3597 (1988).
622. Hirano, A., Ippommastu, M. and Tsujishita, M., Opt. Lett. 17, 303 (1992).
623. Aldén, M., Hertz, H. M., Svanberg, S. and Wallin, S., Appl. Opt. 23, 3255 (1984).
624. Hiller, B., Cohen, L. M. and Hanson, R. K., AIAA paper 86-0161, 24th Aerospace Sciences Meeting, Reno, U.S.A., January 6-9 (1986).
625. McDaniel, J. C., Hiller, B. and Hanson, R. K., Opt. Lett. 8, 51 (1983).
626. Hiller, B. and Hanson, R. K., Opt. Lett. 10, 206 (1985).
627. McDaniel, J. C., Hollo, S. D. and Klavuhn, K. G., In: New Trends in Instrumentation for Hypersonic Research A. Boutier (Ed.) NATO-ASI Series E Vol. 224, p. 381, Kluwer Academic Publishers, Dordrecht, The Netherlands (1993).
628. Hollo, S. D., Hartfield, R. J. and McDaniel, J. C., Opt. Lett. 19, 216 (1994).
629. Hiller, B., Booman, R. A., Hassa, C. and Hanson, R. K., Rev. Sci. Instrum. 55, 1964 (1984).
630. Lee, M. P., Paul, P. H., McMillin, B. K. and Hanson, R. K., Western States Section of the Combus-

tion Institute, Fall Meeting, Paper No. 89-40 (1989).
631. Paul, P. H., Lee, M. P. and Hanson, R. K., Opt. Lett. 14, 417 (1989).
632. Palmer, J. L. and Hanson, R. K., AIAA Paper 93-2020, AIAA SAE ASME ASEE 29th Joint Propulsion Conference, Monterey, U.S.A., June 28-30 (1993).
633. Palmer, J. L. and Hanson, R. K., AIAA Paper 94-0618, 32nd Aerospace Sciences Meeting, Reno, U.S.A., January 10-13 (1994).
634. Boedeker, L. R., AIAA Paper 92-0003, 30th Aerospace Sciences Meeting, Reno, U.S.A., Jan 6-9, (1992).
635. Miles, R., Connors, J., Markovitz, E., Howard, P. and Roth, G., Phys. Fluids A1, 389 (1989).
636. Miles, R. B., Lempert, W R., Zhang, B., Zhang, L., Zhou, D. and She, Z. S., AIAA Paper 92-0007, 30th Aerospace Sciences Meeting, Reno, January 6-9 (1992).
637. Miles, R., Lempert, W., Forkey, J., Zhang, B. and Zhou, D., In New Trends in Instrumentation for Hypersonic Research A. Boutier (Ed.) p. 391, NATO-ASI Series E Vol. 224, Kluwer Academic Publishers, Dordrecht, The Netherlands (1993).
638. Miles, R. B., Zhou, D., Zhang, B., Lempert, W. R., and She, Z. S., AIAA Jl. 31, 447 (1993).
639. Melton, L. A., Appl. Opt. 22, 2224 (1983).
640. Melton, L. A. and Verdieck, J. F., Combust Sci. Tech. 42, 217 (1985).
641. Rotunno, A. A., Winter, M., Dobbs, G. M. and Melton, L. A., Combust Sci Tech 71, 247 (1990).
642. Nickle, S. K. and Melton, L. A, Appl Spectrosc 43, 1406 (1989).
643. Winter, M. and Melton, L. A., Appl. Opt. 29, 4574 (1990).
644. Arnold, A., Becker, H., Suntz, R., Monkhouse, P., Wolfrum, J., Maly, R. and Pfister, W., Opt. Lett. 15, 831 (1990).
645. Tait, N. P. and Greenhalgh, D. A., Twenty-Fourth Symposium (International) on Combustion, p. 1621, The Combustion Institute, Pittsburgh (1992).
646. Lozano, A., Yip, B. and Hanson, R. K., Exp. Fluids 13, 369 (1992).
647. Lawrenz, W., Köhler, J., Meier, F., Stolz, W., Wirth, R., Bloss, W. H., Maly, R. R., Wagner, E. and Zahn, M., SAE Paper 92-2320, SAE International Fuels and Lubricants Meeting, San Francisco, U.S.A., October 19-22 (1992).
648. Serpengüzel, A., Swindal, J. C., Chang, R. K. and Acker, W. P., Appl. Opt. 31, 3543 (1992).
649. Koch, A., Chryssostomou, A., Andresen, P. and Bornscheuer, W., Appl. Phys. B56, 165 (1993).
650. Winter, M., Hermanson, J. C. and Dobbs, G. M., AIAA Paper 92-0381, 30th Aerospace Sciences Meeting, Reno, U.S.A. January 6-9 (1992).
651. Yip, B., Lozano, A. and Hanson, R. K., AIAA Paper 93-0221, 31st Aerospace Sciences Meeting, Reno, U.S.A., January 11-14 (1993).
652. Paul, P. H. and Clemens, N. T., Opt. Lett. 18, 161 (1993).
653. Aldén, M., Wallin, S. and Wendt, W., Appl. Phys. B33, 205 (1984).
654. Norton, T. S. and Smyth, K. C., Combust. Sci. Tech. 76, 1 (1991).
655. Ni, T. and Melton, L. A., Appl. Spectrosc. 45, 938 (1991).
656. Hirano, A., Ricoul, F. and Tsushihita, M., Jpn. J. Appl. Phys. 32, 3300 (1993).
657. Barlow, R. S. and Collignon, A., AIAA Paper 91-0179, 29th Aerospace Sciences Meeting, Reno, U.S.A., January 7-10 (1991).
658. Atakan, B., Meier, U., Meier, W. and Kohse-Höinghaus, K., unpublished results (1993).
659. Dyer, M. J. and Crosley, D. R., Opt. Lett. 9, 217 (1984).

660. YIP, B., LAM, J. K., WINTER, M. and LONG, M. B., *Science* 235, 1209 (1987).

661. WINTER, M. and LONG, M. B., *Combust. Sci. Tech.* 66, 181 (1989).

662. FORKEY, J., COGNE, S., SMITS, A., BOGDONOFF, S., LEMPERT, W. R. and MILES, R. B., AIAA Paper 93-2300, AIAA SAE ASME ASEE 29th Joint Propulsion Conference, Monterey, U.S.A., June 28-30 (1993).

663. MILES, R. and LEMPERT, W., *Appl. Phys.* B51, 1 (1990).

664. VAN CRUYINGEN, I., LOZANO, A., MUNGAL, M. G. and HANSON, R. K., *AIAA Jl* 29, 479 (1991).

665. YANEY, P. P., GRAYSON, T. P. and PARISH, J. W., *Twenty-Third Symposium (International) on Combustion*, p. 1877, The Combustion Institute, Pittsburgh (1990).

666. ATAKAN, B., JÖRRES, V. and KOHSE-HÖINGHAUS, K., *Ber. Bunsenges Phys. Chem.* 97, 1706 (1993).

667. ABRAMS, R. L. and LIND, R. C., *Opt. Lett.* 2, 94 (1978).

668. ABRAMS, R. L. and LIND, R. C., *Opt. Lett.* 3, 205 (1978).

669. SHEN, Y. R., *IEEE J. Quantum Electron.* QE-22, 1196 (1986).

670. FARROW, R. L. and RAKESTRAW, D. J., *Science* 257, 1894 (1992).

671. EWART, P. and SNOWDON, P., *Opt. Lett.* 15, 1403 (1990).

672. JEFFRIES, I. P., YATES, A. J. and EWART, P., Proceedings of the 11th European CARS Workshop: *Coherent Raman Spectroscopy: Applications and New Developments*, F. Castellucci, R. Righini and P. Foggi (Eds), World Scientific Publishing, Singapore (1992).

673. EWART, P. and O'LEARY, S. V., *Opt. Lett.* 11, 279 (1986).

674. EWART, P., SNOWDON, P. and MAGNUSSON, I., *Opt. Lett.* 14, 563 (1989).

675. RAKESTRAW, D. J., FARROW, R. L. and DREIER, T., *Opt. Lett.* 15, 709 (1990).

676. EWART, P. and KACZMAREK, M., *Appl. Opt.* 30, 3996 (1991).

677. MANN, B. A., O'LEARY, S. V., ASTILL, A. G. and GREENHALGH, D. A., *Appl. Phys.* B54, 271 (1992).

678. RAKESTRAW, D. J., THORNE, L. R. and DREIER, T., *Twenty-Third Symposium (International) on Combustion*, p. 1901, The Combustion Institute, Pittsburgh (1990).

679. DREIER, T. and RAKESTRAW, D. J., *Appl. Phys.* B50, 479 (1990).

680. BROWN, M. S., RAHN, L. A. and DREIER, T., *Opt. Lett.* 17, 76 (1992).

681. GEORGIEV, N. and ALDÉN, M., *Appl. Phys.* B56, 281 (1993).

682. VANDER WAL, R. L., FARROW, R. L. and RAKESTRAW, D. J., *Twenty-Fourth Symposium (International) on Combustion*, p. 1653, The Combustion Institute, Pittsburgh (1992).

683. FARROW, R. L., RAKESTRAW, D. J. and DREIER, T., *J. Opt. Soc. Am.* B9, 1770 (1992).

684. MEIJER, G. and CHANDLER, D. W., *Chem. Phys. Lett.* 192, 1 (1992).

685. VANDER WAL, R. L., HOLMES, B. E., JEFFRIES, J. B.,

DANEHY, P. M., FARROW, R. L. and RAKESTRAW, D. J., *Chem. Phys. Lett.* 191, 251 (1992).

686. WILLIAMS, S., GREEN, D. S., SETHURAMAN, S. and ZARE, R. N., *J. Am. Chem. Soc.* 114, 9122 (1992).

687. NYHOLM, K., KAIVOLA M. and AMINOFF, C. G., *Opt. Commun.* 107, 406 (1994).

688. GEORGIEV, N., WESTBLOM, U. and ALDÉN, M., *Opt. Commun.* 94, 99 (1992).

689. HALL, G., SUITS, A. G. and WHITAKER, B. J., *Chem. Phys. Lett.* 203, 277 (1993).

690. DREIER, T. and RAKESTRAW, D. J., *Opt. Lett.* 15, 72 (1990).

691. EWART, P., *Opt. Commun.* 55, 124 (1985).

692. YIP, B., DANEHY, P. M. and HANSON, R. K., *Opt. Lett.* 17, 751 (1992).

693. COOPER, J., CHARLTON, A., MEACHER, D. R., EWART, P. and ALBER, G., *Phys. Rev.* A40, 5705 (1989).

694. MEACHER, D. R., CHARLTON, A., EWART, P., COOPER, J. and ALBER, G., *Phys. Rev.* A42, 3018 (1990).

695. KACZMAREK, M., MEACHER, D. R. and EWART, P., *J. Modern Opt.* 37, 1561 (1990).

696. DANEHY, P. M., FRIEDMAN-HILL, E. J., LUCHT, R. P. and FARROW, R. L., *Appl. Phys.* B57, 243 (1993).

697. LUCHT, R. P., FARROW, R. L. and RAKESTRAW, D. J., *J. Opt. Soc. Am.* B10, 1508 (1993).

698. LINNE, M. A. and FIECHTNER, G. J., *Opt. Lett.* 19, 667 (1994).

699. HEMMERLING, B. and STAMPANONI-PANARIELLO, A., *Appl. Phys.* B57, 281 (1993).

700. GOLDSMITH, J. E. M., *J. Opt. Soc. Am.* B6, 1979 (1989).

701. HEARD, D. E. and JEFFRIES, J. B., Western States Section of the Combustion Institute, Spring Meeting, Paper No. 91-21 (1991).

702. ALDÉN, M., WESTBLOM, U. and GOLDSMITH, J. E. M., *Opt. Lett.* 14, 305 (1989).

703. BERGSTRÖM, H., HALLSTADIUS, H., LANDBERG, H. and PERSSON, A., *Chem. Phys. Lett.* 155, 27 (1989).

704. ALDÉN, M., BENGTSSON, P.-E. and WESTBLOM, U., *Opt. Commun.* 71, 263 (1989).

705. SAPPEY, A. D. and JEFFRIES, J. B., *Appl. Phys. Lett.* 55, 1182 (1989).

706. WESTBLOM, U., AGRUP, S., ALDÉN, M., HERTZ, H. M. and GOLDSMITH, J. E. M., *Appl. Phys.* B50, 487 (1990).

707. GEORGIEV, N., NYHOLM, K., FRITZON, R. and ALDÉN, M., *Opt. Commun.* 180, 71 (1994).

708. ZIZAK, G., LANAUZE, J. A. and WINEFORDNER, J. D., *Appl. Opt.* 25, 3242 (1986).

709. NYHOLM, K., MAIER, R., AMINOFF, C. G. and KAIVOLA, M., *Appl. Opt.* 32, 919 (1993).

710. NYHOLM, K., FRITZON, R. and ALDÉN, M., *Opt. Lett.* 18, 1672 (1993).

711. FIECHTNER, G. J., JIANG, Y., KING, G. B., LAURENDEAU, N. M., KNEISLER, R. J. and LYTLE, F. E., *Twenty-Second Symposium (International) on Combustion*, p. 1915, The Combustion Institute, Pittsburgh (1988).

712. FIECHTNER, G. J., KING, G. B., LAURENDEAU, N. M. and LYTLE, F. E., *Appl. Opt.* 31, 2849 (1992).

713. KNEISLER, R. J., LYTLE, F. E., FIECHTNER, G. J., JIANG, Y., KING, G. B. and LAURENDEAU, N. M., *Opt. Lett.* 14, 260 (1989).